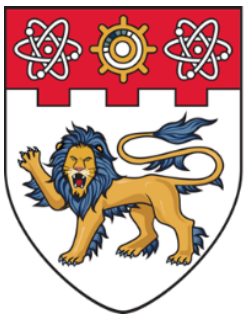

NANYANG TECHNOLOGICAL UNIVERSITY
SINGAPORE

ADAPTIVE COOPERATIVE CONTROL OF MULTI-AGENT SYSTEMS

YING ZOU

SCHOOL OF ELECTRICAL AND ELECTRONIC ENGINEERING

2020

ADAPTIVE COOPERATIVE CONTROL OF MULTI-AGENT SYSTEMS

YING ZOU

School of Electrical & Electronic Engineering

A thesis submitted to the Nanyang Technological University
in partial fulfillment of the requirement for the degree of
Doctor of Philosophy

2020

Statement of Originality

I hereby certify that the work embodied in this thesis is the result of original research, is free of plagiarised materials, and has not been submitted for a higher degree to any other University or Institution.

10/01/2020

. . . . . .

Date

. . . . . .

YING ZOU

Supervisor Declaration Statement

I have reviewed the content and presentation style of this thesis and declare it is free of plagiarism and of sufficient grammatical clarity to be examined. To the best of my knowledge, the research and writing are those of the candidate except as acknowledged in the Author Attribution Statement. I confirm that the investigations were conducted in accord with the ethics policies and integrity standards of Nanyang Technological University and that the research data are presented honestly and without prejudice.

10/01/2020

. . . . . .

Date

. . . . . .

CHANGYUN WEN

Authorship Attribution Statement

This thesis contains material from 4 papers submitted to and published in the following peer-reviewed journals in which I am listed as an author.

Chapter 3 is submitted to *IET Control Theory & Applications* as Y. Zou, C. Wen, and M. Guan. "Distributed output feedback consensus tracking control of multiple nonholonomic mobile robots with directed communication graph and sensor faults,"

The contributions of the co-authors are as follows:

- I prepared the drafts of the manuscript, designed the control algorithm and performed the simulations.
- Prof. Wen provided comments on the algorithm design and revised the manuscript drafts.
- Mr. Guan assisted in simulations and revision of the manuscript.

Chapter 4 is submitted to *IEEE Transactions on Systems, Man and Cybernetics: Systems* as Y. Zou, C. Wen, and C. Deng. "Distributed output feedback consensus tracking control of multiple nonholonomic mobile robots with only position information of leader,"

The contributions of the co-authors are as follows:

- I prepared the drafts of the manuscript, designed the control algorithm and performed the simulations.
- Prof. Wen provided comments on the algorithm design and revised the manuscript drafts.
- Dr. Deng assisted in the mathematical derivations, simulations and revision of the manuscript.

Chapter 5 is published as Y. Zou, C. Wen, and M. Guan. "Adaptive estimator-based formation maneuvering control of nonholonomic mobile robots," *International Journal of Adaptive Control and Signal*

Processing, https://doi.org/10.1002/acs.3078.

The contributions of the co-authors are as follows:

- I prepared the drafts of the manuscript, designed the control algorithm and performed the simulations.
- Prof. Wen provided comments on the algorithm design and revised the manuscript drafts.
- Mr. Guan assisted in the simulations and revision of the manuscript.

Chapter 6 is published as Y. Zou, C. Wen, and M. Guan. "Distributed adaptive control for distance-based formation and flocking control of multi-agent systems," *IET Control Theory & Applications*, vol. 13, no. 6, 878-885, 2019.

The contributions of the co-authors are as follows:

- I prepared the drafts of the manuscript, designed the control algorithm and performed the simulations.
- Prof. Wen provided comments on the algorithm design and revised the manuscript drafts.
- Mr. Guan assisted in the simulations and revision of the manuscript.

10/01/2020

. . . . . .

Date

. . . . . .

YING ZOU

Acknowledgements

I would like to take this opportunity to thank all who have helped me during the past four-year study in NTU.

First and foremost, I would like to express my deepest appreciation to my supervisor, Prof. Changyun Wen, for his continuous support, professional guidance and positive encouragement during the PhD study. I still remember when I first came to NTU in 2015, all the PhD students in the laboratory told me that Prof. Wen is very amiable. After the first meeting with him, I really agree with what they said. During the past four years, his admirable patience and academic sense gives me great help on my research. For example, he will explain some theorems or lemmas by completing the mathematical derivations step by step and takes some examples to help me understand them. He will revise my QE report and research articles sentence by sentence. His attitude towards research and rigor in mathematics have a great influence on me and will benefit me in all my life. In addition to research, he is always concerned with my daily life and encourages me to exercise more. To me, he is not only a supervisor, but also like a father.

I am also very thankful to Dr. Fanghong Guo, Dr. Jie Ding and Dr. Mao Shan. Dr. Guo helped me to complete my application process before I came to NTU. When I first came to NTU to take TPT examination in 2015, he took me for a campus tour and a city tour. After I started my study in NTU, Dr. Guo and Dr. Ding helped me a lot to get familiar with the campus quickly. During the first year, when I encountered problems in my study, they always helped me to solve them patiently. After I joined in the ST Engineering-NTU Corporate Laboratory, Dr. Shan has helped me significantly to find theoretical problems from practical

applications. Even though now Dr. Shan is not working in Singapore, he is still concerned with my research and discussed with me via Wechat.

My colleagues and friends in ST Engineering-NTU Corporate Laboratory and Robotics I Laboratory also give me a lot of help throughout the past four years. I am thankful to Mr. Mingyang Guan for his assistances and advices in the simulation. I also would like to thank Mr. Yijie Zeng and Mr. Kun Cao for their patient discussions and generous help in mathematical derivations. Special thanks go to my friends, Ms. Keyu Wu, Dr. Yuanzhe Wang, Dr. Chule Yang, and Dr. Chao Deng etc., for their support and company. My deep gratitude also goes go to Alex for his delicious food, friendly guidance in cooking and patiently assistances during my stay in the corporate laboratory.

Last but not the least, I would like to express the deepest gratitude to my family for their love and support.

Contents

Summary

Cooperative control of multi-agent systems has achieved rapid development during the past decades due to its broad applications in various areas, such as robotics, intelligent transportation systems, surveillance and monitoring. Consensus is one of the most popular topics in this area, which has attracted considerable attention of numerous researchers. Although a large number of effective control approaches have been proposed to address the consensus problem of multi-agent systems, there are still a lot of open problems in this area. Among them distributed output feedback consensus tracking control of multiple nonholonomic mobile robots in the situations that i) sensor faults occur and ii) limited information of the reference trajectory is available are two important problems to be studied in this thesis.

First of all, distributed output feedback consensus tracking control of multiple nonholonomic mobile robots with sensor faults and communication through a directed graph is studied. In the presence of sensor faults, the main challenge to achieve distributed consensus tracking control lies in that both individual position measurements and relative position between pairs of robots are faulty. To address this issue, an adaptive output feedback fault-tolerant control scheme which involves estimator, observer and controller design is proposed to compress the effects of sensor faults and realize consensus tracking, by estimating the reference trajectory and velocity information. With the designed control algorithm, all the signals in the resulting closed-loop system can be guaranteed to be bounded, and the consensus tracking error of the system can converge to an adjustable neighborhood of zero by appropriately choosing design parameters even in the presence of sensor faults.

Secondly, distributed output feedback consensus tracking control of multiple nonholonomic mobile robots with only position information of leader is considered.

To solve such a problem, an adaptive output feedback control scheme which involves estimator, observer and controller design is proposed. Since only position information of leader is available to a subset of following robots, a fully distributed adaptive estimator is constructed to estimate the position information of leader for each robot. Utilizing the estimated information, an observer-based adaptive output feedback control law is designed to estimate unavailable velocity information and unknown dynamic parameters and achieve trajectory tracking for each robot. It is shown that the boundedness of all the signals in the resulting closed-loop system and the convergence of consensus error to an adjustable neighborhood of zero is established.

Another class of cooperative control problem arises when one wants all agents in a formation to take up a desired shape which is described by the inter-agent distances and assume a common velocity. This is a combined problem of flocking and distance-based formation control, namely flocking with distance-based formation control. To solve such a control problem, most existing algorithms are proposed just based on simple linear models, such as single- and double-integrators. Thus, to overcome this restriction, distance-based formation and flocking control with nonholonomic dynamics and parametric uncertainty are considered respectively in the second part of this thesis.

Aiming to achieve the desired formation shape and an overall maneuvering velocity for nonholonomic mobile robots, a control scheme consisting of an adaptive estimator and a modified gradient control law is proposed. The adaptive estimator is constructed to estimate the desired maneuvering velocity which can be either constant or time-varying. Utilizing the estimated velocity, a modified gradient control law is developed based on the nonholonomic kinematic model to maintain the desired formation shape. Local asymptotic convergence of the overall system is guaranteed by choosing appropriate control parameters.

For distance-based formation and flocking control of multi-agent system with parametric uncertainty, an adaptive distributed control strategy is firstly proposed

based on a 3-agent leader–first-follower (LFF) system model. By introducing two new variables that involve distance error and velocity error and utilizing them in the controller design, it is shown that all agents will globally converge to the desired formation and move with the velocity of the leader. Then the three-agent case is inductively extended to N-agent case. The stability and the effectiveness of the proposed control strategy are analyzed in theory and demonstrated through simulation results, respectively.

List of Figures

Chapter 1

Introduction

The introduction of this thesis is presented in this chapter. Firstly, the background and motivation for conducting the research is introduced. Then, major contributions are summarized. Finally, the outline of the thesis is presented.

1.1 Background and Motivation

Cooperative control of multi-agent systems has attracted considerable attention and achieved rapid development during the past decades due to its broad applications in both civilian and military fields, such as intelligent transportation systems, unknown environment exploration and target tracking. Cooperative control aims to employ a group of agents with interaction capacities to execute some tasks, such as exploration, search and monitoring. Up to now, there are already some papers that have comprehensively reviewed the existing works in this area, see [3–7] for examples. The typical problems in cooperative control of multi-agent systems are consensus, formation control, flocking, shape control and cooperative localization, to name a few. Among the above-mentioned research topics, consensus is one of the hottest topics and has attracted considerable attention of numerous researchers. Consensus is usually aimed to reach an agreement for interested variables of the

agents in a group, by only sharing information among neighbors through the communication network. The interested variables can be position in rendezvous, pose in coordination of robots or velocity in flocking.

1.1.1 Distributed output feedback consensus tracking control of multiple nonholonomic mobile robots

In recent years, considerable consensus approaches have been proposed which can be essentially divided into two broad categories, namely, consensus without a leader (i.e., leaderless consensus) and consensus with a leader (i.e., leader-follower consensus or distributed tracking). Due to the increasing applications of nonholonomic mobile robots in a large number of practical projects, the research on distributed consensus tracking control of multiple nonholonomic mobile robots has attracted an increasing interest in the past decades. However, to implement these proposed approaches into practical applications, most of the existing approaches may suffer from a variety of challenges due to different constraints. These constraints include but not limited to the listed cases as follows.

(1) *Sensor faults.* Sensor fault-tolerant control is of both practical and theoretical importance. Although some results on the sensor fault-tolerant control of individual system have been achieved, few efforts have been made on such an issue with respect to multi-agent systems due to its significant challenge to deal with both faulty individual measurements and faulty relative states/outputs. There have been some attempts in the literature, however, only with additive sensor faults. Similar to actuator faults, multiplicative faults also exist in practice and thus need to be considered in real applications. Furthermore, these existing results are established for linear systems and cannot be directly applied to nonholonomic mobile robots.

(2) *Limited information of the leader.* Provided that the reference trajectory is prescribed or generated by a virtual leader with similar dynamics, most of

the existing consensus methods are developed under the assumption that the velocity or input information of the leader can be obtained by all followers or a subset of followers. In some tasks, such information may not be obtained by the followers.

(3) *Independence of global communication information.* Since consensus is achieved based on the information transmission between neighboring agents, it is necessary to consider the constraints and challenges associated with the communication network topology. One common feature of most existing works is that the knowledge of some eigenvalue information of the Laplacian matrix associated with the communication graph is required to implement the proposed controllers. Specifically, in the case that the communication topologies are undirected graphs, the smallest nonzero eigvenvalue of the Laplacian matrix is required, while the smallest real part of the nonzero eigenvalues of the Laplacian matrix is required for directed communication topologies. However, it is worth mentioning that such information is global information which means it requires the entire communication graph to be known by each agent in the group.

1.1.2 Flocking with Distance-Based Formation Control

In terms of flocking behavior, it means the phenomenon that all agents in a formation move with identical velocity. This is a velocity consensus problem. Distance-based formation control focuses on the inter-agent distances and aims to control the agents in a formation such that the formation achieves the desired shape which is described by the desired inter-agent distances and is invariant to combination of translation and rotation. Thus, another class of consensus problem, namely flocking with distance-based formation control, arises when a multi-agent system is required to take up a particular shape and share a common velocity. Although flocking with distance-based formation control has been studied in many research works, there exist several important issues that deserve further attention.

(1) *Motion constraint.* Almost existing works on flocking with distance-based formation control are developed based on single-integrator or double-integrator models, which cannot fully express the dynamic model of real agents because of the existence of motion constraints. Specifically, the velocity of a single integrator can be arbitrarily assigned whereas the velocity of a nonholonomic mobile robot is subject to nonholonomic dynamics. Thus, theses results cannot be directly applied to multiple nonholonomic mobile robots.

(2) *Intrinsic model uncertainty.* In some practical applications, it is difficult to obtain the exact intrinsic model for each agent. However, intrinsic model uncertainty has been less studied in distance-based formation control, even though it is a hot-spot in other control areas.

(3) *Time-varying leading velocity.* In most of existing results, the desired leading velocity is assumed to be an unknown constant vector. Thus, some efforts have been made to achieve flocking with distance-based formation control of double-integrator agents with time-varying leading velocity. Nevertheless, one important issue that remains open is to realize flocking with distance-based formation control by considering time-varying leading velocity and motion constraint or dynamic uncertainty.

1.2 Contributions

This thesis investigates two categories consensus problems: distributed output feedback consensus tracking control of multiple nonholonomic mobile robots (Chapter 3 and 4) and adaptive distance-based formation and flocking control (Chapter 5 and 6). The main contributions of this thesis are summarized as follows.

(1) Distributed output feedback consensus tracking control of multiple nonholonomic mobile robots

(i) In Chapter 3, distributed output feedback consensus tracking control is investigated for multiple nonholonomic mobile robots with directed graph in the presence of sensor faults. An adaptive-based output feedback scheme which involves estimator, observer and controller design is proposed to address the fault tolerance issue. To avoid using the global information of the communication graph, a fully distributed adaptive estimator is constructed to estimate the reference trajectory information for each robot. Moreover, to realize feedback control, an adaptive observer is constructed for each robot to estimate velocity information. Based on the estimated information from the estimator and observer, a feedback control law is developed to compress the effects of sensor faults and realize trajectory tracking. It is shown that the boundedness of all the signals in the resulting closed-loop system can be guaranteed, and the consensus tracking error of the system can converge to an adjustable neighborhood of zero by appropriately choosing design parameters even in the presence of sensor faults.

(ii) In Chapter 4, distributed output feedback consensus tracking control of multiple nonholonomic mobile robots with directed graphs is addressed by using only position information of the leader. To design the controller without using the global information of the communication graph, a fully distributed adaptive estimator is firstly constructed to estimate the position of leader for each robot. To realize feedback control and handle system uncertainty, an adaptive observer is constructed for each robot to estimate the velocity information and unknown dynamic parameters. Based on the estimated information, an adaptive observer-based output feedback controller is designed to realize tracking control. The boundedness of all the signals in the resulting closed-loop system is guaranteed. Moreover, the convergence of consensus tracking error of the system to an adjustable neighborhood of zero is established by appropriately choosing design parameters.

(2) Adaptive distance-based formation and flocking control

(i) In Chapter 5, the formation maneuvering control problem of a group of nonholonomic mobile robots is studied with the objective of having a desired formation shape described by distances between pairs of robots and an overall maneuvering velocity. The desired maneuvering velocity, which can be constant or time-varying, is only known to a set of agents. A control scheme consisting of an adaptive estimator and a modified gradient control law is proposed to solve this problem. The adaptive estimator is developed to estimate the desired maneuvering velocity in either constant or time-varying situation. Utilizing the estimated velocity, a modified gradient control law is designed based on the nonholonomic kinematic model so that the objective is achieved. Local asymptotic convergence of the overall system is guaranteed by choosing appropriate control parameters.

(ii) In Chapter 6, distributed distance-based formation and flocking control of multi-agent system with parametric uncertainty is considered. A 3-agent LFF system is considered first. The agents are supposed to have non-identical dynamics, whereas with similar structure. By introducing two new variables that involve distance error and velocity error and utilizing them in the controller design, it is shown that all agents in the formation will globally converge to the desired formation and move with the velocity of the leader. Finally, the three-agent case is inductively extended to N-agent case. The stability and the effectiveness of the proposed control scheme are analyzed in theory and demonstrated through simulation results, respectively.

1.3 Organization of the Thesis

The thesis is mainly divided into two parts: distributed output feedback consensus tracking control of multiple nonholonomic mobile robots and adaptive distance-based formation and flocking control (Chapter 5 and 6).

In Chapter 2, we review existing approaches in literature on two categories of consensus problems: distributed consensus tracking and flocking with distance-based formation control. In Chapter 3 and Chapter 4, distributed output feedback consensus tracking control is investigated for multiple nonholonomic mobile robots with directed graphs in the cases that i) sensor faults occur and ii) only position information of leader is available to a subset of follower robots. In Chapter 5 and Chapter 6, adaptive control schemes are developed to address flocking with distance-based formation control of a group of nonholonomic mobile robots with undirected graphs and a second-order multi-agent system with directed graphs and dynamic uncertainty, respectively. In Chapter 7, this thesis is summarized and recommendations for the future work are provided.

Chapter 2

Literature Review

In the past decades, consensus problem has been studied extensively in the field of cooperative control of multi-agent systems, considerable consensus approaches have been proposed. According to whether the final consensus values are predetermined, these approaches can be essentially divided into two broad categories, namely, consensus without a leader (i.e., leaderless consensus) and consensus with a leader (i.e., leader-follower consensus or distributed tracking).

In this chapter, a deep survey of the existing results on two categories control problems i) distributed consensus tracking and ii) flocking with distance-based shape control, is presented.

2.1 Distributed Consensus Tracking

The main idea behind consensus problem is to design distributed consensus protocols for multi-agent systems. As is known, consensus always focuses on the motion of multiple agents. Thus, the dynamic model of each agent should be taken into consideration when studying the consensus problem for multi-agent systems. In this section, we firstly introduce some basic concepts of graph theory and then

review distributed consensus tracking control problem for integrator type, linear, nonlinear and nonholonomic dynamics.

2.1.1 Graph Theory

Suppose that the interaction and information transmission among N agents are governed by graph $\mathcal{G} = (\mathcal{V}, \mathcal{E})$, where $\mathcal{V} = \{1, 2, \cdots, N\}$ denotes the set of vertices corresponding to each agent and $\mathcal{E} \subset \mathcal{V} \times \mathcal{V}$ is the set of edges between two distinct agents. If $\mathcal{G}$ is undirected, then the edge $(i, j) \in \mathcal{E}$ indicates that agent i and agent j can obtain information transmitted by each other. In this case, agent j is called a neighbor of agent i, and vice versa. Otherwise if the graph is directed, then the edge $(i, j) \in \mathcal{E}$ indicates that robot i is a neighbor of robot j and only robot i can obtain information from robot j. The set of neighbors of agent i is denoted as $\mathcal{N}_i = \{j \in \mathcal{V} | (i, j) \in \mathcal{E}\}$. The connectivity matrix $\mathcal{A} = [a_{ij}] \in \Re^{N \times N}$ is defined as $a_{ij} = 1$ if $(i, j) \in \mathcal{E}$ and $a_{ij} = 0$ if $(i, j) \in \mathcal{E}$. Note that $\mathcal{A}$ is symmetric for an undirected graph.An in-degree matrix $\mathcal{D} = diag(d_{ii}) \in \Re^{N \times N}$ is defined such that $d_{ii} = \sum_{j=1}^{N} a_{ij}$. Then, the Laplacian matrix of $\mathcal{G}$ is defined as $\mathcal{L} = \mathcal{D} - \mathcal{A}$.

If the graph is undirected, then $\mathcal{G}$ is connected means that there is a undirected path between any two agents. A directed graph $\mathcal{G}$ is strongly connected means that there is a directed path from each agent to each other agent. A spanning tree of a directed graph is a directed tree formed by graph edges that connect all the vertices of the graph. A directed graph has a directed spanning tree, if there is an agent called root, such that there is a directed path from the root to each other agent in the graph.

2.1.2 Integrator Type Dynamics

For consensus problem of multi-agent systems, earlier studies start with single-integrator or double-integrator dynamic systems. The distributed consensus tracking control problems for multi-agent systems with single-integrator dynamics is addressed in [8], where distributed control laws are introduced and convergence is analyzed in three cases i) directed fixed communication topologies; ii) directed switching communication topologies; and iii) undirected fixed communication topologies with time delays. In [9], by developing an identifier to estimate the unknown disturbances and unmodelled dynamics, asymptotic consensus tracking is achieved for multi-agent systems with integrator-type dynamics in the presence of disturbances and unmodelled dynamics. Under directed noisy networks without/with communication delays, leader-following consensus controllers are developed for multi-agent systems with single-integrator dynamics in [10, 11].

Note that, the results mentioned above are developed for single-integrator multi-agents systems. Since it is a fact that the single integrator dynamic model sometimes cannot well express the dynamics of a real agent, some efforts have been made to study double-integrator multi-agent systems. A consensus control scheme is proposed in [12] for double-integrator agents. Distributed finite-time consensus tracking control of multi-agent systems with double-integrator dynamics are solved in [13–16]. Specially, the presence of external disturbances is considered in [13, 14]; in [15], both fixed and switching topologies are analyzed with the aid of graph theory, matrix theory, homogeneity with dilation and LaSalle's invariance principle; while the absence of velocity measurements is addressed in [16]. A consensus algorithm is proposed in [17] to address the double-integrator leader-following problem subjects to input delay. Furthermore, a distributed event-triggered sampling approach is proposed in [18], where the double-integrator agents communicate with their neighbors via a limited communication medium .

Besides single- and double-integrator type systems, finite-time consensus problem has been extensively studied for high-order integrator systems with or without

bounded disturbances in [19, 20].

2.1.3 Linear Dynamics

Besides the simple integrator type multi-agent systems, different topics on general linear multi-agent systems have been discussed. For example, leader-follower consensus control problems are discussed in [21–28] for multi-agent systems with general linear dynamics. In [24], two distributed control schemes are developed for leader-following consensus of general linear multi-agent systems by utilizing full state feedback and output measurements, respectively. Using local information, controller design and convergence analysis is presented for both fixed and switching topologies in [23]. In [28], distributed consensus tracking control is addressed for linear multi-agent systems in the presence of bounded transmission channels, where the transmission channel bound is expressed by applying a saturation function to each channel. It is worth noting that one common feature of results in [21–28] is that the control input of the leader is assumed to be zero or available to all the followers. In some scenarios, to achieve some certain objectives, nonzero input may need to be applied on the leader. Furthermore, the input of leader may only be available to a subset of followers or may not available to any follower in some circumstances. Thus, a distributed fault-tolerant control law is designed in [29] to deal with leader-following consensus problem under undirected communication topologies against actuator faults and a dynamic leader with nonzero input. In [30], based on the assumption that the control input of leader might be nonzero, time-varying and not available to any follower and the communication network topology of the followers is governed by an undirected graph, two distributed discontinuous controllers with, respectively, static and adaptive coupling gains, are proposed to realize consensus tracking. To remove the assumption of zero control input, distributed consensus tracking control of linear multi-agent systems with directed switching topology and exogenous disturbances is investigated in [31].

It should be pointed out that the eigenvalue information of the Laplacian matrix associated with the communication topology is required to be known by each follower for the controller design in [21–31]. However, the eigenvalues of the Laplacian matrix is global information, which means the entire communication graph is required to be known by each follower in the networks to obtain such information. Therefore, these control schemes cannot be implemented by only using the local information. To address this issue, some fully distributed consensus tracking control schemes are proposed in [32–40] based on adaptive control, where the controller is designed without utilizing any global information of the communication networks. Based on the assumption that the control input of leader is zero, adaptive consensus control laws are designed in [32, 33] for multi-agent systems with undirected graphs. Adaptive consensus tracking control approaches are developed in [34, 35] for linear multi-agent systems with directed graphs and zero leader input. By assuming the reference signal is constant, an adaptive distributed control law together with an internal model are presented in [36] to achieve output tracking for unknown linear multi-agent systems under directed graphs. Based on the assumption that the control input of leader is nonzero and bounded, leader-following consensus problem of linear multi-agent systems is solved in [37, 38] with considering parametric uncertainties and external disturbances. In [39], fully consensus tracking problem is addressed for linear multi-agent systems by assuming the unknown leader input and time-varying disturbances are linearly parameterized with the basis functions being known by all agents. In [40], a fully distributed output feedback consensus control law is developed for linear multi-agent systems under directed graphs, where the nonzero control input of leader is assumed to be bounded.

2.1.4 Nonlinear Dynamics

It is worth noting that the dynamics of almost all physical systems are nonlinear in practice. Thus, besides integrator type dynamics and linear dynamics, research attention also has been put on leader-follower consensus of nonlinear multi-agent systems, which is more challenging to deal with because of its intrinsic complicated

nonlinear dynamics. The leader-follower consensus control problems of first-order nonlinear multi-agent systems are studied in [41–45]. In [43] and [45], adaptive neural networks and a fuzzy observer are respectively employed to address the system uncertainties derive from the unknown nonlinear dynamics and ensure that consensus errors are uniformly ultimately bounded.

Distributed consensus tracking control problems of second-order nonlinear multi-agent systems are studied in [46–56]. In [53], the control input of each follower is assumed to be subject to unknown nonlinear dead zone. To address this issue, an adaptive neural networks-based distributed controller is designed to guarantee the consensus errors are semi-globally uniformly ultimately bounded. In [50], assume the control input of leader is unknown to all follower agents, an adaptive distributed nonlinear controller is constructed to achieve leader-following consensus under directed communication graphs by only using relative state information between neighboring agents. In [48], to handle multiple actuator faults and time-varying dynamic uncertainties which is dependent on state and/or input, a robust fault-tolerant leader-following consensus control strategy is proposed for a class of nonlinear second-order nonlinear multi-agent systems. To avoid using the global information of the communication graph, distributed adaptive gain-design strategies are proposed in [46, 55, 56] for multi-agent systems with second-order nonlinear dynamics over undirected or directed communication topology.

Leader-follower consensus problem of multi-agent systems with high-order nonlinear dynamics also has been investigated in some works. For example, the result in [44] is extended in [57] to address finite-time consensus problem of higher-order nonlinear multi-agent systems with undirected graph based on adaptive control. In [58–62], distributed tracking control of high-order nonlinear multi-agent systems with directed communication topologies and dynamic uncertainties is studied. In [61], under the condition that the time-varying control gains of each agent are unknown and some control directions are unknown, an adaptive control strategy is designed to relax the requirement of identical unknown control directions of all the agents. It is worth pointing out that the proposed control schemes in [57–61]

can only deal with nonlinearities which in the control input channel. Technically, these schemes are not applicable for nonlinear multi-agent systems with lower triangular dynamics. Thus, distributed consensus tracking controllers are proposed in [63–70] to address such an issue. In [70], the implementation of the proposed adaptive control law requires only relative output measurements and the local information of the communication networks, thus the proposed adaptive controller is fully distributed.

Note that, most of existing works on distributed consensus control problem are developed for multi-agent systems with integer-order dynamics. However, many phenomena in nature cannot be well approximated by an integer-order dynamic model, such as food seeking of microbes and the collective motion of bacteria in lubrications perspired by themselves [71, 72]. Therefore, it is of significant importance to study the consensus problem of multi-agent systems with fractional-order dynamics. Consensus of fractional-order multi-agent systems is first investigated in [73]. Leader-following consensus control of fractional-order nonlinear multi-agent systems under undirected or directed graphs is discussed in [74–76].

2.1.5 Nonholonomic Dynamics

Due to the increasing applications of nonholonomic mobile robots in various fields, the research on distributed consensus tracking control of multiple nonholonomic mobile robots has attracted an increasing interest in recent years. Most of current research on distributed consensus tracking control problem has mainly focused on the controller design of kinematic model. In these works, it is common to transform the nonholonomic kinematic model into a chained form model by applying a group of new variables. Based on the chained form model, distributed consensus tracking control of multiple nonholonomic mobile robots with undirected or directed communication topologies is investigated in [77–84]. Based on dynamic feedback linearization, a consensus-based formation control scheme is proposed for nonholonomic mobile robots without global position measurement in [85]. Distributed

fixed-time consensus tracking control of nonholonomic chained-form systems with undirected graphs and directed graphs are respectively studied in and [78] and [84]. In [79], a switching finite-time control strategy is designed to achieve leader-following consensus under undirected graphs based on time-rescalling technique and graph theory. Based on the kinematic model and assume the desired velocities are bounded but not equal to zero, distributed finite-time tracking controllers are developed for a group of nonholonomic mobile robots to handle time-varying unknown parameters and external disturbances in [86, 87]. Finite-time consensus-based formation control of multiple nonholonomic mobile robots is considered in [88], where a distributed finite-time observer is proposed for each follower to estimate the states of leaders in a finite time.

For practical reasons, it will be a motivation to design distributed consensus tracking control algorithms for nonholonomic mobile robots with higher-order models which involves both kinematics and dynamics. Thus, the corresponding distributed consensus tracking controller is proposed in [89] for nonholonomic mobile robots with undirected graphs and partial known dynamics. In [69], distributed adaptive consensus-based formation control scheme is proposed to deal with intrinsic mismatched unknown parameters for nonholonomic mobile robots with undirected or balanced directed graph. Under general directed communication graph, distributed consensus tracking for multiple nonholonomic mobile robots is address in [90, 91]. Furthermore, due to technology limitations or cost considerations, the velocity information for a mobile robot is unavailable in some circumstances. Hence, it is meaningful in practice and worthy research to design distributed consensus tracking controller by utilizing output measurements for nonholonomic mobile robots. Distributed output feedback tracking control of nonholonomic unmanned aerial vehicles is considered in [92], where the controller is designed without linear and angular velocities measurements by introducing a state observer. In [93], to handle unavailable velocity measurements, some finite-time convergent observers are constructed to estimate both the unknown velocity information and the disturbance

in finite time. Utilizing the estimated information, a finite-time consensus control law is developed for a group of nonholonomic mobile robots under undirected communication topology.

2.2 Flocking with Distance-based Formation Control

In recent years, formation control, as a typical hot topic in cooperative control of multi-agent systems, also has attracted considerable attention. According to the variables to be controlled, the formation control problems can be categorized as position-based, displacement-based, and distance-based formation control problems [4]. In position-based formation control, the desired formation is described by desired positions with respect to global coordinate system. Global positions of agents in the group are controlled to achieve the desired formation [94, 95]. In displacement-based formation control, the desired formation is formulated by the desired relative displacements with respect to global coordinate system. Relative displacements among neighboring agents are controlled to achieve the desired formation [96–98]. Different from position- and displacement-based formation control, distance-based formation control focuses on the inter-agent distances. That is, the desired formation is formulated by the desired inter-distances between pairs of agents. Thus, the desired formation can be treated as a given rigid body, which means the desired formation is invariant to combination of translation and rotation. The inter-distances between pairs of agents are controlled to achieve the desired formation [99–101]. To achieve the desired formation shape by controlling the inter-agent distances, the interaction graph needs to be rigid or persistent as discussed in [4]. In distance-based formation control, control laws are nonlinear even if agent models are linear. Although the nonlinearity of the proposed control laws complicates the stability analysis of the multi-agent system, much effort has been made in this research area. Utilizing relative position obtained in the local frames

instead of global position information in controller design, gradient descent controllers have been widely used to address distance-based formation control problem in [99–104].

In some practical applications, such as moving target enclosure, source seeking and maneuvering of autonomous vehicles [105–107], one may want to achieve both objectives of formation shape control and sharing a common velocity. Thus, another control problem of multi-agent systems arises when it is required to maintain the desired formation shape and achieve velocity consensus for all agents in the formation simultaneously. This control problem is referred as flocking with distance-based formation control, in which the interaction graphs involve velocity consensus graph and formation shape graph. We review flocking with distance-based formation control under undirected and directed formation shape graphs in the following,.

2.2.1 Undirected Graph

In the case that the formation shape graph of a multi-agent system is undirected, the requirement on the interaction graph is characterized by rigidity [108]. Suppose the undirected graphs for velocity consensus and formation shape control are the same, and assume this undirected interaction graph is minimally and infinitesimally rigid, flocking with distance-based formation control problem is addressed in [109] for a group of agents with double-integrator dynamics. With the proposed gradient descent control law, it is shown that local asymptotic convergence to the desired formation shape is established and the final velocities of all agents can converge to the average of the initial velocities of the agents. Under the same assumption, local finite time convergence for the flocking of the desired formation shape is guaranteed in [110, 111]. In [2, 112], consider the general case where the graphs for velocity consensus and formation shape control can be different, assume the undirected formation shape graph is rigid, flocking with distance-based formation control is studied for double-integrator agents with undirected and directed velocity

consensus graphs, respectively. Furthermore, in this work, the cases that there is a leader or a group of leaders in the velocity consensus and formation shape graph are investigated when both two graphs are undirected. It is needed to point out that in [2, 109–112], the velocities of all agents converge to a constant value, which may limit the application of the proposed control schemes. Thus, in [113], consider a group of n agents modeled by single integrator dynamics and assume the desired velocity is available to only a subset of agents, observer-based control schemes are proposed to drive all the agents to maintain the desired formation shape while moving with the desired translational velocity. In the proposed control schemes, two different observers are designed to estimate the constant and time-varying reference velocity for each agent, respectively.

2.2.2 Directed Graph

In the case that the formation shape graph of a multi-agent system is directed, the requirement on the interaction graph is characterized by persistence [114]. Analogous to minimally rigid graph, minimal persistent graph is studied widely in the distance-based formation control under directed graphs. Note that, any minimally persistent formations belong to one of leader-first-follower, leader-remote-follower (LRF), or co-leader-follower [115]. Thus, most of existing works on flocking with distance-based formation control under directed graphs are studied based on these three types of formations.

Focus on the case that there are two leaders and one follower which are all governed by single integrator dynamics, and assume the constant reference velocity is available to leaders but unavailable to follower, flocking with distance-based formation control is addressed in [116–118]. Based on adaptive control, the proposed control schemes enable all the agents in the group to form a desired formation shape and to maintain the desired moving velocity by employing an adaptive law to estimate the reference velocity. Furthermore, in [116, 117], the proposed control law is generalized to a N-agent case. In [1, 119], assume the unknown velocity of

leader is constant, distributed formation control laws are developed for the multi-agent systems with LFF formation. Additionally, the three-agent LFF case is extended to N-agent case by an inductive way in [1]. Note that, in [1, 116–119], the reference velocity is assumed to be constant and all the agents are modeled by single integrator dynamics. As mentioned in last section, the control algorithms ensure that the velocities of all agents converge to a time-varying value may have a wider applications. Furthermore, it is worthy noting that extension of distributed formation control algorithms from the first-order case to the second-order case is nontrivial even in the linear formation control as shown in [12]. Thus, in [120], suppose the desired formation is co-leader type and all agents are modeled by double integrators, a backstepping controller is proposed to ensure that all agents in the formation maintain the desired formation shape and move with a common velocity. In the proposed control algorithm, the reference velocity can be time-varying but is assumed to be known by all agents.

Chapter 3

Distributed Output Feedback Consensus Tracking Control of Multiple Nonholonomic Mobile Robots with Directed Communication Graph and Sensor Faults

In this chapter, we address the issue of distributed output feedback consensus tracking control for multiple nonholonomic mobile robots with directed graph in the presence of sensor faults, by developing an adaptive-based fault tolerant scheme consisting of a fully distributed adaptive estimator and an observer-based output feedback controller. The controller design involves three steps. Firstly, a fully distributed adaptive estimator is constructed to estimate the reference trajectory information for each robot. Secondly, to realize feedback control, an adaptive observer is designed for each robot to estimate velocity information. Thirdly, utilizing the estimated information from the estimator and observer, a feedback control law

is designed based on backstepping technique to compress the effects of sensor faults and realize decentralized trajectory tracking control. Consequently, the main contributions and novelty of this paper are summarized as follows:

- To the best of our knowledge, this is the first sensor fault tolerant method for distributed consensus tracking control of multiple nonholonomic mobile robots with directed communication topology.
- A fully distributed adaptive estimator is constructed to estimate the reference trajectory information without using the global information of communication networks topology.
- The boundedness of all the signals in the resulting closed-loop system are ensured. The consensus tracking error of the system can converge to an adjustable neighborhood of zero by appropriately choosing design parameters.

3.1 Problem Formulation

Consider a group of N Type(2,0) wheeled mobile robots (WMRs) which is composed of two driving wheels and one passive wheel. The posture of a WMR in Catesian coordinates is described in Figure 3.1. The mass of centre is located at C, the midpoint of the axis between two wheels is P. Taking the actuator into account, the kinematic and dynamic models of the WMR can be given as follows [121],

$$\dot{q}_i = S\left(q_i\right)\eta_i \tag{3.1}$$

$$\bar{M}_i\dot{\eta}_i + \bar{V}\left(q_i, \dot{q}_i\right)\eta_i + \bar{\tau}_{d,i} = \frac{n_i K_{T,i}}{R_{a,i}}\bar{B}_i u_i - \frac{n_i^2 K_{T,i}K_{b,i}}{R_{a,i}}\bar{B}_i\bar{B}_i^T\eta_i \tag{3.2}$$

where $i = 1, \cdots, N$, $q_i = [x_i, y_i, \phi_i]^T$; $p_i = [x_i, y_i]^T$ is the position of the centre of mass C and ϕ_i is the orientation of robot i. $\eta_i = [v_i, \omega_i]^T$ where v_i and ω_i are the linear and angular velocity respectively, u_i is the input voltage, $\bar{\tau}_{d,i}$ represents the external disturbance. n_i is the gear ratio, $K_{T,i}$ is the motor torque constant, $K_{b,i}$ is the counter electromotive force coefficient, and $R_{a,i}$ is the electric resistance.

$$S(q_i) = \begin{bmatrix} \cos\phi_i & -a_i \sin\phi_i \\ \sin\phi_i & a_i \cos\phi_i \\ 0 & 1 \end{bmatrix}, \ \bar{M}_i = \begin{bmatrix} m_i & 0 \\ 0 & I_{m,i} - m_i a_i^2 \end{bmatrix},$$

$$\bar{V}(q_i, \dot{q}_i) = \begin{bmatrix} 0 & 0 \\ 0 & 0 \end{bmatrix}, \ \bar{B}_i = \tfrac{1}{r_i} \begin{bmatrix} 1 & 1 \\ b_i & -b_i \end{bmatrix}.$$

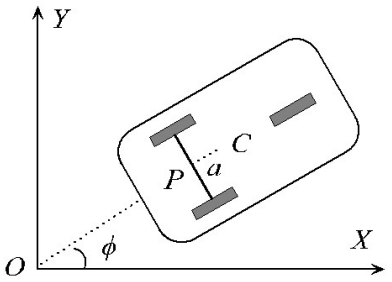

FIGURE 3.1: A type(2,0) wheeled mobile robot.

In these expressions, m_i is the mass of the robot, $I_{m,i}$ is the moment of inertia, b_i is the half width of axis between two wheels and r_i is the radius of each wheel, a_i is the distance between C and P.

In this chapter, multiplicative sensor failures are considered for the position measurement p_i of each robot. The failures that may occur on the position sensor in system (1) at the time are modeled as

$$\bar{p}_i(t) = \rho_i(t) p_i(t), \ \rho_i(t) = \begin{bmatrix} \rho_{i,x}(t) & 0 \\ 0 & \rho_{i,y}(t) \end{bmatrix}. \tag{3.3}$$

where $\rho_{i,x}$ and $\rho_{i,y}$ represent the sensor gain of position measurement x_i and y_i. Sensor fault occurs if $\rho_{i,x}(\rho_{i,y}) \neq 1$, otherwise senor works formally.

Suppose that the interaction and information transmission among the N WMRs are governed by a directed graph $\mathcal{G}$ and the virtual leader moves along predefined trajectory $p_r(t) = [x_r(t), y_r(t)]^T$. We use $\mu_i = 1$ to indicate that robot i has access to the reference trajectory information $p_r(t)$; otherwise, $\mu_i = 0$.

Assume the reference trajectory information is represented by a virtual leader labeled by 0. The control objective is, while only part of the robots in the group

have access to the leader, to design distributed control input u_i for each robot by utilizing only locally available information obtained from the intrinsic robot and its neighbors such that

- All the signals in the resulting closed-loop system are globally uniformly bounded;
- For each robot, the measured tracking error $\|\bar{p}_i - p_r\|$ can converge to an adjustable neighborhood of zero.

To achieve the above mentioned objectives,the following assumptions are imposed.

Assumption 3.1. The first 2nd-order derivatives of reference trajectory $p_r(t)$ are bounded and piecewise continuous, and there exists a constant vector such that $|\ddot{x}_r(t)| \leq \sigma_1$ and $|\ddot{y}_r(t)| \leq \sigma_2$. Thus, $\sigma = [\sigma_1, \sigma_2]^T$ is available to robot i if $\mu_i = 1$.

Note that the virtual leader can also be nonholonomic, as long as it is driven to move along a predefined trajectory $p_r(t)$ which satisfies Assumption 1.

Assumption 3.2. The directed graph contains a spanning tree with the root being the leader.

Assumption 3.3. The unknown external disturbances $\bar{\tau}_{i,d}$ are bounded.

Assumption 3.4. $\rho_{i,x}$ ($\rho_{i,y}$) and $\dot{\rho}_{i,x}$ ($\dot{\rho}_{i,y}$) are bounded, and there exist unknown constants ρ_{min} and ρ_{min} such that $0 < \rho_{min} \leq \rho_{i,x}, \rho_{i,y} \leq \rho_{max}$.

To develop and analyze the proposed control scheme, the following lemmas are then introduced.

Lemma 3.1 ([122])**.** Under Assumption 3.2, the matrix $H = \mathcal{L} + \mu$ is a positive matrix, where $\mu = diag(\mu_1, \mu_2, \cdots, \mu_N)$. Define

$$\theta = [\theta_1, \theta_2, \cdots, \theta_N]^T = H^{-1} 1_N$$

$$\Theta = diag\left\{\frac{1}{\theta_1}, \frac{1}{\theta_2}, \cdots, \frac{1}{\theta_N}\right\}$$
$$W = \Theta H + H^T\Theta \tag{3.4}$$

Then $\theta_i > 0$ for $i = 1, 2, \cdots, N$ and W is a positive definite matrix.

Lemma 3.2 ([123])**.** Given any real-valued continuous function $f(\alpha, \beta) \in \mathbb{R}^m$ with $\alpha \in \mathbb{R}^{m_\alpha}$ and $\beta \in \mathbb{R}^{m_\beta}$, there exist a smooth scalar function $f_1(\alpha) \geq 0$ and a continuous scalar function $f_2(\beta) \geq 0$ such that $\|f(\alpha, \beta)\| \leq f_1(\alpha) f_2(\beta)$.

Lemma 3.3 ([124])**.** For any scalars $\epsilon > 0$ and $z \in \mathbb{R}$, the following relationship holds: $0 \leq |z| - \frac{z^2}{\sqrt{z^2+\epsilon^2}} < \epsilon$.

3.2 Controller Design

Under Assumption 3.2, in most existing works, to realize consensus tracking control in the absence of sensor faults, the error variable $s_i = \sum a_{ij}(p_i - p_j) + \mu_i(p_i - p_r)$ is usually utilized to design control input to ensure $s_i \to 0$. Since $s = H(p - 1_N \otimes p_0)$ and H is nonsingular, then $s_i \to 0 \Rightarrow p_i \to p_0$, which means consensus tracking control will be achieved. However, when sensor faults occur, each robot can only obtain that

$$\bar{s}_i = \sum a_{ij}(\rho_i p_i - \rho_j p_j) + \mu_i(\rho_i p_i - p_r). \tag{3.5}$$

In this case, the effects of sensor faults of itself and its neighbors needs to be compressed in controller design for each robot. Hence, to address our issue, a fully distributed adaptive estimator is firstly introduced to estimate the states of the leader. Based on the estimated states, a decentralized observer-based output feedback controller is developed to compress the effects of sensor faults and achieve trajectory tracking control for the whole group.

3.2.1 Estimator design

Firstly, the reference trajectory is represented by a virtual leader expressed by the following dynamic model,

$$\dot{r}_0 = Ar_0 + Bv_0 \tag{3.6}$$

where $r_0 = \left[p_r^T, \dot{p}_r^T\right]^T$, $v_0 = \ddot{p}_r$,

$$A = \begin{bmatrix} 0_2 & I_2 \\ 0_2 & 0_2 \end{bmatrix}, \quad B = \begin{bmatrix} 0_2 \\ I_2 \end{bmatrix}.$$

Based on the information transmission among neighbors, the following fully distributed adaptive estimator is introduced to estimate the states of leader for each robot,

$$\begin{aligned} \dot{r}_i &= Ar_i + Bv_i \\ v_i &= -\left(c_i + \beta_i\right) Ks_i - \mathrm{diag}(sgn\left(Ks_i\right))\hat{\sigma}_i \\ \dot{c}_i &= s_i^T PBB^T Ps_i \\ \dot{\hat{\sigma}}_i &= -\sum_{j=1}^{N} a_{ij}\left(\hat{\sigma}_i - \hat{\sigma}_j\right) - \mu_i\left(\hat{\sigma}_i - \sigma\right) \end{aligned} \tag{3.7}$$

where $r_i = [r_{i,1}^T, r_{i,2}^T]^T$, $s_i = \sum_{j=1}^{N} a_{ij}\left(r_i - r_j\right) + \mu_i\left(r_i - r_0\right)$, $\hat{\sigma}_i$ is the estimation of σ of robot i, gain matrix $K = B^T P$ and $\beta_i = s_i^T Ps_i$ with $P > 0$.

Define the estimation errors as $\tilde{r}_i = r_i - r_0$ and $\tilde{\sigma} = \hat{\sigma}_i - \sigma$. Let $\tilde{r} = \left[\tilde{r}_1^T, \cdots, \tilde{r}_N^T\right]^T$ and $s = \left[s_1^T, \cdots, s_N^T\right]^T$, then $s = \left(H \otimes I_4\right)\tilde{r}$. From (3.6) and (3.7), the estimation error dynamics can be given as,

$$\begin{aligned} \dot{\tilde{r}}_i &= A\tilde{r}_i + B\left(v_i - v_0\right) \\ &= A\tilde{r}_i - \left(c_i + \beta_i\right) Ks_i - \mathrm{diag}\left(sig\left(Ks_i\right)\right)\hat{\sigma}_i - Bv_0 \end{aligned} \tag{3.8}$$

Theorem 3.1. Suppose that Assumptions 3.1 and 3.2 hold. Then the estimation error $\tilde{r}$ and the adaptive gains c_i, $i = 1, 2, \cdots, N$ are bounded if K and $P > 0$

satisfy the following linear matrix inequality

$$AP^{-1} + P^{-1}A^T - 2BB^T < 0. \tag{3.9}$$

Moreover, $\tilde{r}$ and $\tilde{\sigma}$ asymptotically converges to zero, i.e. $\lim_{t\to 0}\|\tilde{r}\| = \lim_{t\to 0}\|\tilde{\sigma}\| = 0$.

Proof. The proof of Theorem 3.1 is given in Appendix. □

Remark 3.1. Note that, the designed adaptive estimator (3.7) is independent of any global information of the communication graph, thus it is fully distributed. The estimator design is motivated by the distributed consensus controller proposed in [40]. However, σ is assumed to be known by all the agents in [40]. In this chapter, σ is only available by a subset of robots and will be estimated by adaptive control for the rest robots that cannot access the reference trajectory.

Remark 3.2. Utilizing the estimated trajectory information r_i as the reference trajectory for each robot, the consensus tracking problem for a group of WMRs can be transformed into decentralized trajectory tracking control of WMRs, which makes it possible to individually compress the effects of sensor faults for each robot.

3.2.2 Observer design

In this chapter, velocity measurements η_i are unavailable, thus to design observer to estimate η_i, the system models in (3.1) and (3.2) are rewritten as follows,

$$\begin{aligned} \dot{p}_i &= J_i\eta_i \\ \dot{\phi}_i &= \omega_i \\ \dot{\eta}_i &= -R_i\eta_i + B_iu_i + \tau_{d,i} \end{aligned} \tag{3.10}$$

where

$$J_i = \begin{bmatrix} \cos\phi_i & -a_i\sin\phi_i \\ \sin\phi_i & a_i\cos\phi_i \end{bmatrix}, \quad R_i = \frac{2n_iK_{T,i}K_{b,i}}{R_{a,i}r_i^2}\begin{bmatrix} 1/m_i & 0 \\ 0 & b_i^2/\left(I_{m,i} - m_ia_i^2\right) \end{bmatrix},$$

$$B_i = \frac{n_i K_{T,i}}{R_{a,i} r_i} \begin{bmatrix} 1/m_i & 0 \\ 0 & b_i^2/\left(I_i - m_i a_i^2\right) \end{bmatrix}, \quad \tau_{d,i} = \bar{M}_i^{-1} \bar{\tau}_{d,i}.$$

The observer is designed for (3.10) as follows,

$$\begin{aligned} \dot{\hat{p}}_i &= J_i \hat{\eta}_i + L_{i,1} \left(\bar{p}_i - \hat{p}_i\right) \\ \dot{\hat{\eta}}_i &= -R_i \hat{\eta}_i + B_i u_i + L_{i,2} J_i^T \left(\bar{p}_i - \hat{p}_i\right) \end{aligned} \tag{3.11}$$

where $\hat{p}_i$ and $\hat{\eta}_i$ are the estimations of p_i and η_i, respectively. $L_{i,1}$ and $L_{i,2}$ are observer gain matrices.

Define the observer errors as $\tilde{p}_i = p_i - \hat{p}_i$ and $\tilde{\eta}_i = \eta_i - \hat{\eta}_i$. Let $\tilde{e}_i = \left[\tilde{p}_i^T, \tilde{\eta}_i^T\right]^T$. Then from (3.10) and (3.11), the dynamics of observer error can be expressed as,

$$\dot{\tilde{e}}_i = A_i^c \tilde{e}_i + L_i \left(\rho_i^{-1} - I_2\right) \bar{p}_i + d_i \tag{3.12}$$

where

$$A_i^c = \begin{bmatrix} -L_{i,1} & J_i \\ -L_{i,2} J_i^T & -R_i \end{bmatrix}, \; L_i = \begin{bmatrix} L_{i,1} \\ L_{i,2} J_i^T \end{bmatrix}, \; d_i = \begin{bmatrix} 0_2 \\ \tau_{i,d} \end{bmatrix}.$$

The observer gain matrices $L_{i,1}$ and $L_{i,2}$ are chosen such that A_i^c is Hurwitz. Then $\tilde{e}_i$ can be directly calculated based on (3.11) as

$$\tilde{e}_i\left(t\right) = \underbrace{e^{A_i^c t} \tilde{e}_i\left(0\right)}_{e_{ai}} + \underbrace{\int_0^t e^{A_i^c (t-\tau)} \left[L_i \left(\rho_i^{-1} - I\right) \bar{p}_i + d_i\right] d\tau}_{e_{bi}} \tag{3.13}$$

Since A_i^c is Hurwitz, there exist known constants $\varrho_{i,1} \geq 1$ and $\varrho_{i,2} > 0$ such that

$$\| E_2 e^{A_i^c t} \| \leq \varrho_{i,1} e^{-\varrho_{i,2} t}, \; \forall t \geq 0 \tag{3.14}$$

where $E_2 = [0_2, I_2]^T$.

From Lemma 2, there exit a smooth function $f_1(\bar{p}_i) \geq 0$ and a continuous function $f_2(\rho_i) \geq 0$ such that

$$\|L_i\left(\rho_i^{-1} - I\right)\bar{p}_i\| \leq f_1\left(\bar{p}_i\right) f_2\left(\rho_i\right). \tag{3.15}$$

Define $\vartheta_0 = \underset{t\geq 0}{sup}\|\rho_i J_i\|$ and

$$\vartheta_{i,1} = \max\left\{\underset{t\geq 0}{sup}\vartheta_0\varrho_{i,1}\|d_i\left(t\right)\|, \underset{t\geq 0}{sup}\vartheta_0\varrho_{i,1}f_2\left(\rho_i\right)\right\}.$$

Let $e_{ai} = \left[e_{ai,1}^T, e_{ai,2}^T\right]^T$ and $e_{bi} = \left[e_{bi,1}^T, e_{bi,2}^T\right]^T$. Then, from (3.10), (3.11) and (3.13), the time derivative of $\bar{p}_i$ can be expressed as

$$\begin{aligned}\dot{\bar{p}}_i =& \dot{\rho}_i\rho_i^{-1}\bar{p}_i + \rho_i J_i\eta_i \\ =& \dot{\rho}_i\rho_i^{-1}\bar{p}_i + \rho_i J_i\hat{\eta}_i + \bar{e}_{ai,2} + \bar{e}_{bi,2}\end{aligned} \tag{3.16}$$

where $\bar{e}_{ai,2} = \rho_i J_i e_{ai,2}$ and $\bar{e}_{bi,2} = \rho_i J_i e_{bi,2}$. Based on (3.13)-(3.15), we have

$$\begin{aligned}&\|\rho_i J_i e_{bi,2}\| \\ &\leq \|\rho_i J_i\|\int_0^t \|E_2 e^{A_i^c(t-\tau)}\|\left(f_1\left(\bar{p}_i\right) f_2\left(L_i, \rho_i\right) + \|d_i\left(t\right)\|\right)d\tau \\ &\leq \vartheta_{i,1}\int_0^t e^{-\varrho_{i,2}(t-\tau)}\left(f_1\left(\bar{p}_i\right) + 1\right)d\tau\end{aligned} \tag{3.17}$$

Construct an auxiliary filter as follows,

$$\dot{\varsigma}_i = -\varrho_{i,2}\varsigma_i + f_1\left(\bar{p}_i\right) + 1, \quad \varsigma_i\left(0\right) \geq 0. \tag{3.18}$$

Then $\varsigma_i\left(t\right)$ can be calculated as,

$$\varsigma_i\left(t\right) = e^{-\varrho_{i,2}t}\varsigma_i\left(0\right) + \int_0^t e^{-\varrho_{i,2}(t-\tau)}\left(f_1\left(\bar{p}_i\right) + 1\right)d\tau. \tag{3.19}$$

Since $\varsigma_i\left(0\right) \geq 0$, we can have

$$\|\rho_i J_i e_{bi,2}\| \leq \vartheta_{i,1}\varsigma_i. \tag{3.20}$$

3.2.3 Controller design

Based the estimated states r_i from (3.11), an observer-based failure tolerating control law will be designed by using backstepping technique to realize trajectory tracking control for each robot. Firstly, we define

$$z_i^r = p_i - r_{i,1},\ z_{i,1} = \bar{p}_i - r_{i,1},\ z_{i,2} = \hat{\eta}_i - \eta_i^c. \tag{3.21}$$

where z_i^r and $z_{i,1}$ are the real and the measured tracking errors, respectively, and η_i^c is the virtual command to be designed for η_i.

Based on (3.10), (3.13) and (3.21), the time derivative of $z_{i,1}$ can be expressed as

$$\begin{aligned}\rho_i^{-1}\dot{z}_{i,1} = J_i\left(\eta_i^c + z_{i,2}\right) - \alpha_1\rho_i^{-1}z_{i,1} - 0.5\dot{\rho}_i^{-1}z_{i,1} \\ +\Xi_{i,1}\chi_{i,1} + \rho_i^{-1}\bar{e}_{ai,2} + \rho_i^{-1}\bar{e}_{bi,2}\end{aligned} \tag{3.22}$$

where $\Xi_{i,1} = \left[\rho_i^{-1}\dot{\rho}_i\rho_i^{-1}, \rho_i^{-1}, \dot{\rho}_i^{-1}\right]$ and $\chi_{i,1} = [\bar{p}_i^T, \alpha_1 z_{i,1}^T - r_{i,2}^T, 0.5z_{i,1}^T]^T$.

Noting that $\Xi_{i,1}$ is bounded, define

$$\vartheta_{i,2} = \max\left\{\sup_{t\geq 0}\|\Xi_{i,1}\|, \sup_{t\geq 0}\|\rho_i^{-1}\|, \sup_{t\geq 0}\vartheta_{i,1}\|\rho_i^{-1}\|\right\} \tag{3.23}$$

Considering (3.20) and (3.23) and applying Lemma 3, it can be obtained that

$$\begin{aligned}z_{i,1}^T\Xi_{i,1}\chi_{i,1} + z_{i,1}^T\rho_i^{-1}\bar{e}_{bi,2} &\leq \vartheta_{i,2}\|z_{i,1}\|\left(\|\chi_{i,1}\| + \varsigma_i\right) \\ &\leq \vartheta_{i,2}\|z_{i,1}\|\sqrt{2\chi_{i,1}^T\chi_{i,1} + 2\varsigma_i^2} \\ &\leq \vartheta_{i,2}\varphi_{i,2}z_{i,1}^T z_{i,1} + \epsilon_2\vartheta_{i,2}\end{aligned} \tag{3.24}$$

where $\varphi_{i,2} = \frac{2\chi_{i,1}^T\chi_{i,1}+2\varsigma_i^2}{\sqrt{\left(2\chi_{i,1}^T\chi_{i,1}+2\varsigma_i^2\right)z_{i,1}^T z_{i,1}+\epsilon_2^2}}$. Also utilizing Young's inequality yields

$$z_{i,1}^T\rho_i^{-1}\bar{e}_{ai,2} \leq \alpha_1 z_{i,1}^T\rho_i^{-1}z_{i,1} + \Delta_{i,1} \tag{3.25}$$

where $\Delta_{i,1} = \frac{1}{4\alpha_1}e_{ai,2}^T\rho_i^{-1}\bar{e}_{ai,2}$.

Then to use Lyapunov stability theory, consider the following Lyapunov function

$$V_{i,1} = \frac{1}{2} z_{i,1}^T \rho_i^{-1} z_{i,1} + \frac{1}{2\gamma_{i,2}} \tilde{\vartheta}_{i,2}^2 \tag{3.26}$$

where $\gamma_{i,2} > 0$ is a design parameter, $\tilde{\vartheta}_{i,2} = \vartheta_{i,2} - \hat{\vartheta}_{i,2}$ with $\hat{\vartheta}_{i,2}$ being the estimation of $\vartheta_{i,2}$.

From (3.22) and (3.24), the time derivative of $V_{i,1}$ can be computed as

$$\begin{aligned} \dot{V}_{i,1} &= z_{i,1}^T \rho_i^{-1} \dot{z}_{i,1} + \frac{1}{2} z_{i,1}^T \dot{\rho}_i^{-1} z_{i,1} + \frac{1}{\gamma_{i,2}} \tilde{\vartheta}_{i,2} \dot{\tilde{\vartheta}}_{i,2} \\ &= z_{i,1}^T J_i \left(\eta_i^c + z_{i,2} \right) - \alpha_1 z_{i,1}^T \rho_i^{-1} z_{i,1} + z_{i,1}^T \Xi_{i,1} \chi_{i,1} \\ &+ z_{i,1}^T \rho_i^{-1} \bar{e}_{ai,2} + z_{i,1}^T \rho_i^{-1} \bar{e}_{bi,2} - \frac{1}{\gamma_{i,2}} \tilde{\vartheta}_{i,2} \dot{\hat{\vartheta}}_{i,2} \\ &\leq z_{i,1}^T J_i \left(\eta_i^c + z_{i,2} \right) + \vartheta_{i,2} \varphi_{i,2} z_{i,1}^T z_{i,1} + \epsilon_1 \vartheta_{i,2} \\ &+ \Delta_{i,1} - \frac{1}{\gamma_{i,2}} \tilde{\vartheta}_{i,2} \dot{\hat{\vartheta}}_{i,2} \end{aligned} . \tag{3.27}$$

Design the virtual command η_i^c and the adaptive law of $\hat{\vartheta}_{i,2}$ as

$$\eta_i^c = J_i^{-1} \left(-k_1 - \hat{\vartheta}_{i,2} \varphi_{i,2} \right) z_{i,1} \tag{3.28}$$

$$\dot{\hat{\vartheta}}_{i,2} = \gamma_{i,2} \varphi_{i,2} z_{i,1}^T z_{i,1} - \delta_{i,2} \hat{\vartheta}_{i,2} \tag{3.29}$$

where k_1 and $\delta_{i,2}$ are positive design parameters.

Substituting (3.28)-(3.29) into (3.27) results in

$$\dot{V}_{i,1} \leq -k_1 z_{i,1}^T z_{i,1} + z_{i,1}^T J_i z_{i,2} + \frac{\delta_{i,2}}{\gamma_{i,2}} \tilde{\vartheta}_{i,2} \hat{\vartheta}_{i,2} + \Delta_{i,1} + \epsilon_2 \vartheta_{i,2}. \tag{3.30}$$

Then we need to design control input u_i such that $\hat{\eta}_i$ will follow the virtual command η_i^c, i.e., stabilize the dynamic of error $z_{i,2}$. From (3.11) and (3.16), we have

$$\begin{aligned} \dot{z}_{i,2} &= \dot{\hat{\eta}}_i - \dot{\eta}_i^c \\ &= B_i u_i + g_i - h_{i,1} \Xi_{i,2} \chi_{i,2} - h_{i,2} \left(\bar{e}_{ai,2} + \bar{e}_{bi,2} \right) \end{aligned} \tag{3.31}$$

where $g_i = L_{i,2}J_i^T(\bar{p}_i - \hat{p}_i) - R_i\hat{\eta}_i - \frac{\partial\eta_i^c}{\partial\chi_{i,3}}\dot{\chi}_{i,3} - \frac{\partial\eta_i^c}{\partial\phi_i}e_2^T\hat{\eta}_i$ with $\chi_{i,3} = [r_{i,1}^T, r_{i,2}^T, \hat{\vartheta}_{i,2}, \varsigma_i]^T$, $e_2 = [0,1]^T$, $\Xi_{i,2} = [\dot{\rho}_i\rho_i^{-1}, \rho_i]$, $\chi_{i,2} = [\bar{p}_i^T, (J_i\hat{\eta}_i)^T]^T$, $h_{i,1} = \frac{\partial\eta_i^c}{\partial\bar{p}_i}$ and $h_{i,2} = \frac{\partial\eta_i^c}{\partial\bar{p}_i} + \frac{\partial\eta_i^c}{\partial\phi_i}e_2^T$.

Define $\vartheta_{i,3} = \underset{t\geq 0}{sup}\|\Xi_{i,2}(t)\|$ and choose another Lyapunov function

$$V_{i,2} = V_{i,1} + \frac{1}{2}z_{i,2}^T z_{i,2} + \frac{1}{2\gamma_{i,1}}\tilde{\vartheta}_{i,1}^2 + \frac{1}{2\gamma_{i,3}}\tilde{\vartheta}_{i,3}^2 \tag{3.32}$$

where $\gamma_{i,1}$ and $\gamma_{i,3}$ are positive design parameters, $\tilde{\vartheta}_{i,\kappa} = \vartheta_{i,\kappa} - \hat{\vartheta}_{i,\kappa}, \kappa = 1,3$ with $\hat{\vartheta}_{i,\kappa}$ being the estimation of $\vartheta_{i,\kappa}$. Utilizing Young's inequality again, we can have

$$-z_{i,2}^T h_{i,1}\Xi_{i,2}\chi_{i,2} \leq \vartheta_{i,3}\varphi_{i,3}z_{i,2}^T h_{i,1}h_{i,1}^T z_{i,2} + \epsilon_3\vartheta_{i,3} \tag{3.33}$$

$$-z_{i,2}^T h_{i,2}\bar{e}_{bi,2} \leq \vartheta_{i,1}\varphi_{i,1}z_{i,2}^T h_{i,2}h_{i,2}^T z_{i,2} + \epsilon_1\vartheta_{i,1} \tag{3.34}$$

$$-z_{i,2}^T h_{i,2}\bar{e}_{ai,2} \leq \alpha_2 z_{i,2}^T h_{i,2}h_{i,2}^T z_{i,2} + \Delta_{i,2} \tag{3.35}$$

where $\varphi_{i,3} = \frac{\chi_{i,2}^T\chi_{i,2}}{\sqrt{z_{i,2}^T h_{i,1}h_{i,1}^T z_{i,2}\chi_{i,2}^T\chi_{i,2} + \epsilon_3^2}}$,

$\varphi_{i,1} = \frac{\varsigma_i^2}{\sqrt{z_{i,2}^T h_{i,1}h_{i,1}^T z_{i,2}\varsigma_i^2 + \epsilon_1^2}}$ and $\Delta_{i,2} = \frac{1}{4\alpha_2}e_{ai,2}^T\bar{e}_{ai,2}$.

Taking (3.33) - (3.35) into consideration, we can get the time derivative of $V_{i,2}$ as

$$\begin{aligned}\dot{V}_{i,2} &= \dot{V}_{i,1} + z_{i,2}^T\dot{z}_{i,2} + \frac{1}{\gamma_{i,1}}\tilde{\vartheta}_{i,1}\dot{\tilde{\vartheta}}_{i,1} + \frac{1}{\gamma_{i,3}}\tilde{\vartheta}_{i,3}\dot{\tilde{\vartheta}}_{i,3} \\ &\leq \dot{V}_{i,1} + z_{i,2}^T B_i u_i + z_{i,2}^T g_i + \vartheta_{i,3}\varphi_{i,3}z_{i,2}^T h_{i,1}h_{i,1}^T z_{i,2} \\ &+\vartheta_{i,1}\varphi_{i,1}z_{i,2}^T h_{i,2}h_{i,2}^T z_{i,2} + \alpha_2 z_{i,2}^T h_{i,2}h_{i,2}^T z_{i,2} + \Delta_{i,2} \\ &-\frac{1}{\gamma_{i,1}}\tilde{\vartheta}_{i,1}\dot{\hat{\vartheta}}_{i,1} - \frac{1}{\gamma_{i,3}}\tilde{\vartheta}_{i,3}\dot{\hat{\vartheta}}_{i,3} + \epsilon_1\vartheta_{i,1} + \epsilon_3\vartheta_{i,3}\end{aligned} \tag{3.36}$$

Then design the control input u_i and the adaptive law for $\hat{\vartheta}_{i,1}$ and $\hat{\vartheta}_{i,3}$ as

$$\begin{aligned}u_i = B_i^{-1}(&-k_2 z_{i,2} - J_i^T z_{i,2} - g_{i,2} - \alpha_2 h_{i,2}h_{i,2}^T z_{i,2} \\ &- \vartheta_{i,3}\varphi_{i,3}h_{i,1}h_{i,1}^T z_{i,2} - \vartheta_{i,1}\varphi_{i,1}h_{i,2}h_{i,2}^T z_{i,2})\end{aligned} \tag{3.37}$$

$$\dot{\hat{\vartheta}}_{i,3} = \gamma_{i,3}\varphi_{i,3}z_{i,2}^T h_{i,1}h_{i,1}^T z_{i,2} - \delta_{i,3}\hat{\vartheta}_{i,3} \tag{3.38}$$

$$\dot{\hat{\vartheta}}_{i,1} = \gamma_{i,1}\varphi_{i,1}z_{i,2}^T h_{i,2}h_{i,2}^T z_{i,2} - \delta_{i,1}\hat{\vartheta}_{i,1} \tag{3.39}$$

where k_2, $\delta_{i,1}$ and $\delta_{i,3}$ are positive design parameters. Substituting (3.37)-(3.39) into (3.36) results in

$$\dot{V}_{i,2} \leq -k_1 z_{i,1}^T z_{i,1} - k_2 z_{i,2}^T z_{i,2} - \sum_{k=1}^{3} \frac{\delta_{i,k}}{2\gamma_{i,k}}\tilde{\vartheta}_{i,k}^2 + \Delta_i + \Omega_i \tag{3.40}$$

where $\Delta_i = \Delta_{i,1} + \Delta_{i,2}$ and $\Omega_i = \sum_{\kappa=1}^{3}\left(\frac{\delta_{i,\kappa}}{2\gamma_{i,\kappa}}\vartheta_{i,\kappa}^2 + \epsilon_\kappa\vartheta_{i,\kappa}\right)$.

Now we are in the position to present our tracking results, as summarized in the following theorem.

Theorem 3.2. With the application of the observer (3.11) and the controller (3.37) to the system modelled in (3.1) and (3.2), the boundedness of all the signals in the resulting closed-loop system is guaranteed even in the presence of sensor faults (3.3). Furthermore, it ensures that $\|\bar{p}_i - p_r\|$ will converge to a set which is adjustable by appropriately choosing design parameters.

Proof. Let $C_i = \min\left(2k_1\rho_{\min}, 2k_2, \delta_{i,1}, \delta_{i,2}, \delta_{i,3}\right)$, (3.40) can be rewritten as

$$\dot{V}_{i,2} \leq -C_i V_{i,2} + \Delta_i + \Omega_i. \tag{3.41}$$

From (3.41), we have

$$V_{i,2}(t) \leq V_{i,2}(0)\, e^{-C_i t} + \frac{\Omega_i}{C_i}(1 - e^{-C_i t}) + \bar{V}_i \tag{3.42}$$

where $\bar{V}_i$ represents the effect of Δ_i and decays to zero exponentially. From (3.42) it can be concluded that all the signals in the resulting closed-loop system are bounded. Furthermore, we can obtain that

$$\lim_{t\to\infty} 2\rho_{\max}V_{i,2}(t) \leq \frac{2\rho_{\max}\Omega_i}{C_i}. \tag{3.43}$$

By choosing design parameters appropriately, then the bound $\sqrt{2\rho_{\max}\Omega_i/C_i}$ can be adjusted as small as desired for each robot.

From Theorem 3.1 and (3.43), $\lim_{t\to\infty}\|r_{i,1}-p_r\|=0$ and $\|z_{i,1}\|^2 \leq 2\rho_{\max}V_{i,2}(t)$. Then we can obtain that $\|\bar{p}_i-p_r\|$ is bounded by a function that converges towards a set

$$\Lambda=\{\bar{p}_i-p_r|\|p_i-p_r\|\leq\|p_i-r_{i,1}\|+\|r_{i,1}-p_r\|\leq\varepsilon\} \tag{3.44}$$

where

$$\varepsilon=\max(\sqrt{2\rho_{\max}\Omega_i/C_i}),\ i=1,2,\cdots,N. \tag{3.45}$$

□

Remark 3.3. From (3.44) and (3.45), it can be noted that the ultimate bound of the tracking error depends on the constants Ω_i and C_i. Furthermore, decreasing Ω_i/C_i can be achieved by decreasing Ω_i and increasing C_i. From the expressions of Ω_i and C_i, it can be seen that they share some common design parameters, such as $\delta_{i,\kappa}$, $\kappa=1,2,3$, thus it is difficult to decrease Ω_i/C_i by adjusting these parameters. Therefore, it is possible to decrease Ω_i by increasing $\gamma_{i,\kappa}$, while increasing C_i can be achieved by increasing $k_{i,1}$ and $k_{i,2}$.

Remark 3.4. Note that $z_i^r=z_{i,1}+\left(\rho_i^{-1}-I_2\right)\bar{p}_i$. Thus, if $\lim_{t\to+\infty}\rho_i=I_2$, i.e., no sensor faults exist after a finite time instant or the sensors recover accurate measurement gradually, in this case, with the proposed fault tolerant control scheme, z_i^r can converge to a residual set which can be made arbitrarily small by adjusting the design parameters.

3.3 Simulation

To verify the established theoretical results, simulation study has been carried out by considering a group of four identical WMRs with their physical parameters set as follows, $m_i=30$, $I_{m,i}=19$, $b_i=0.5$, $a_i=0.3$, $r_i=0.1$, $n_i=20$, $K_{b,i}=0.019$, $K_{T,i}=0.2639$ and $R_{a,i}=1.6$. The disturbance is assumed as $\bar{\tau}_{d,i}=$

$[\cos(\pi t/8), \sin(\pi t/8)]^T$ for simulation purpose, while it is unknown to designer. The reference trajectory is given as $p_r(t) = [3sin(\pi t/16) + 1, -2cos(\pi t/16)]^T$. The communication topology of the group is shown in Figure2.

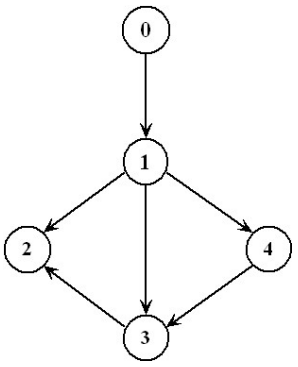

FIGURE 3.2: Communication topology of the 4 WMRs.

The initial positions and orientations of the four WMRs are set as $p_1(0) = [0, -2, 0]^T$, $p_2(0) = [-0.5, -2.5, 0]^T$, $p_3(0) = [1, -2.5, 0]^T$ and $p_4(0) = [0, -3, 0]^T$. The following sensor faults are considered in the simulation for each WMR.

$$\rho_1 = \text{diag}(1 - 0.04e^{-0.1t},\ 1 - 0.05e^{-0.1t}),$$

$$\rho_2 = \text{diag}(1 + 0.05e^{-0.1t},\ 1 + 0.05e^{-0.1t}),$$

$$\rho_3 = \text{diag}(1 - 0.05e^{-0.1t},\ 1 - 0.07e^{-0.1t}\cos(\pi t/10)),$$

$$\rho_4 = \text{diag}(1 + 0.1e^{-0.1t}\cos(\pi t/10),\ 1 + 0.1e^{-0.1t}\sin(\pi t/10)).$$

The initial values of the estimator are set as $r_{i,1}(0) = p_i(0)$, $r_{i,2}(0) = [0, 0]^T$, $c_i(0) = 2$ and $\hat{\sigma}_i(0) = [0, 0]^T$. The initial values of the observer are set as $\hat{p}_i = \hat{\eta}_i = [0, 0]^T$. The design parameters in the control scheme are chosen as follows, $L_{i,1} = 3I_2$, $L_{i,2} = 2I_2$, $k_1 = k_2 = 2$, $\delta_{i,2} = 0.2$, $\delta_{i,1} = \delta_{i,3} = 0.3$, $\gamma_{i,\kappa} = 0.4$, $\kappa = 1, 2, 3$.

The simulation results are shown in Figure 3-9, which verify the effectiveness of the proposed observer-based output feedback consensus tracking control scheme for nonholonomic mobile robots under sensor faults.

The proposed control scheme involves estimator, observer and controller design. The estimator errors $\tilde{r}_{i,1} = [\tilde{r}_{i,11}, \tilde{r}_{i,12}]^T$ and $\tilde{\sigma}_i = [\tilde{\sigma}_{i,1}, \tilde{\sigma}_{i,2}]^T$ are shown in Figure 3.3 and Figure 3.4 respectively, which show that the proposed estimator can estimate the trajectory information of the leader for each robot with bounded estimation error and thus effectively illustrate the results in Theorem 3.1.

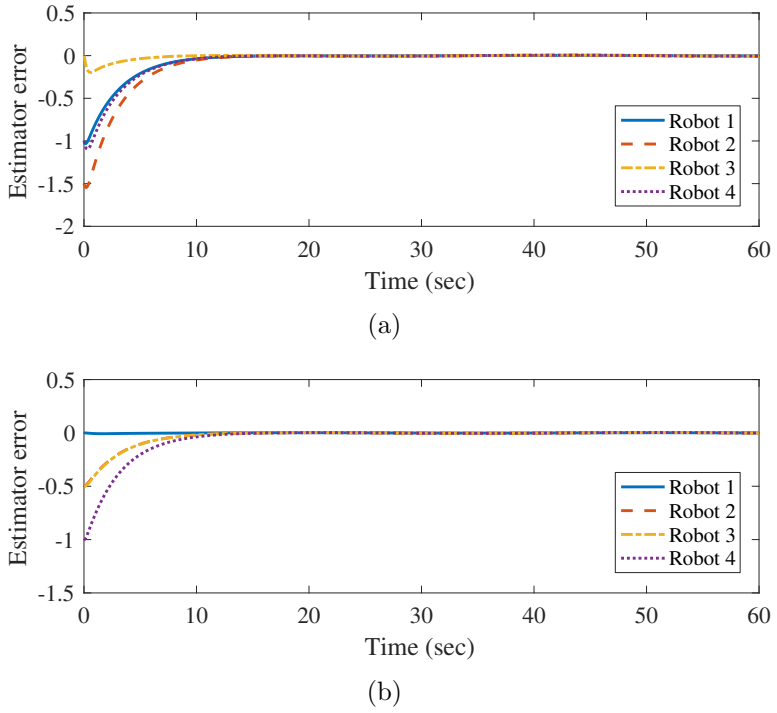

FIGURE 3.3: The estimation errors $\tilde{r}_{i,1}$ of four robots. Figures in (a) and (b) respectively show $\tilde{r}_{i,11}$ and $\tilde{r}_{i,12}$, $i = 1, 2, 3, 4$.

Overall, the trajectories and tracking errors of four robots generated by the proposed controller are illustrated in Figure 3.5 - Figure 3.6, from which, it can be seen that the effects of sensor faults can be compressed and the consensus tracking performance can be achieved with the proposed control scheme. The control input u_i is illustrated in Figure 3.7.

To illustrate the discussions made in Remark 3.3, take Robot 1 as an example. In terms of the observer-based controller, we also consider the following two cases:

Case 1: Change k_1 by setting $k_1 = 2$, 6 and 12 respectively, while other design parameters are fixed as the values given above.

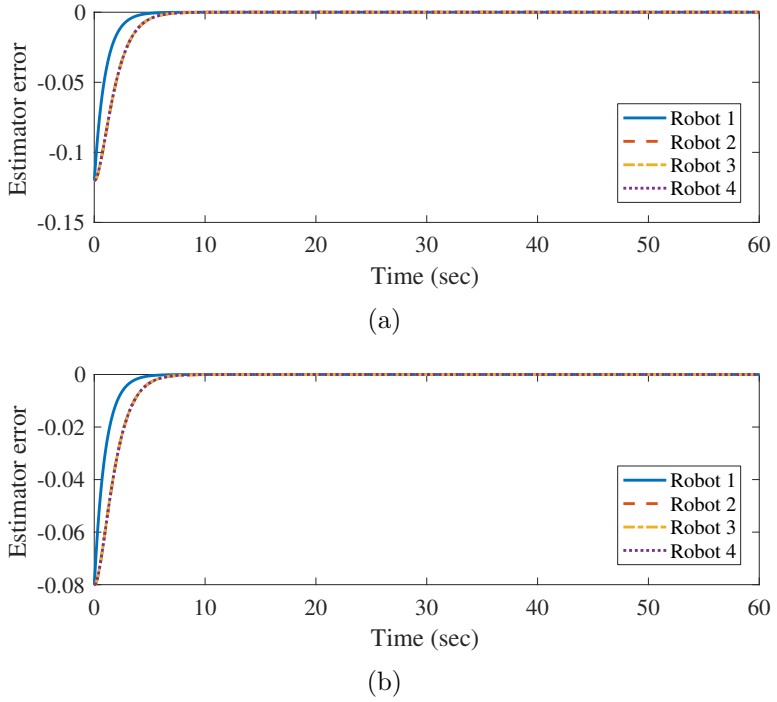

FIGURE 3.4: The estimation errors $\tilde{\sigma}_i$ of four robots. Figures in (a) and (b) respectively show $\tilde{\sigma}_{i,1}$ and $\tilde{\sigma}_{i,2}$, $i = 1, 2, 3, 4$.

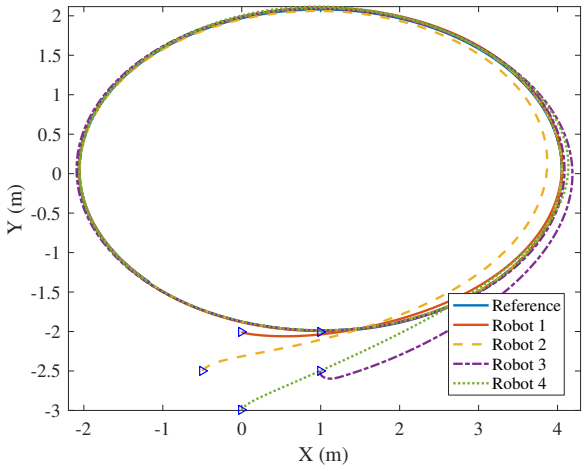

FIGURE 3.5: The trajectories of the four robots with the proposed control scheme. The triangles represent the initial positions of the leader and four robots.

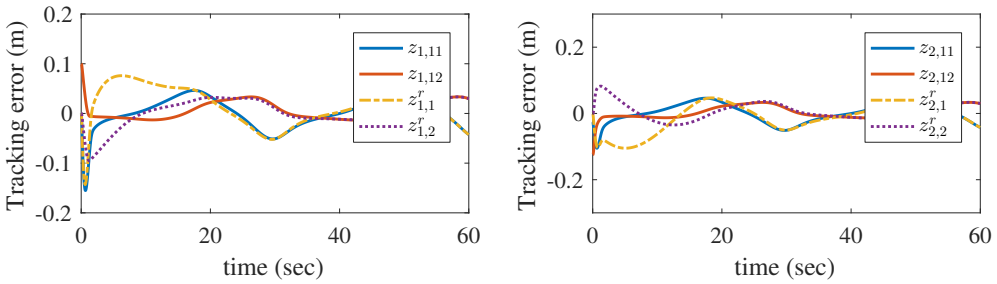

(a) Robot 1 (b) Robot 2

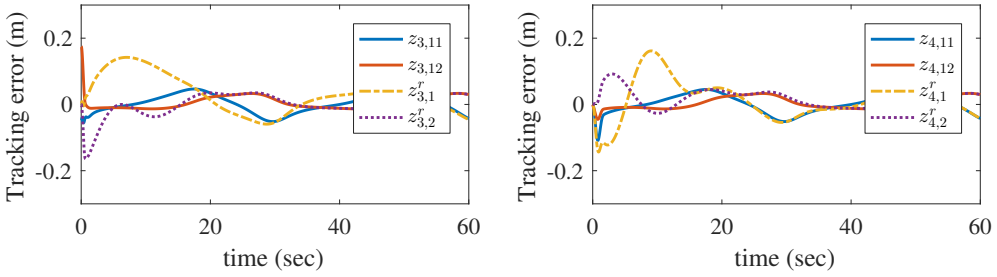

(c) Robot 3 (d) Robot 4

FIGURE 3.6: The measured tracking errors $z_{i,1} = [z_{i,11}, z_{i,12}]^T$ and the real tracking error $z^r_i = [z^r_{i,1}, z^r_{i,2}]^T$ of four robots with the proposed control scheme, $i = 1, 2, 3, 4$.

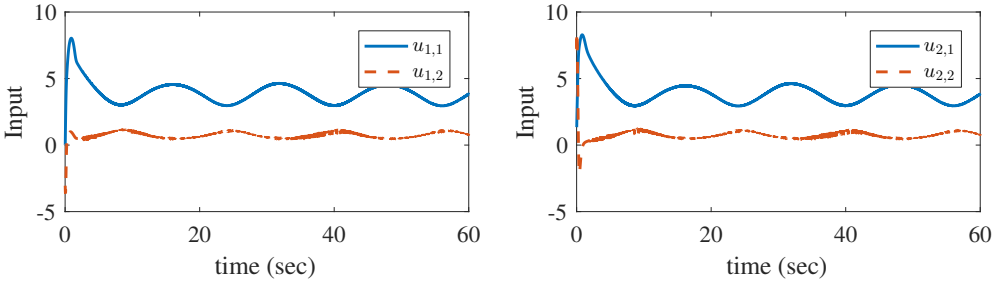

(a) Robot 1 (b) Robot 2

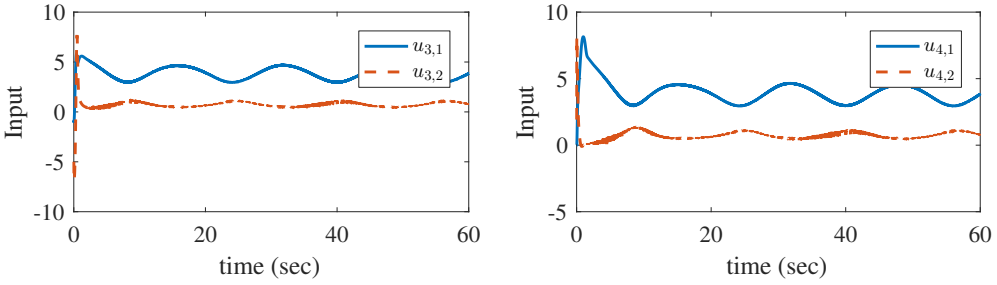

(c) Robot 3 (d) Robot 4

FIGURE 3.7: The control input u_i of four robots, $i = 1, 2, 3, 4$.

Case 2: Vary $\gamma_{1,1}$ by setting $\gamma_{1,1} = 0.1$, 0.4 and 0.8 respectively, with the remaining design parameters the same as the values given earlier.

The measured tracking errors of Robot 1, $z_{1,11}$, with different k_1 and different $\gamma_{1,1}$ are respectively shown in Figure 3.8 and 3.9, from which it can be observed that the ultimate measured tracking error decrease as k_1 and $\gamma_{1,1}$ increase.

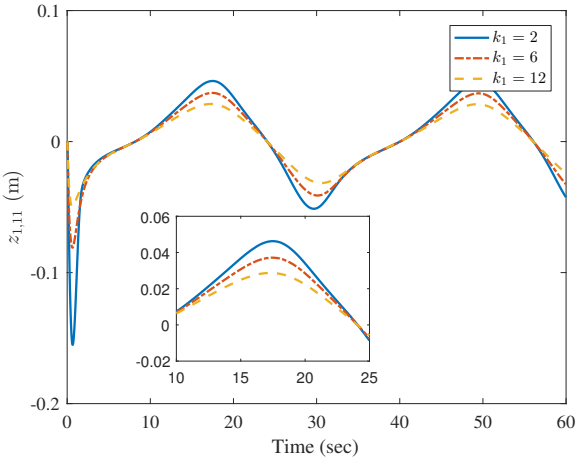

FIGURE 3.8: $z_{1,11}$ with different k_1.

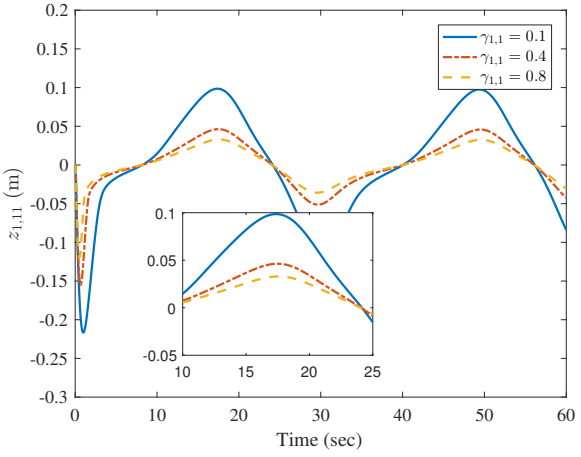

FIGURE 3.9: $z_{1,11}$ with different $\gamma_{1,1}$.

3.4 Conclusion and Future Work

In this chapter, distributed output feedback consensus tracking control is studied for multiple nonholonomic mobile robots with directed communication graph in

the presence of sensor faults. In the proposed control scheme, a fully distributed estimator is firstly constructed to estimate the reference trajectory for each robot without using any global information of communication network topology. In the presence of sensor faults, to compress the effects of sensor faults and realize decentralized trajectory tracking, an observer-based output feedback control law is designed based on backstepping technique and the estimated information. The proposed control scheme can guarantee the boundedness of all the signals in the resulting closed-loop system. Moreover, the consensus tracking error of the system can converge to an adjustable neighborhood of zero by appropriately choosing design parameters. The simulation results verify the effectiveness of the proposed control scheme.

3.5 Appendix

Consider the following Lyapunov function,

$$V_e = \frac{1}{2}\sum_{i=1}^{N}\left(\frac{2c_i+\beta_i}{\theta_i}s_i^T P s_i + \frac{\tilde{c}_i^2}{\theta_i} + \frac{1}{\theta_i\gamma_\sigma}\tilde{\sigma}_i^T\tilde{\sigma}_i\right), \tag{3.46}$$

where $\tilde{c}_i = c_i - c^*$ with c^* being a constant will be defined hereinafter. Based on (3.6) and (3.7), the time derivative of V_e can be computed as

$$\begin{aligned}
\dot{V}_e &= \sum_{i=1}^{N}\left(\frac{2\left(c_i+\beta_i\right)}{\theta_i}s_i^T P\dot{s}_i + \frac{\dot{c}_i}{\theta_i}s_i^T P s_i + \frac{\tilde{c}_i\dot{c}_i}{\theta_i} + \frac{1}{\theta_i\gamma_\sigma}\tilde{\sigma}_i^T\dot{\tilde{\sigma}}_i\right)\\
&= s^T\left[\left(c+\beta\right)\Theta\otimes\left(A^TP+PA\right)\right]s\\
&- s^T\left[\left(c+\beta\right)W\left(c+\beta\right)\otimes PBB^TP\right]s\\
&-2s^T\left[\left(c+\beta\right)\Theta H\otimes PB\right]\mathrm{diag}\left(sgn\left[\left(H\otimes K\right)\tilde{r}\right]\right)\left(1\otimes\sigma\right)\\
&-2s^T\left[\left(c+\beta\right)\Theta H\otimes PB\right]\left(1\otimes v_0\right)\\
&- 2s^T\left[\left(c+\beta\right)\Theta H\otimes PB\right]\mathrm{diag}\left(sgn\left[\left(H\otimes K\right)\tilde{r}\right]\right)\tilde{\sigma}\\
&+ s^T\left[\left(c+\beta-c^*I\right)\otimes PBB^TP\right]s - \frac{1}{\gamma_\sigma}\tilde{\sigma}^T\left(W\otimes I_2\right)\tilde{\sigma}
\end{aligned} \tag{3.47}$$

where $c = \text{diag}(c_1, c_2, \cdots, c_N)$, $\beta = \text{diag}(\beta_1, \beta_2, \cdots, \beta_N)$, $\tilde{\sigma} = [\tilde{\sigma}_1^T, \tilde{\sigma}_2^T, \cdots, \tilde{\sigma}_N^T]^T$.

Since $H = \mathcal{D} - \mathcal{A} + \mu$ and based on Lemma 3.1, it follows that

$$\begin{aligned} &-s^T[(c+\beta)\,\Theta D \otimes PB]\,\text{diag}\left(sgn\left[(H\otimes K)\,\tilde{r}\right]\right)(1\otimes\sigma) \\ &\quad = -\sum_{i=1}^{N}\frac{c_i+\beta_i}{\theta_i}d_{ii}\left|s_i^T K^T\right|\sigma \\ &\quad = -\sum_{i=1}^{N}\sum_{k=1}^{N}\frac{c_i+\beta_i}{\theta_i}a_{ik}\left|s_i^T K^T\right|\sigma \end{aligned} \tag{3.48}$$

$$\begin{aligned} &s^T[(c+\beta)\,\Theta A \otimes PB]\,\text{diag}\left(sgn\left[(H\otimes K)\,\tilde{r}\right]\right)(1\otimes\sigma) \\ &\quad \le \sum_{i=1}^{N}\sum_{k=1}^{N}\frac{c_i+\beta_i}{\theta_i}a_{ik}\left|s_i^T K^T\right|\sigma \end{aligned} \tag{3.49}$$

$$\begin{aligned} &-s^T[(c+\beta)\,\Theta\mu \otimes PB]\,\text{diag}\left(sgn\left[(H\otimes K)\,\tilde{r}\right]\right)(1\otimes\sigma) \\ &\quad = \sum_{i=1}^{N}\frac{c_i+\beta_i}{\theta_i}\mu_i\left|s_i^T K^T\right|\sigma \end{aligned} \tag{3.50}$$

$$\begin{aligned} &-2s^T\left[(c+\beta)\,\Theta H \otimes PB\right]\text{diag}\left(sgn\left[(H\otimes K)\,\tilde{r}\right]\right)\tilde{\sigma} \\ &\quad \le s^T\left[\varsigma\bar{\lambda}_U\,(c+\beta)^2\otimes PBB^TP\right]z + \frac{1}{\varsigma}\tilde{\sigma}^T\tilde{\sigma} \end{aligned} \tag{3.51}$$

where $U = \Theta H H^T \Theta$ and $\bar{\lambda}_U = \lambda_{\max}(U)$.

Thus, substituting (3.48)-(3.51) into (3.47) results in

$$\begin{aligned} \dot{V}_e \le\ & s^T\left[(c+\beta)\,\Theta\otimes\left(A^TP+PA\right)\right]s \\ & - s^T\left[\left(\lambda_W - \varsigma\bar{\lambda}_U\right)(c+\beta)^2\otimes PBB^TP\right]s \\ & + s^T\left[(c+\beta-c^*I)\otimes PBB^TP\right]s - \left(\frac{\lambda_W}{\gamma_\sigma}-\frac{1}{\varsigma}\right)\tilde{\sigma}^T\tilde{\sigma} \end{aligned} \tag{3.52}$$

where $\lambda_W = \lambda_{\min}(W)$. Choose ς and γ_σ such that

$$\lambda_W > \varsigma\bar{\lambda}_U,\ \frac{\lambda_W}{\gamma_\sigma} > \frac{1}{\varsigma}. \tag{3.53}$$

Furthermore, since

$$\begin{aligned} & s^T\left[(c+\beta)\,\Theta\otimes 3PBB^TP\right]s \\ & \quad\le s^T\left[\left(\left(\lambda_W-\varsigma\bar{\lambda}_U\right)(c+\beta)^2+c^*\Theta\right)\otimes PBB^TP\right]s \end{aligned} \tag{3.54}$$

where $c^*=9\lambda_{\max}(\Theta)/4\left(\lambda_W-\varsigma\bar{\lambda}_U\right)$, we can obtain

$$\begin{aligned} \dot{V}_e &\le s^T\left[(c+\beta)\,\Theta\otimes\left(A^TP+PA-2PBB^TP\right)\right]s \\ &\quad - s^T\left[(c+\beta-c^*I)\,\Theta\otimes PBB^TP\right]s \\ &\quad + s^T\left[(c+\beta-c^*I)\,\Theta\otimes PBB^TP\right]s-\left(\frac{\lambda_W}{\gamma_\sigma}-\frac{1}{\varsigma}\right)\tilde{\sigma}^T\tilde{\sigma} \\ &\le s^T\left[(c+\beta)\,\Theta\otimes\left(A^TP+PA-2PBB^TP\right)\right]s-\left(\frac{\lambda_W}{\gamma_\sigma}-\frac{1}{\varsigma}\right)\tilde{\sigma}^T\tilde{\sigma} \end{aligned} \tag{3.55}$$

Let $\bar{s}=(I_{N\times N}\otimes P)s$. (3.55) can be rewritten as

$$\begin{aligned} \dot{V}_e &\le \bar{s}^T\left[(c+\beta)\,\Theta\otimes\left(\ AP^{-1}+P^{-1}A^T-2BB^T\right)\right]\bar{s} \\ &\quad -\left(\frac{\lambda_W}{\gamma_\sigma}-\frac{1}{\varsigma}\right)\tilde{\sigma}^T\tilde{\sigma}\triangleq -\bar{V}_e\left(\bar{s},\tilde{\sigma}\right) \end{aligned} \tag{3.56}$$

It follows from (3.8) that $AP^{-1}+P^{-1}A^T-2BB^T=-Q<0$, $\bar{V}_e\left(\bar{s},\tilde{\sigma}\right)$ is positive definite. Thus we can obtain from (3.56) that $\dot{V}_e\le 0$, which means $\bar{s}$, $\tilde{c}_i$, $\tilde{\sigma}$ and V_e are bounded. It can also be checked that s, $\dot{s}$ and $\dot{\bar{s}}$ are bounded. By taking integration of both sides of (3.56), it has

$$V_e\left(\infty\right)+\int_0^\infty \bar{V}_e\left(\bar{s},\tilde{\sigma}\right)d\tau\le V_e\left(0\right) \tag{3.57}$$

which means $\int_0^\infty \bar{V}_e\left(\bar{s},\tilde{\sigma}\right)d\tau$ is bounded. So based on Barbalat's lemma, it has

$$\lim_{t\to 0}\|\bar{s}\|=\lim_{t\to 0}\|\tilde{\sigma}\|=0. \tag{3.58}$$

Since P and H are non-sigular, it ensures that r_i asymptotically converge to r_0, i.e. $\lim\limits_{t\to\infty} r_i=r_0$.

Chapter 4

Distributed Output Feedback Consensus Tracking Control of Multiple Nonholonomic Mobile Robots with Only Position Information of Leader

In the previous chapter, distributed output feedback consensus tracking control of multiple nonholonomic mobile robots with directed graph is investigated. However the control scheme is developed based on the assumption that the reference trajectory is represented by a virtual leader whose position and velocity information is available to a set of follower robots. The first 2nd-order derivatives of reference trajectory are bounded and piecewise continuous. Furthermore, dynamic uncertainty is not taken into consideration. In this chapter, we address the issue of distributed output feedback consensus tracking control of multiple nonholonomic mobile robots under directed graph by using only position information of the leader. To solve the problem, a new control design scheme involving three steps is proposed.

Firstly, a fully distributed adaptive estimator is constructed to estimate the position of leader for each robot via the communication topology. Secondly, to realize feedback control, an adaptive observer is designed for each robot to estimate the velocity information and unknown dynamic parameters. Thirdly, utilizing the estimated information from the estimator and observer, a feedback control law is designed based on backstepping technique to realize trajectory tracking control for each robot. Consequently, the main contributions and novelty of this paper are summarized as follows:

- To the best of our knowledge, this is the first work to achieve fully distributed consensus tracking control for multiple nonholonomic mobile robots under directed communication topology.
- Only position information of the leader is available to a subset of followers, adaptive control is employed to deal with the requirement of velocity information of the leader in the controller design.
- The dynamic model considered in this chapter involves parametric uncertainty and unknown external disturbances.
- The boundedness of all the signals in the resulting closed-loop system are ensured. The consensus tracking error of the system can converge to an adjustable neighborhood of zero by appropriately choosing design parameters.

4.1 Problem Formulation

Consider a group of N wheeled mobile robots (WMRs) which is composed of two driving wheels and one passive wheel. The posture of a WMR in Catesian coordinates is described in Figure 4.1. The mass of centre is located at C, the midpoint of the axis between two wheels is P. Taking the actuator into account, the kinematic and dynamic models of the WMR can be given as follows [121],

$$\dot{q}_i = S\left(q_i\right)\eta_i \tag{4.1}$$

$$\bar{M}_i\dot{\eta}_i + \bar{V}\left(q_i, \dot{q}_i\right)\eta_i + \bar{\tau}_{d,i} = \frac{\bar{N}_i K_{T,i}}{R_{a,i}}\bar{B}_i u_i - \frac{\bar{N}_i^2 K_{T,i} K_{b,i}}{R_{a,i}}\bar{B}_i\bar{B}_i^T\eta_i \tag{4.2}$$

where $i = 1, \cdots, N$, $q_i = [x_i, y_i, \phi_i]^T$; (x_i, y_i) is the position of P and ϕ_i is the orientation of robot i. $\eta_i = [v_i, \omega_i]^T$ where v_i and ω_i are the linear and angular velocity respectively, u_i is the input voltage, $\bar{\tau}_{d,i}$ represents the external disturbance. N_i is the gear ratio, $K_{T,i}$ is the motor torque constant, $K_{b,i}$ is the counter electromotive force coefficient, and $R_{a,i}$ is the electric resistance.

$$S\left(q_i\right) = \begin{bmatrix} \cos\phi_i & 0 \\ \sin\phi_i & 0 \\ 0 & 1 \end{bmatrix},\ \bar{M}_i = \begin{bmatrix} m_i & 0 \\ 0 & I_{m,i} - m_i a_i^2 \end{bmatrix},$$

$$\bar{V}\left(q_i, \dot{q}_i\right) = \begin{bmatrix} 0 & 0 \\ 0 & 0 \end{bmatrix},\ \bar{B}_i = \tfrac{1}{r_i}\begin{bmatrix} 1 & 1 \\ b_i & -b_i \end{bmatrix}.$$

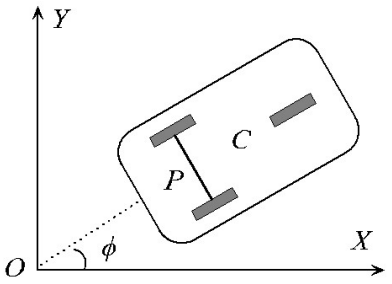

FIGURE 4.1: A type(2,0) wheeled mobile robot.

In these expressions, m_i is the mass of the robot, $I_{m,i}$ is the moment of inertia, b_i is the half width of axis between two wheels and r_i is the radius of each wheel, a_i is the distance between C and P.

Suppose that the interaction and information transmission among the N WMRs are governed by a directed graph $\mathcal{G}$. Labeling the leader robot as agent 0, we use $\mu_i = 1$ to indicate that robot i has access to the position information of the leader $p_0(t) = [x_0(t), y_0(t)]^T$; otherwise, $\mu_i = 0$.

The control objective is to design distributed control input u_i for each robot by utilizing only locally available information obtained from the intrinsic robot and its neighbors such that

- All the signals in the resulting closed-loop system are globally uniformly bounded;
- The design parameters are independent of the global information of the graph.
- The consensus error of the whole group can converge to an adjustable neighborhood of zero under the situation that only position information of the leader is available for a subset of followers.

To achieve the above mentioned objectives, the following assumptions are imposed.

Assumption 4.1. The linear and angular velocities of the leader are bounded and piecewise continuous, and there exists a constant vector $\sigma = [\sigma_1, \sigma_2]^T$ such that $|\dot{x}_0(t)| \leq \sigma_1$ and $|\dot{y}_0(t)| \leq \sigma_2$. Furthermore, σ is available to the ith robot if $\mu_i = 1$.

Assumption 4.2. The directed graph contains a spanning tree with the root being the leader.

Assumption 4.3. The unknown external disturbances $\bar{\tau}_{i,d}$ are bounded.

To develop and analyze the proposed control scheme, the following lemmas from [122] and [124] are then introduced.

Lemma 4.1 ([122])**.** Under Assumption 4.2, the matrix $H = \mathcal{L} + \mu$ is a positive matrix, where $\mu = diag(\mu_1, \mu_2, \cdots, \mu_N)$. Define

$$\begin{aligned} \theta &= [\theta_1, \theta_2, \cdots, \theta_N]^T = H^{-1} 1_N \\ \Theta &= diag\left\{ \frac{1}{\theta_1}, \frac{1}{\theta_2}, \cdots, \frac{1}{\theta_N} \right\} \\ W &= \Theta H + H^T \Theta \end{aligned} \tag{4.3}$$

Then $\theta_i > 0$ for $i = 1, 2, \cdots, N$ and W is a positive definite matrix.

Lemma 4.2 ([124])**.** For any scalars $\epsilon > 0$, $z \in \mathbb{R}$, the following relationship holds: $0 \leq |z| - \frac{z^2}{\sqrt{z^2+\epsilon^2}} < \epsilon$.

4.2 Controller Design

In this section, we will show the above described control problem is solvable by our proposed scheme.

4.2.1 Estimator design

Denote $\bar{p}_i$ as the estimation of p_0 from the estimator designed for the ith robot. Introduce the error variable

$$s_i = \sum_{j=1}^{N} a_{ij} \left(\bar{p}_i - \bar{p}_j\right) + \mu_i \left(\bar{p}_i - p_0\right) \tag{4.4}$$

and define the estimation error as $e_i = \bar{p}_i - p_0$. Let $e = \left[e_1^T, \cdots, e_N^T\right]^T$ and $s = \left[s_1^T, \cdots, s_N^T\right]^T$, then

$$s = \left(H \otimes I_2\right) e. \tag{4.5}$$

Based on the communication among neighbors, design the fully distributed adaptive estimator for the ith robot to estimate the position information of leader as follows

$$\dot{\bar{p}}_i = -c_0 s_i - \operatorname{diag}\left(sig\left(s_i\right)\right) \hat{\sigma}_i \tag{4.6}$$

$$\dot{\hat{\sigma}}_i = -\sum_{j=1}^{N} a_{ij} \left(\hat{\sigma}_i - \hat{\sigma}_j\right) - \mu_i \left(\hat{\sigma}_i - \sigma\right). \tag{4.7}$$

where $c_0 > 0$ is a design parameter, $\hat{\sigma}_i$ is the estimation of σ and $sig\left(s_i\right) = \left[\frac{s_{i,1}}{\sqrt{s_{i,1}^2+\epsilon^2}}, \frac{s_{i,2}}{\sqrt{s_{i,2}^2+\epsilon^2}}\right]^T$ with ϵ being a positive constant. Then, we can have

$$\dot{s} = \left(H \otimes I_2\right) \left(-c_0 s - \operatorname{diag}\left(sig\left(s\right)\right) \hat{\sigma} - 1_N \otimes \dot{p}_0\right) \tag{4.8}$$

Define $\tilde{\sigma}_i = \sigma - \hat{\sigma}_i$, and let $\hat{\sigma} = \left[\hat{\sigma}_1^T, \cdots, \hat{\sigma}_2^T\right]^T$ and $\tilde{\sigma} = \left[\tilde{\sigma}_1^T, \cdots, \tilde{\sigma}_2^T\right]^T$, then

$$\dot{\tilde{\sigma}} = -\left(H \otimes I_2\right) \tilde{\sigma}. \tag{4.9}$$

Theorem 4.1. Under Assumptions 4.1 and 4.2 and with the proposed adaptive estimator given in (4.6) and (4.7), the estimation errors e and $\tilde{\sigma}$ are bounded. Moreover, it ensures that $\|e\|$ will converge to an adjustable neighborhood of zero by appropriately choosing design parameters.

Proof. Consider the following Lyapunov function for the closed-loop system

$$V_e = \frac{1}{2} s^T (\Theta \otimes I_2) s + \frac{1}{2\gamma_e} \tilde{\sigma}^T (\Theta \otimes I_2) \tilde{\sigma} \tag{4.10}$$

where γ_e is a positive design parameter. Then

$$\begin{aligned}
\dot{V}_e &= -\frac{c_0}{2} s^T \left[\left(\Theta \mathrm{H} + \mathrm{H}^{\mathrm{T}} \Theta \right) \otimes I_2 \right] s - s^T (\Theta H \otimes I_2) \operatorname{diag}(sig(s)) \hat{\sigma} \\
&\quad - s^T (\Theta H \otimes I_2) (1_N \otimes \dot{p}_0) - \frac{1}{2\gamma_e} \tilde{\sigma}^T \left[\left(\Theta \mathrm{H} + \mathrm{H}^{\mathrm{T}} \Theta \right) \otimes I_2 \right] \tilde{\sigma} \\
&= -\frac{c_0}{2} s^T (W \otimes I_2) s - \frac{1}{2\gamma_e} \tilde{\sigma}^T (W \otimes I_2) \tilde{\sigma} \\
&\quad + s^T (\Theta H \otimes I_2) \chi (1_N \otimes \sigma) - s^T (\Theta H \otimes I_2) (1_N \otimes \dot{p}_0) \\
&\quad - s^T (\Theta H \otimes I_2) \operatorname{diag}(sgn(s)) (1_N \otimes \sigma) + s^T (\Theta H \otimes I_2) \operatorname{diag}(sig(s)) \tilde{\sigma}
\end{aligned} \tag{4.11}$$

where $\chi = \operatorname{diag}(sgn(s) - sig(s))$.

From the definition of H we can obtain that,

$$\begin{aligned}
-s^T (\Theta \mathcal{D} \otimes I_2) \operatorname{diag}(sgn(s)) (1_N \otimes \sigma) &= -\sum_{i=1}^{N} \frac{d_{ii}}{\theta_i} \left| s_i^T \right| \sigma \\
&= \sum_{i=1}^{N} \sum_{k=1}^{N} \frac{a_{ik}}{\theta_i} \left| s_i^T \right| \sigma
\end{aligned} \tag{4.12}$$

$$s^T (\Theta \mathcal{A} \otimes I_2) \operatorname{diag}(sgn(s)) (1_N \otimes \sigma) \leq \sum_{i=1}^{N} \sum_{k=1}^{N} \frac{a_{ik}}{\theta_i} \left| s_i^T \right| \sigma \tag{4.13}$$

$$- s^T (\Theta \mu \otimes I_2) \operatorname{diag}(sgn(s)) (1_N \otimes \sigma) = -\sum_{i=1}^{N} \frac{\mu_i}{\theta_i} \left| s_i^T \right| \sigma \tag{4.14}$$

$$- s^T (\Theta H \otimes I_2) (1_N \otimes \dot{p}_0) = \sum_{i=1}^{N} \frac{\mu_i}{\theta_i} s_i^T \dot{p}_0 \leq \sum_{i=1}^{N} \frac{\mu_i}{\theta_i} \left| s_i^T \right| \sigma \tag{4.15}$$

where $\left|s_i^T\right| = [|s_{i,1}|, |s_{i,2}|]$. Substituting (4.12)-(4.15) into (4.11) and using Young's inequality yield,

$$\begin{aligned}\dot{V}_e \leq & -\frac{c_0}{2} s^T (W \otimes I_2) s + s^T (\Theta H \otimes I_2) \chi (1_N \otimes \sigma) \\ & + s^T (\Theta H \otimes I_2) \operatorname{diag}(sig(s)) \tilde{\sigma} - \frac{1}{2\gamma_e} \tilde{\sigma}^T (W \otimes I_2) \tilde{\sigma} \\ \leq & -\frac{\bar{c}_0}{2} s^T s - \frac{1}{2} \left(\frac{\lambda_{\min}(W)}{\gamma_e} - \frac{\|\Theta H\|^2}{\lambda_{\min}(W)} \right) \tilde{\sigma}^T \tilde{\sigma} + \Delta_e\end{aligned} \tag{4.16}$$

where $\bar{c}_0 = (c_0 - \xi_e - 1) \lambda_{\min}(W)$ and $\Delta_e = \frac{\|\Theta H\|^2 \|n\epsilon\sigma\|^2}{2\xi_e \lambda_{\min}(W)}$ with ξ_e being a positive constant.

Choose c_0 and γ_e such that

$$c_0 > \xi_e + 1 \tag{4.17}$$

$$0 < \gamma_e < \frac{\lambda_{\min}^2(W)}{\|\Theta H\|^2}, \tag{4.18}$$

then we obtain

$$\dot{V}_e \leq -c_e V_e + \Delta_e \tag{4.19}$$

where $c_e = \min\{\bar{c}_0, \gamma_e c_\sigma\} / \lambda_{\min}(\Theta)$ with $c_\sigma = \frac{\lambda_{\min}(W)}{\gamma_e} - \frac{\|\Theta H\|^2}{\lambda_{\min}(W)}$. From (4.19), we have

$$V_e(t) \leq V_e(0) e^{-c_e t} + \frac{\Delta_e}{c_e} \left(1 - e^{-c_e t}\right) \tag{4.20}$$

from which it can be concluded that s and $\tilde{\sigma}$ are bounded. Furthermore,

$$\lim_{t \to \infty} 2V_e(t) \leq \frac{2\Delta_e}{c_e}. \tag{4.21}$$

Based on (4.5) and $s^T(\Theta \otimes I_2)s \leq 2V_e(t)$, we also obtain that the estimation error $\|e\|$ converges towards a set

$$\Lambda = \{e | \|e\| \leq \varepsilon_e\} \tag{4.22}$$

where $\varepsilon_e = \sqrt{2\Delta_e / c_e \lambda_{\min}(H^T \Theta H)}$.

□

Remark 4.1. Note that, the designed adaptive estimator given in (4.6) and (4.7) is independent of any global information of the communication graph, thus it is fully distributed. From (4.22), it can be seen that the ultimate bound of the estimation error can be decreased by increasing c_0, ξ_e or decreasing γ_e.

Remark 4.2. In case that the reference trajectory is prescribed or generated by a virtual leader, most existing methods are developed under two types of assumptions: (i) the velocity information of the leader is known by all followers or a subset of followers [79–81], (ii) the bound of velocity or input is known by all followers [82, 84, 93, 125]. As seen from (4.6) and (4.7), our proposed estimator no longer requires the velocity information of the leader. Also the bound σ is only needed by a subset of robots and it is estimated by the adaptive law (4.7) for the rest robots that cannot access the position of the leader.

4.2.2 Observer design

Since velocity measurements η_i are unavailable, thus we need to design an observer to estimate it for controller design. Introduce a new position off the wheel axis of the ith robot by a distance h_i, which is given by

$$p_i = \begin{bmatrix} x_i \\ y_i \end{bmatrix} + h_i \begin{bmatrix} \cos\phi_i \\ \sin\phi_i \end{bmatrix} \tag{4.23}$$

Then the system models in (4.1) and (4.2) can be rewritten as follows,

$$\begin{aligned} \dot{p}_i &= J_i \eta_i \\ \dot{\phi}_i &= \omega_i \\ \dot{\eta}_i &= -R_i \eta_i + B_i u_i + \tau_{d,i} \end{aligned} \tag{4.24}$$

where

$$J_i = \begin{bmatrix} \cos\phi_i & -h_i \sin\phi_i \\ \sin\phi_i & h_i \cos\phi_i \end{bmatrix}, \quad R_i = \frac{2\bar{N}_i K_{T,i} K_{b,i}}{R_{a,i} r_i^2} \begin{bmatrix} 1/m_i & 0 \\ 0 & b_i^2/\left(I_{m,i} - m_i a_i^2\right) \end{bmatrix},$$

$$B_i = \frac{\bar{N}_i K_{T,i}}{R_{a,i} r_i} \begin{bmatrix} 1/m_i & 0 \\ 0 & b_i^2/\left(I_i - m_i a_i^2\right) \end{bmatrix}, \quad \tau_{d,i} = \bar{M}_i^{-1} \bar{\tau}_{d,i}.$$

Based on (4.24), the observer is designed as follows,

$$\begin{aligned} \dot{\hat{p}}_i &= J_i \hat{\eta}_i + L_{i,1}\left(p_i - \hat{p}_i\right) \\ \dot{\hat{\eta}}_i &= -\hat{R}_i \hat{\eta}_i + \hat{B}_i u_i + L_{i,2}\left(p_i - \hat{p}_i\right) \end{aligned} \tag{4.25}$$

where $\hat{p}_i$ and $\hat{\eta}_i$ are the estimations of p_i and η_i, respectively, $L_{i,1}$ and $L_{i,2}$ are observer gain matrices, $\hat{R}_i = \text{diag}(\hat{R}_{i,1}, \hat{R}_{i,2})$ and $\hat{B}_i = \text{diag}(\hat{B}_{i,1}, \hat{B}_{i,2})$ with $\hat{R}_{i,k}$ and $\hat{B}_{i,k}$ representing the estimation of $R_{i,k}$ and $B_{i,k}$ respectively, $k = 1, 2$.

Define the observer errors as $\tilde{p}_i = p_i - \hat{p}_i$ and $\tilde{\eta}_i = \eta_i - \hat{\eta}_i$. Then from (4.24) and (4.25), the dynamics of observer errors can be expressed as,

$$\begin{aligned} \dot{\tilde{p}}_i &= J_i \tilde{\eta}_i - L_{i,1} \tilde{p}_i + L_{i,1} \tilde{h}_i \bar{p}_i \\ \dot{\tilde{\eta}}_i &= -R_i \tilde{\eta}_i - \tilde{R}_i \hat{\eta}_i + \tilde{B}_i u_i - L_{i,2} \tilde{p}_i + \tau_{i,d} \end{aligned} \tag{4.26}$$

where $\tilde{R}_i = diag(\tilde{R}_{i,1}, \tilde{R}_{i,2})$ and $\tilde{B}_i = diag(\tilde{B}_{i,1}, \tilde{B}_{i,2})$ with $\tilde{R}_{i,k} = R_{i,k} - \hat{R}_{i,k}$ and $\tilde{B}_{i,k} = B_{i,k} - \hat{B}_{i,k}$, $k = 1, 2$.

The observer gain matrices $L_{i,1}$ and $L_{i,2}$ are then chosen such that

$$L_{i,1}^T P_{i,1} + P_{i,1} L_{i,1} = Q_{i,1} > 0 \tag{4.27}$$

$$J_i^T P_{i,1} - P_{i,2} L_{i,2} = 0 \tag{4.28}$$

with $P_{i,1}$ and $P_{i,2}$ being given diagonal positive definite matrices.

Based on Lyapunov stability theory, a Lyapunov function with the following form is chosen to develop the adaptive laws for $\hat{R}_{i,k}$ and $\hat{B}_{i,k}$

$$V_{i,0} = \tilde{p}_i^T P_{i,1} \tilde{p}_i + \tilde{\eta}_i^T P_{i,2} \tilde{\eta}_i + \sum_{k=1}^{2} \left(\frac{\tilde{R}_{i,k}^2}{2\gamma_{i,rk}} + \frac{\tilde{B}_{i,k}^2}{2\gamma_{i,bk}} \right) \tag{4.29}$$

where $\gamma_{i,rk} > 0$ and $\gamma_{i,bk} > 0$ are design parameters. Let $Q_{i,2} = R_i^T P_{i,2} + P_{i,2} R_i$. Using (4.27) and (4.28), the time derivative of $V_{i,0}$ can be computed as,

$$\begin{aligned}
\dot{V}_{i,0} &= -\tilde{p}_i^T Q_{i,1} \tilde{p}_i - \tilde{\eta}_i^T Q_{i,2} \tilde{\eta}_i - 2\tilde{\eta}_i^T P_{i,2} \tilde{R}_i \hat{\eta}_i \\
&\quad + 2\tilde{\eta}_i^T P_{i,2} \tilde{B}_i u_i + 2\tilde{\eta}_i^T P_{i,2} \tau_{i,d} - \sum_{k=1}^{2} \left(\frac{\tilde{R}_{i,k} \dot{\hat{R}}_{i,k}}{\gamma_{i,rk}} + \frac{\tilde{B}_{i,k} \dot{\hat{B}}_{i,k}}{\gamma_{i,bk}} \right) \\
&\leq -\alpha_{i,1} \tilde{p}_i^T \tilde{p}_i - \alpha_{i,2} \tilde{\eta}_i^T \tilde{\eta}_i - \tilde{\eta}_i^T \tilde{R}_i \hat{\eta}_i + \tilde{\eta}_i^T \tilde{B}_i u_i \\
&\quad - \sum_{k=1}^{2} \left(\frac{\tilde{R}_{i,k} \dot{\hat{R}}_{i,k}}{\gamma_{i,rk}} + \frac{\tilde{B}_{i,k} \dot{\hat{B}}_{i,k}}{\gamma_{i,bk}} \right) + \xi_{i,1} D^2
\end{aligned} \tag{4.30}$$

where $\alpha_{i,1} = \lambda_{\min}(Q_{i,1})$, $\alpha_{i,2} = \lambda_{\min}(Q_{i,2}) - \|P_{i,2}\|^2 / \xi_{i,1}$ with $\xi_{i,1}$ being a positive design parameter, $\|\tau_{i,d}\| \leq D$ and

Since $\tilde{\eta}_i = J_i^{-1} \dot{\tilde{p}}_i + J_i^{-1} L_{i,1} \tilde{p}_i$, we can have,

$$\begin{aligned}
&-\tilde{\eta}_i^T \tilde{R}_i \hat{\eta}_i + \tilde{\eta}_i^T \tilde{B}_i u_i \\
&\quad = \left(J_i^{-1} \dot{\tilde{p}}_i + J_i^{-1} L_{i,1} \tilde{p}_i \right)^T \left(\tilde{B}_i u_i - \tilde{R}_i \hat{\eta}_i \right) \\
&\quad = \sum_{k=1}^{2} \left(\tilde{R}_{i,k} \varphi_{i,rk} + \tilde{B}_{i,k} \varphi_{i,bk} \right) + \sum_{k=1}^{2} \left(\tilde{R}_{i,k} \psi_{i,rk}^T \dot{\tilde{p}}_i + \tilde{B}_{i,k} \psi_{i,bk}^T \dot{\tilde{p}}_i \right)
\end{aligned} \tag{4.31}$$

where $\varphi_{i,rk} = -\left(J_i^{-1} L_{i,1} \tilde{p}_i \right)_k \hat{\eta}_{i,k}$, $\varphi_{i,bk} = \left(J_i^{-1} L_{i,1} \tilde{p}_i \right)_k u_{i,k}$, $\psi_{i,rk}^T = -\left(J_i^{-1} \right)_k \hat{\eta}_{i,k}$ and $\psi_{i,bk}^T = \left(J_i^{-1} \right)_k u_{i,k}$.

Let $\hat{R}_{i,k} = \hat{R}_{i,k}^c + \Upsilon_{i,rk}$ and $\hat{B}_{i,k} = \hat{B}_{i.k}^c + \Upsilon_{i,bk}$, $k = 1, 2$. Then the adaptive laws of $\hat{R}_{i,k}$ and $\hat{B}_{i,k}$ are respectively designed as

$$\dot{\hat{R}}_{i,k}^c = \gamma_{i,rk} \varphi_{i,rk} - \delta_{i,rk} \hat{R}_{i,\kappa}, \ \Upsilon_{i,rk} = \gamma_{i,rk} \int_{\tilde{p}_{ik}(0)}^{\tilde{p}_{ik}(t)} \psi_{i,rk}^T d\varsigma \tag{4.32}$$

$$\dot{\hat{B}}_{i.k}^c = \gamma_{i,bk} \varphi_{i,bk} - \delta_{i,bk} \hat{B}_{i,k}, \ \Upsilon_{i,bk} = \gamma_{i,bk} \int_{\tilde{p}_{ik}(0)}^{\tilde{p}_{ik}(t)} \psi_{i,bk}^T d\varsigma \tag{4.33}$$

where $\delta_{i,rk}$ and $\delta_{i,bk}$ are positive design parameters.

Substituting (4.31)-(4.33) into (4.30) results in

$$\begin{aligned}\dot{V}_{i,0} \leq & -\alpha_{i,1}\tilde{p}_i^T\tilde{p}_i - \alpha_{i,2}\tilde{\eta}_i^T\tilde{\eta}_i + \xi_{i,1}D^2 - \sum_{k=1}^{2}\left(\frac{\tilde{R}_{i,k}\dot{\hat{R}}_{i,k}}{\gamma_{i,rk}} + \frac{\tilde{B}_{i,k}\dot{\hat{B}}_{i,k}}{\gamma_{i,bk}}\right) \\ & + \sum_{k=1}^{2}\left(\tilde{R}_{i,k}\psi_{i,rk}\dot{\tilde{p}}_{ik} + \tilde{B}_{i,k}\psi_{i,bk}\dot{\tilde{p}}_{ik}\right) + \sum_{k=1}^{2}\left(\tilde{R}_{i,k}\varphi_{i,rk} + \tilde{B}_{i,k}\varphi_{i,bk}\right) \\ \leq & -\alpha_{i,1}\tilde{p}_i^T\tilde{p}_i - \alpha_{i,2}\tilde{\eta}_i^T\tilde{\eta}_i - \sum_{k=1}^{2}\left(\frac{\delta_{i,rk}}{2\gamma_{i,rk}}\tilde{R}_{i,k}^2 + \frac{\delta_{i,bk}}{2\gamma_{i,bk}}\tilde{B}_{i,k}^2\right) + \Delta_{i,0}\end{aligned} \tag{4.34}$$

where $\Delta_{i,0} = \xi_{i,1}D^2 + \sum_{k=1}^{2}\left(\frac{\delta_{i,rk}}{2\gamma_{i,rk}}R_{i,k}^2 + \frac{\delta_{i,bk}}{2\gamma_{i,bk}}B_{i,k}^2\right)$.

4.2.3 Controller design

Based on the estimated position $\bar{p}_i$ from (4.6), an observer-based output feedback control law will be designed by using backstepping technique to realize trajectory tracking control for each robot. Firstly, we introduce two error variables

$$z_{i,1} = p_i - \bar{p}_i \tag{4.35}$$

$$z_{i,2} = \hat{\eta}_i - \eta_i^c \tag{4.36}$$

where η_i^c is the virtual command for η_i.

Since $\eta_i = \eta_i^c + z_{i,2} + \tilde{\eta}_i$, we have,

$$\begin{aligned}z_{i,1}^T\dot{z}_{i,1} &= z_{i,1}^T\left(J_i\eta_i - \dot{\bar{p}}_i\right) \\ &= z_{i,1}^T\left(J_i\eta_i^c - \dot{\bar{p}}_i + J_iz_{i,2} + J_i\tilde{\eta}_i\right)\end{aligned}. \tag{4.37}$$

From Theorem 3.1, we know $\|s\|$ and $\|\tilde{\sigma}\|$ are bounded, which implies that $\|\hat{\sigma}\|$ and $\dot{\bar{p}}_i$ are bounded. Let $|\dot{\bar{p}}_{i,1}| \leq \vartheta_{i,1}$, $|\dot{\bar{p}}_{i,2}| \leq \vartheta_{i,2}$, and $\vartheta_i = [\vartheta_{i,1}, \vartheta_{i,2}]^T$. To stabilize the dynamic of $z_{i,1}$, the virtual command η_i^c is designed as

$$\eta_i^c = J_i^{-1}\left(-\bar{c}_{i,1}z_{i,1} - \mathrm{diag}\left(sig\left(z_{i,1}\right)\right)\hat{\vartheta}_i\right) \tag{4.38}$$

where $\bar{c}_{i,1}$ is a positive design parameter and $\hat{\vartheta}_i$ is the estimation of ϑ_i with $\tilde{\vartheta}_i = \vartheta_i - \hat{\vartheta}_i$. Furthermore, utilizing Young's inequality, we can obtain,

$$z_{i,1}^T J_i \tilde{\eta}_i \leq \frac{z_{i,1}^T z_{i,1}}{2} + \frac{\tilde{\eta}_i^T \tilde{\eta}_i}{2} \tag{4.39}$$

Substituting (4.38) and (4.39) into (4.37) results in

$$\begin{aligned} z_{i,1}^T \dot{z}_{i,1} &= -\bar{c}_{i,1} z_{i,1}^T z_{i,1} - z_{i,1}^T \mathrm{diag}\left(sig\left(z_{i,1}\right)\right) \hat{\vartheta}_i - z_{i,1}^T \dot{\bar{p}}_i + z_{i,1}^T J_i z_{i,2} + z_{i,1}^T J_i \tilde{\eta}_i \\ &\leq -c_{i,1} z_{i,1}^T z_{i,1} - z_{i,1}^T \mathrm{diag}\left(sig\left(z_{i,1}\right)\right) \hat{\vartheta}_i + \left| z_{i,1}^T \right| \vartheta + z_{i,1}^T J_i z_{i,2} + \frac{\tilde{\eta}_i^T \tilde{\eta}_i}{2} \\ &\leq -c_{i,1} z_{i,1}^T z_{i,1} + z_{i,1}^T \mathrm{diag}\left(sig\left(z_{i,1}\right)\right) \tilde{\vartheta}_i + \sqrt{2}\epsilon \|\vartheta\| + z_{i,1}^T J_i z_{i,2} + \frac{\tilde{\eta}_i^T \tilde{\eta}_i}{2} \end{aligned} \tag{4.40}$$

where $c_{i,1} = \bar{c}_{i,1} - 0.5$.

By considering the following Lyapunov function

$$V_{i,1} = V_{i,0} + \frac{1}{2} z_{i,1}^T z_{i,1} + \frac{1}{2\gamma_{i,c}} \tilde{\vartheta}_i^T \tilde{\vartheta}_i \tag{4.41}$$

where $\gamma_{i,x} > 0$ and $\gamma_{i,y} > 0$ are design parameters, we design the adaptation law for $\hat{\vartheta}_i$ as

$$\dot{\hat{\vartheta}}_i = \gamma_{i,c} \mathrm{diag}\left(sig\left(z_{i,1}\right)\right) z_{i,1} - \delta_{i,c} \hat{\vartheta}_i \tag{4.42}$$

where $\delta_{i,c}$ is positive design parameter. From (4.40) and (4.42), the time derivative of $V_{i,1}$ can be computed as

$$\begin{aligned} \dot{V}_{i,1} &= \dot{V}_{i,0} + z_{i,1}^T \dot{z}_{i,1} - \frac{1}{\gamma_{i,c}} \tilde{\vartheta}_i^T \dot{\hat{\vartheta}}_i \\ &\leq \dot{V}_{i,0} - c_{i,1} z_{i,1}^T z_{i,1} + \frac{\delta_{i,c}}{\gamma_{i,c}} \tilde{\vartheta}_i^T \hat{\vartheta}_i + \sqrt{2}\epsilon \|\vartheta\| + z_{i,1}^T J z_{i,2} + \frac{\tilde{\eta}_i^T \tilde{\eta}_i}{2} \\ &\leq \dot{V}_{i,0} - c_{i,1} z_{i,1}^T z_{i,1} - \frac{\delta_{i,c}}{2\gamma_{i,c}} \tilde{\vartheta}_i^T \tilde{\vartheta}_i + \Delta_{i,1} + z_{i,1}^T J z_{i,2} + \frac{\tilde{\eta}_i^T \tilde{\eta}_i}{2} \end{aligned} \tag{4.43}$$

where $\Delta_{i,1} = \sqrt{2}\epsilon \|\vartheta\| + \frac{\delta_{i,c}}{2\gamma_{i,c}} \|\vartheta\|^2$.

Then we need to design control input u_i such that $\hat{\eta}_i$ will follow the virtual command η_i^c, i.e., stabilize the dynamic of error $z_{i,2}$. From (4.36) and (4.38), we have

$$\begin{aligned} z_{i,2}^T \dot{z}_{i,2} &= z_{i,2}^T \left(\dot{\hat{\eta}}_i - \dot{\eta}_i^c \right) \\ &= z_{i,2}^T \left[-\hat{R}_i \hat{\eta}_i + \hat{B}_i u_i + L_{i,2} \left(p_i - \hat{p}_i \right) - \dot{\eta}_i^c \right] \end{aligned} \tag{4.44}$$

$$\dot{\eta}_i^c = \frac{\partial \eta_i^c}{\partial \bar{p}_i} \dot{\bar{p}}_i + \frac{\partial \eta_i^c}{\partial \hat{\vartheta}_i} \dot{\hat{\vartheta}}_i + \frac{\partial \eta_i^c}{\partial p_i} J_i \left(\hat{\eta}_i + \tilde{\eta}_i \right) + \frac{\partial \eta_i^c}{\partial \phi_i} \bar{e}^T \left(\hat{\eta}_i + \tilde{\eta}_i \right) \tag{4.45}$$

where $\bar{e}^T = [0, 1]$.

Utilizing Young's inequality again, we can have

$$- z_{i,2}^T \frac{\partial \eta_i^c}{\partial p_i} J \tilde{\eta}_i \leq \frac{1}{2} z_{i,2}^T \frac{\partial \eta_i^c}{\partial p_i} J \left(\frac{\partial \eta_i^c}{\partial p_i} J \right)^T z_{i,2} + \frac{\tilde{\eta}_i^T \tilde{\eta}_i}{2} \tag{4.46}$$

$$- z_{i,2}^T \frac{\partial \eta_i^c}{\partial p_i} J \tilde{\eta}_i \leq \frac{1}{2} z_{i,2}^T \frac{\partial \eta_i^c}{\partial p_i} J \left(\frac{\partial \eta_i^c}{\partial p_i} J \right)^T z_{i,2} + \frac{\tilde{\eta}_i^T \tilde{\eta}_i}{2}. \tag{4.47}$$

Substituting (4.46) and (4.47) into (4.45) results in

$$z_{i,2}^T \dot{z}_{i,2} \leq z_{i,2}^T \left(\hat{B}_i u_i - g_i \right) + \tilde{\eta}_i^T \tilde{\eta}_i \tag{4.48}$$

where

$$\begin{aligned} g_i = & \frac{\partial \eta_i^c}{\partial \bar{p}_i} \dot{\bar{p}}_i + \frac{\partial \eta_i^c}{\partial \hat{\vartheta}_i} \dot{\hat{\vartheta}}_i + \frac{\partial \eta_i^c}{\partial p_i} J_i \hat{\eta}_i + \frac{\partial \eta_i^c}{\partial \phi_i} \bar{e}^T \hat{\eta}_i \\ & - \frac{1}{2} \frac{\partial \eta_i^c}{\partial p_i} J \left(\frac{\partial \eta_i^c}{\partial p_i} J \right)^T z_{i,2} - \frac{1}{2} \frac{\partial \eta_i^c}{\partial \phi_i} \left(\frac{\partial \eta_i^c}{\partial \phi_i} \right)^T z_{i,2} - L_{i,2} \left(p_i - \hat{p}_i \right) + \hat{R}_i \hat{\eta}_i \end{aligned}.$$

Based on (4.48), the control input u_i is finally designed as

$$u_i = \hat{B}_i^{-1} \left(-c_{i,2} z_{i,2} + g_i - J_i^T z_{i,1} \right) \tag{4.49}$$

where $c_{i,2}$ is a positive design parameter. Then choose a Lyapunov function as

$$V_{i,2} = V_{i,1} + \frac{1}{2} z_{i,2}^T z_{i,2}. \tag{4.50}$$

From (4.48) and (4.49), we can get the time derivative of $V_{i,2}$ as

$$\begin{aligned}\dot{V}_{i,2} &= \dot{V}_{i,1} + z_{i,2}^T \dot{z}_{i,2} \\ &\leq \dot{V}_{i,1} - c_{i,2} z_{i,2}^T z_{i,2} - z_{i,2}^T J_i^T z_{i,1} + \tilde{\eta}_i^T \tilde{\eta}_i \\ &\leq -\alpha_{i,1} \tilde{p}_i^T \tilde{p}_i - \alpha_{i,3} \tilde{\eta}_i^T \tilde{\eta}_i - c_{i,1} z_{i,1}^T z_{i,1} - c_{i,2} z_{i,2}^T z_{i,2} \\ &- \sum_{k=1}^{2} \left(\frac{\delta_{i,rk}}{2\gamma_{i,rk}} \tilde{R}_{i,k}^2 + \frac{\delta_{i,bk}}{2\gamma_{i,bk}} \tilde{B}_{i,k}^2 \right) - \frac{\delta_{i,c}}{2\gamma_{i,c}} \tilde{\vartheta}_i^T \tilde{\vartheta}_i + \ \Delta_i\end{aligned} \tag{4.51}$$

where $\alpha_{i,3} = \alpha_{i,2} - 1.5$, $\Delta_i = \Delta_{i,0} + \Delta_{i,1}$.

Remark 4.3. In trajectory tracking control, the tracking error is normally defined as $z = p - p_0$ and $\dot{p}_0$, $\ddot{p}_0$ are used in controller design based on backstepping technique. However, in this chapter, since the velocity and input information of the leader are unavailable, only estimation of the position information of the leader is obtained from the proposed adaptive estimator given in (4.6) and (4.7), i.e. $\bar{p}_i$. Then in controller design, to avoid the requirement of $\ddot{\bar{p}}_i$ in the design of u_i, the estimation of the bound of $\dot{\bar{p}}_i$ is employed to design the virtual command η_i^c in (4.38).

Now we are in the position to present our practical tracking results, as summarized in the following theorem.

Theorem 4.2. With the application of the estimator (4.6) and (4.7), the observer (4.25) and the controller (4.49) to the system modelled in (4.1) and (4.2), the boundedness of all the signals in the resulting closed-loop system is guaranteed in the presence of parametric uncertainty and external disturbances. Furthermore, it is ensured that $\|p_i - p_0\|$ will converge to a set which is adjustable by appropriately choosing design parameters.

Proof. (4.51) can be rewritten as

$$\dot{V}_{i,2} \leq -C_i \dot{V}_{i,2} + \Delta_i \tag{4.52}$$

where

$$C_i = \min(\frac{\alpha_{i,1}}{\lambda_{\min}(P_{i,1})}, \frac{\alpha_{i,3}}{\lambda_{\min}(P_{i,2})}, 2c_{i,1}, 2c_{i,2}, \delta_{i,rk}, \delta_{i,bk}, \delta_{i,c}).$$

From (4.52), we have

$$V_{i,2}(t) \leq V_{i,2}(0) e^{-C_i t} + \frac{\Delta_i}{C_i}(1 - e^{-C_i t}), \tag{4.53}$$

from which it can be concluded that all the signals in the resulting closed-loop system are bounded. Furthermore, we can obtain that

$$\lim_{t\to\infty} 2V_{i,2}(t) \leq \frac{2\Delta_i}{C_i}. \tag{4.54}$$

By selecting design parameters $P_{i,k}$, $c_{i,k}$, $\gamma_{i,c}$, $\gamma_{i,rk}$ and $\gamma_{i,bk}$ appropriately, then the bound $\sqrt{2\Delta_i/C_i}$ can be adjusted as small as desired for each robot.

From (4.54), we have $\|z_{i,1}\|^2 \leq \frac{2\Delta_i}{C_i}$. Then combing the results in Theorem 4.1, we can obtain that $\|p_i - p_0\|$ converges to a set

$$\Lambda = \{p_i - p_0 | \|p_i - p_0\| \leq \|p_i - \bar{p}_i\| + \|\bar{p}_i - p_0\| \leq \varepsilon\} \tag{4.55}$$

where

$$\varepsilon = \varepsilon_e + \max(\sqrt{2\Delta_i/C_i}),\ i = 1, 2, \cdots, N. \tag{4.56}$$

□

Remark 4.4. From the definition of $\sqrt{2\Delta_i/C_i}$, it can be noted that the ultimate bound of the tracking error of each robot depends on the constants Δ_i and C_i. Furthermore, decreasing $\sqrt{2\Delta_i/C_i}$ can be achieved by decreasing Δ_i and/or increasing C_i. From the expressions of Δ_i and C_i, it can be seen that they are mutually dependent as they share some common design parameters, such as $\delta_{i,rk}$, $\delta_{i,bk}$ and $\xi_{i,3}$, thus it is difficult to decrease $\sqrt{2\Delta_i/C_i}$ by adjusting these parameters. Therefore, it is possible to decrease Δ_i by increasing $\gamma_{i,c}$, $\gamma_{i,rk}$ and $\gamma_{i,bk}$, while increasing C_i can be achieved by increasing $\bar{c}_{i,1}$ and $c_{i,2}$.

4.3 Simulation

To verify the established theoretical results, simulation study has been carried out by considering a group of four identical WMRs with their physical parameters of corresponding SI units set as follows, $m_i = 30$, $I_{m,i} = 19$, $b_i = 0.5$, $a_i = 0.3$, $r_i = 0.1$, $N_i = 20$, $K_{b,i} = 0.019$, $K_{t,i} = 0.2639$ and $R_{a,i} = 1.6$. The disturbance is assumed as $\bar{\tau}_{d,i} = [\cos(\pi t/8), \sin(\pi t/8)]^T$ for simulation purpose, while it is unknown to designer. The communication topology of the group is shown in Figure2.

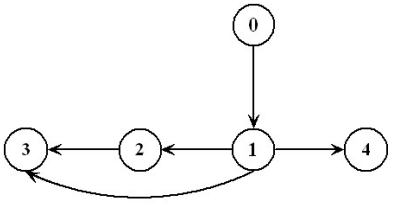

FIGURE 4.2: Communication topology of the 4 WMRs.

The initial positions and orientations of the four WMRs are chosen as $p_1(0) = [-1.5, -1, -0.6]^T$, $p_2(0) = [0, -4, 2]^T$, $p_3(0) = [-1.5, -4, 0.5]^T$, $p_4(0) = [-2.5, -3, 0.7]^T$.

The initial values of the estimator and the observer are respectively given as $\bar{p}_i(0) = p_i(0)$ and $\hat{\sigma}_i(0) = [0.2, 0.2]^T$, and $\hat{p}_i(0) = \hat{\eta}_i(0) = [0, 0]^T$, $\hat{R}_{i,1} = \hat{R}_{i,2} = 0$ and $\hat{B}_{i,1} = \hat{B}_{i,2} = 0.2$. For each robot, h_i is set as $h_i = 0.05$. The design parameters in the control scheme are chosen as follows, $c_0 = 4$, $P_{i,1} = I_2$, $P_{i,2} = 2I_2$, $L_{i,1} = 3I_2$, $\bar{c}_{i,1} = 1$, $c_{i,2} = 2$, $\delta_{1,r1} = \delta_{1,r2} = 0.1$, $\delta_{2,r1} = \delta_{2,r2} = 0.2$, $\delta_{3,r1} = \delta_{3,r2} = 0.4$, $\delta_{4,r1} = 0.1$, $\delta_{4,r2} = 0.4$, $\delta_{i,b1} = \delta_{i,b2} = 0.02$, $\gamma_{1,r1} = 4$, $\gamma_{1,r2} = 2$, $\gamma_{2,r1} = \gamma_{2,r2} = \gamma_{4,r1} = \gamma_{4,r2} = 2$, $\gamma_{3,r1} = 2$, $\gamma_{3,r2} = 1$, $\gamma_{1,b1} = \gamma_{1,b2} = \gamma_{2,b1} = \gamma_{2,b2} = 0.05$, $\gamma_{3,b1} = \gamma_{3,b2} = 0.08$, $\gamma_{4,b1} = \gamma_{4,b2} = 0.1$.

The simulation results are shown in Figure 4.3- Figure 4.10. The estimator errors $e_i = [e_{i,1}, e_{i,2}]^T$ and $\tilde{\sigma}_i = [\tilde{\sigma}_{i,1}, \tilde{\sigma}_{i,2}]^T$ are shown in Figure 4.3 and Figure 4.4 respectively, which show that the proposed estimator can estimate the position of the leader for each robot with bounded estimation error and thus effectively illustrate the results in Theorem 4.1. Utilizing the estimated position information from

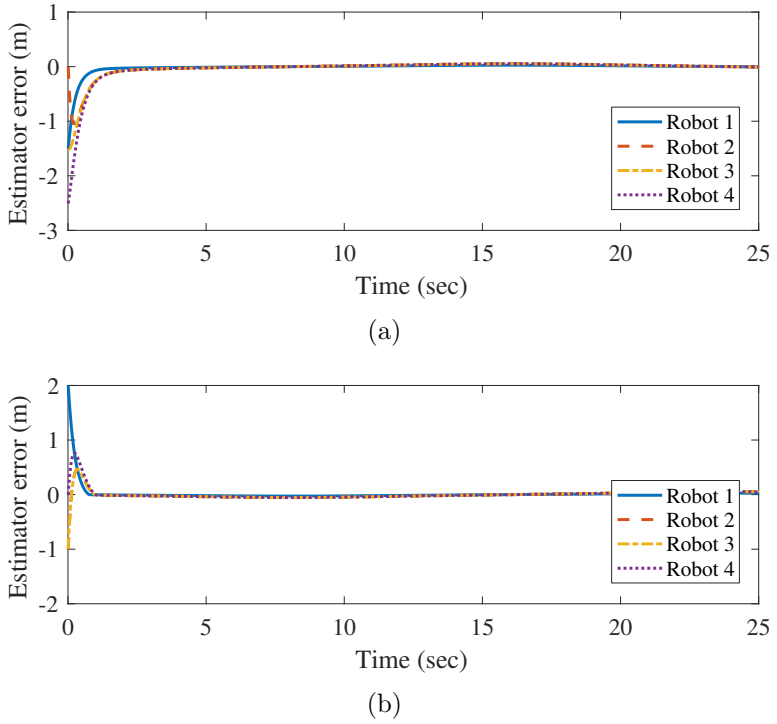

FIGURE 4.3: The estimation errors $e_i = [e_{i,1}, e_{i,2}]^T$ of four robots. Plots in (a) and (b) respectively show $e_{i,1}$ and $e_{i,2}$, $i = 1, 2, 3, 4$.

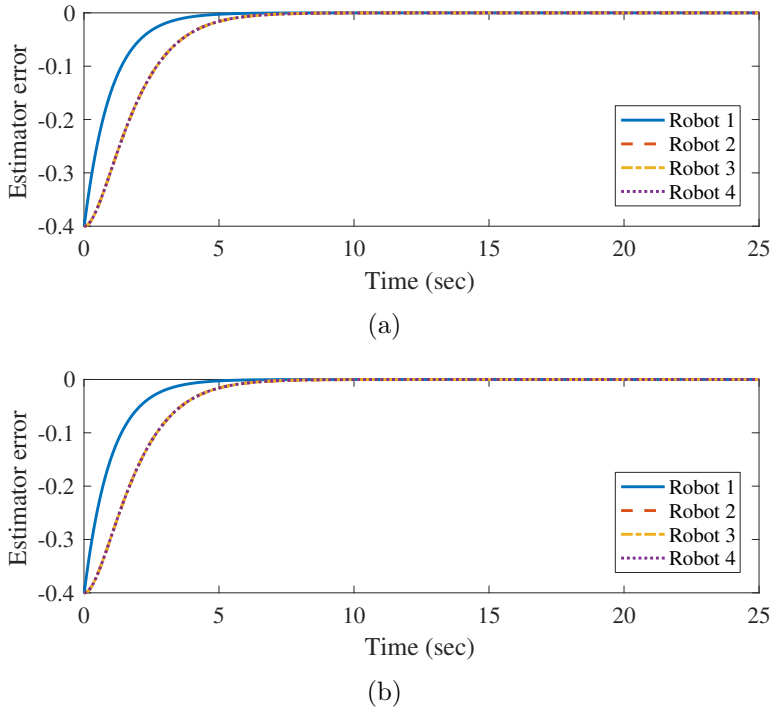

FIGURE 4.4: The estimation errors $\tilde{\sigma}_i$ of four robots. Plots in (a) and (b) respectively show $\tilde{\sigma}_{i,1}$ and $\tilde{\sigma}_{i,2}$, $i = 1, 2, 3, 4$.

the estimator, an observer-based controller is developed to address the parametric uncertainty and realize trajectory tracking control for each robot. The trajectories and tracking errors of four robots are illustrated in Figure 4.5 - Figure 4.6, from which, it can be seen that the consensus tracking performance can be achieved with the proposed control scheme and therefore the results of Theorem 4.2 are validated

.

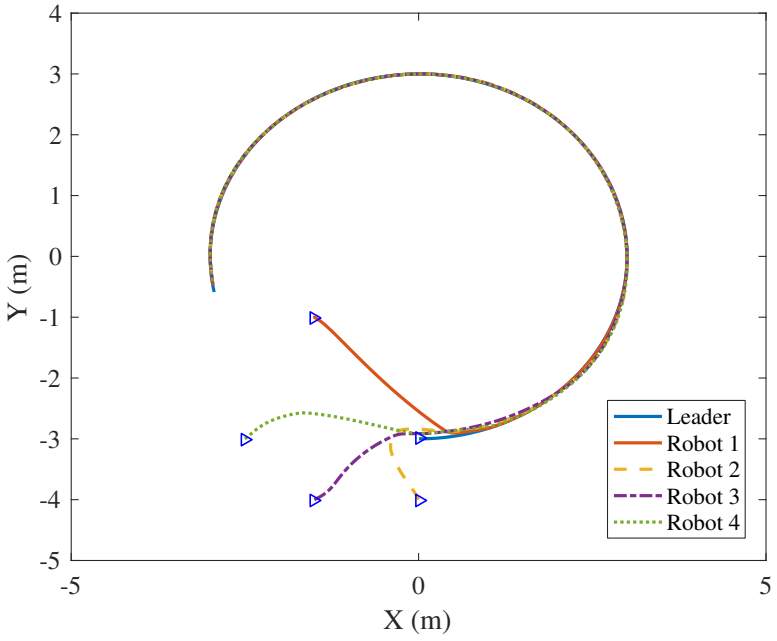

FIGURE 4.5: The trajectories of the four robots with the proposed output feedback control scheme. The triangles represent the initial positions of the leader and four robots.

To further demonstrate performances of the adaptive observer quantitatively, the observer errors are exhibited in Figure 4.7-4.8, from which it can be seen that all these errors are bounded.

To illustrate the discussion made in Remark 4.2 and 4.4, we also consider the following two cases:

Case 1: In terms of the designed estimator, change c_0 by setting $c_0 = 2$, 4 and 8 respectively, while other design parameters are fixed as the values given above.

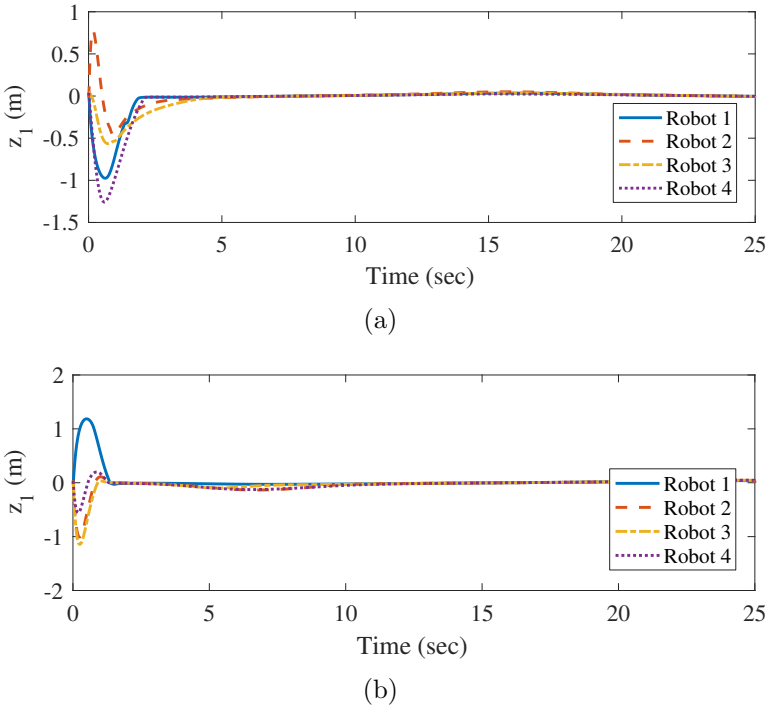

FIGURE 4.6: The tracking errors $z_{i,1} = [z_{i,11}, z_{i,12}]^T$ of four robots. Plots in (a) and (b) respectively show $z_{i,11}$ and $z_{i,12}$, $i = 1, 2, 3, 4$.

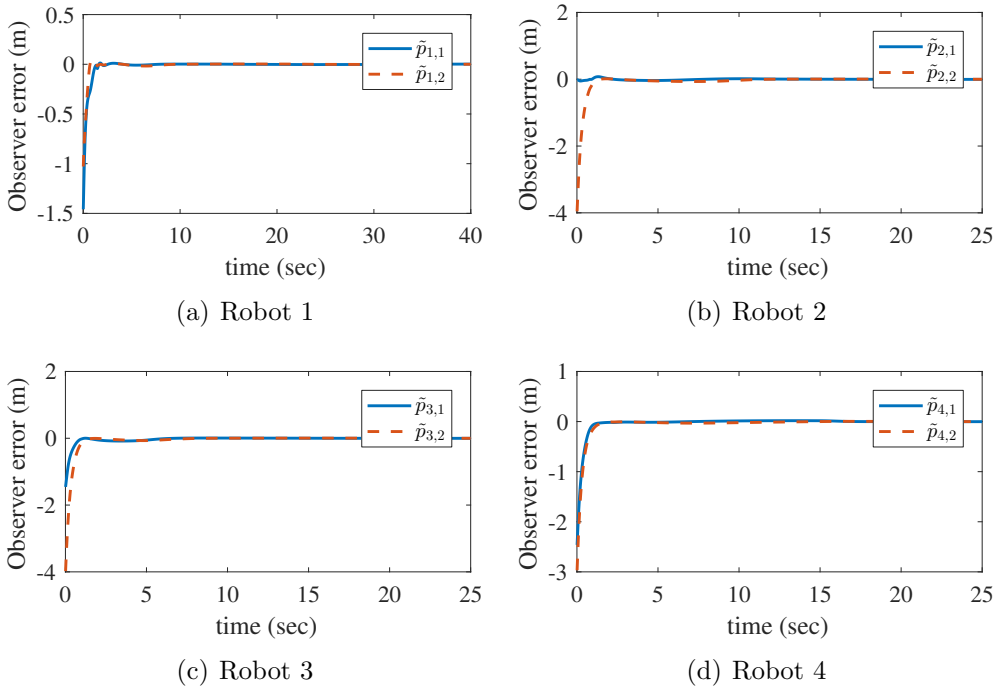

FIGURE 4.7: The observer errors $\tilde{p}_i = [\tilde{p}_{i,1}, \tilde{p}_{i,2}]^T$ of four robots, $i = 1, 2, 3, 4$.

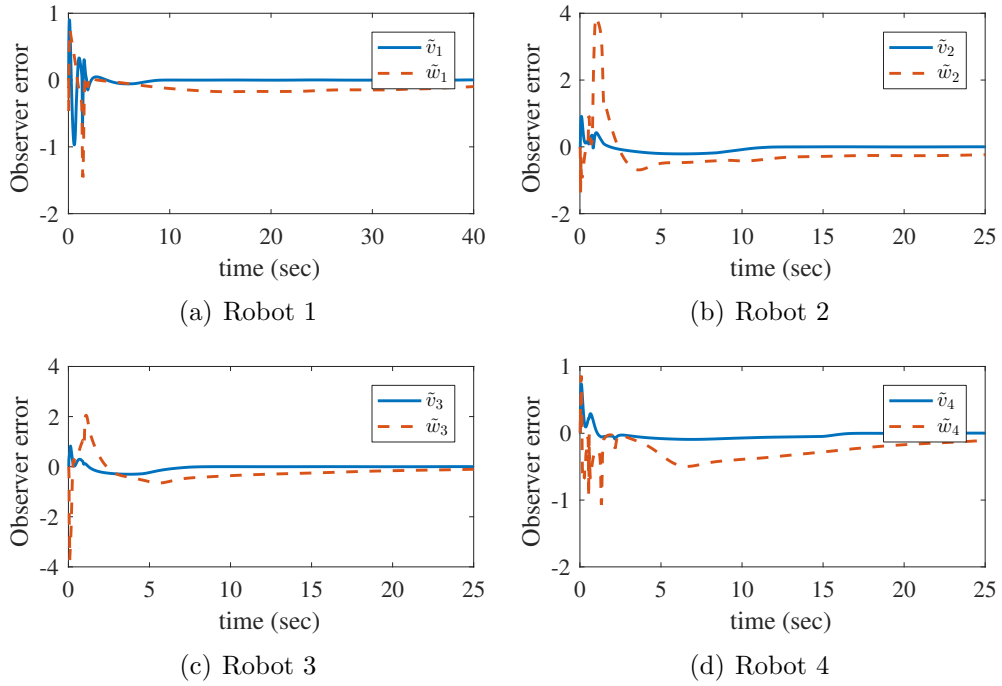

(a) Robot 1 (b) Robot 2

(c) Robot 3 (d) Robot 4

FIGURE 4.8: The observer errors $\tilde{\eta}_i = [\tilde{v}_i, \tilde{\omega}_i]^T$ of four robots, $i = 1, 2, 3, 4$.

Case 2: In terms of the observer-based controller, take Robot 1 as an example, vary $\gamma_{1,c}$ by setting $\gamma_{1,c} = 0.25$, 0.5 and 1.5 respectively, with the remaining design parameters the same as the values given earlier.

The estimation error of Robot 2 $e_{2,1}$ with different c_0 and the tracking error of Robot 1 $z_{1,11}$ with different $\gamma_{i,c}$ are respectively shown in Figure 4.9 and 4.10, from which it can be noted that the ultimate estimation error and tracking error decrease as c_0 and $\gamma_{i,c}$ increase.

4.4 Conclusion

In this chapter, distributed output feedback consensus tracking control is studied for multiple nonholonomic mobile robots under directed graph by using limited information of leader. Since only the position of the leader is available to a set of robots, a fully distributed estimator is firstly constructed to estimate the position of the leader for each robot without using any global information of the graph. Based

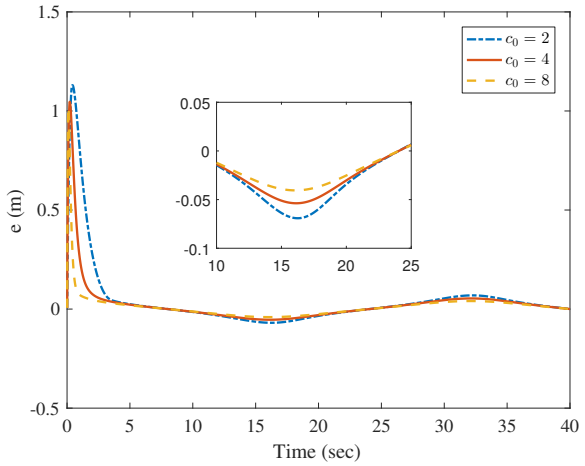

FIGURE 4.9: $e_{2,1}$ with different c_0.

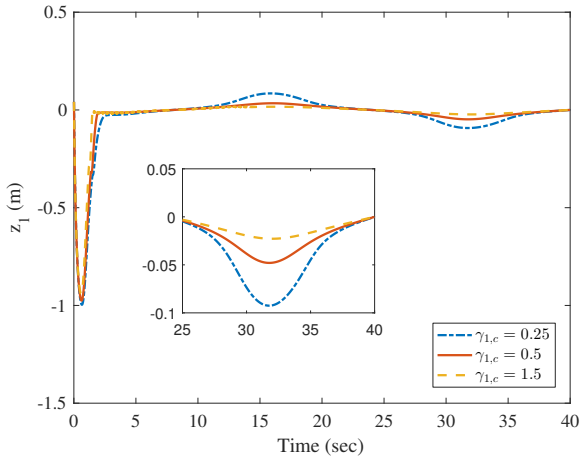

FIGURE 4.10: $z_{1,11}$ with different $\gamma_{1,c}$.

on the estimated position information, to realize trajectory tracking for each robot, an observer-based output feedback control law is designed based on backstepping technique. The proposed control scheme can guarantee the boundedness of all the signals in the resulting closed-loop system. Moreover, the consensus tracking error of the system can converge to an adjustable neighborhood of zero by appropriately choosing design parameters. The simulation results verify the effectiveness of the proposed control scheme.

Chapter 5

Adaptive Estimator-based Formation Maneuvering Control of Nonholonomic Mobile Robots

In the previous two chapters, distributed consensus tracking control problems are studied for multiple nonholonomic mobile robots. From this chapter onwards, another class of consensus problem of multi-agent systems, namely flocking with distance-based formation control problem, will be investigated. In this chapter, a control strategy consisting of an adaptive estimator and a modified gradient control law is designed to address distance-based formation shape and maneuvering control for a group of nonholonomic mobile robots under the condition that the desired maneuvering velocity is only known to a set of robots. The controller design involves two steps. Firstly, an adaptive estimator is designed for each robot to estimate the desired maneuvering velocity in either constant or time-varying situation. Secondly, utilizing the estimated velocity, a modified gradient control law is introduced to design linear and angular velocities based on the nonholonomic kinematic model such that all the robots converge to the desired formation shape and maneuvering velocity.

Consequently, the main contributions and novelty of this paper are summarized as follows:

- An adaptive estimator is proposed to estimate the desired maneuvering velocity, which can be either constant or time-varying and is only known to set of robots. It avoids to use different estimators to address constant and time-varying cases respectively as done in [113].
- With appropriate control parameters, local asymptotic convergence to the desired formation shape and maneuvering velocity is established for a group of mobile robots subject to nonholonomic constraint.

5.1 Problem Formulation

5.1.1 Basic concepts on graph

Consider an undirected graph with n vertices and m edges, denoted by $\mathcal{G} = (\mathcal{V}, \mathcal{E})$, where $\mathcal{V} = \{1, 2, \cdots, n\}$ denotes the set of vertices and $\mathcal{E} \subset \mathcal{V} \times \mathcal{V}$ is the set of edges between two distinct vertices. If $(i, j) \in \mathcal{E}$, agent j is called a neighbor of agent i. Hence the set of neighbors of agent i can be denoted as

$$\mathcal{N}_i = \{j \in \mathcal{V} | (i, j) \in \mathcal{E}\}.$$

Let $p_i \in \mathbb{R}^2$ denote the position assigned to vertex i. The stacked vector $p = \left[p_1^T, p_2^T, \cdots, p_n^T\right]^T \in \mathbb{R}^{2n}$ represents the realization of $\mathcal{G}$ in $\mathbb{R}^2$. A formation of $\mathcal{G}$ in $\mathbb{R}^2$ can be denoted by the pair $(\mathcal{G}, p)$. Based on an arbitrary ordering of the m edges in $\mathcal{E}$, the rigidity function $\psi_{\mathcal{G}}(p) : \mathbb{R}^{2n} \to \mathbb{R}^m$ associated with $(\mathcal{G}, p)$ is given as

$$\psi_{\mathcal{G}}(p) = \frac{1}{2}\left[\cdots, \|p_i - p_j\|^2, \cdots\right]^T, \ (i, j) \in \mathcal{E}$$

where $\|\cdot\|$ denotes the Euclidean norm. The rigidity of a formation is defined as follows.

Definition 5.1. [126] A formation $(\mathcal{G}, p)$ is rigid in $\mathbb{R}^2$ if there exists a neighborhood $\mathcal{U}$ of p such that $\psi_{\mathcal{G}}^{-1}\left[\psi_{\mathcal{G}}\left(p\right)\right] \cap \mathcal{U} = \psi_{\mathcal{K}}^{-1}\left[\psi_{\mathcal{K}}\left(p\right)\right] \cap \mathcal{U}$ where $\mathcal{K}$ is the complete graph of n vertices.

One useful tool to characterize the rigidity property of a formation is the rigidity matrix $R \in \mathbb{R}^{m \times 2n}$, which is defined as

$$R\left(p\right) = \frac{\partial \psi_{\mathcal{G}}\left(p\right)}{\partial p}.$$

Based on the rank property of $R(p)$, the infinitesimal rigidity of a formation is defined as follows.

Definition 5.2. [126] A formation $(\mathcal{G}, p)$, where $p \in \mathbb{R}^{2n}$ and $n \geq 3$, is infinitesimally rigid in 2D space if $rank[R(p)] = 2n - 3$.

Specifically, if the formation is infinitesimally rigid in $\mathbb{R}^2$ and has exactly $2n - 3$ edges, then it is called a minimally and infinitesimally rigid framework.

5.1.2 System model and problem formulation

Consider a group of n nonholonomic mobile robots modeled as follows,

$$\begin{bmatrix} \dot{x}_i \\ \dot{y}_i \\ \dot{\theta}_i \end{bmatrix} = \begin{bmatrix} \cos\theta_i & 0 \\ \sin\theta_i & 0 \\ 0 & 1 \end{bmatrix} \begin{bmatrix} v_i \\ \omega_i \end{bmatrix}, \quad \forall i \in \mathcal{V} \tag{5.1}$$

where $[x_i, y_i]^T = p_i \in \mathbb{R}^2$ and $\theta_i \in \mathbb{R}$ are the position and orientation of robot i, $v_i \in \mathbb{R}$ and $\omega_i \in \mathbb{R}$ are linear and angular velocities.

Suppose that the interactions and information transmission among the n robots are denoted as an undirected graph $\mathcal{G} = (\mathcal{V}, \mathcal{E})$. Robot i can measure the relative positions of its neighboring robots and obtain the information transmitted from them. Let formation $(\mathcal{G}, p^*)$ be the desired formation with desired distances $d =$

$(\cdots, d_{ij}, \cdots)$, $\forall (i,j) \in \mathcal{E}$ where $d_{ij} = \|p_i^* - p_j^*\|$. In this chapter, $(\mathcal{G}, p^*)$ is assumed to be an infinitesimally and minimally rigid formation in $\mathbb{R}^2$.

In terms of formation control, the objective is to realize the desired formation which is formulated by the desired distances d. Define the distance error between robot i and robot j as follows,

$$e_{ij} = \|p_i - p_j\|^2 - d_{ij}^2 \quad \forall (i,j) \in \mathcal{E} \tag{5.2}$$

From (5.2), the distance between robot i and robot j converging to d_{ij} is equivalent to the distance error e_{ij} converging to zero, i.e., $\|z_{ij}\| = d_{ij} \Leftrightarrow e_{ij} = 0$. Furthermore, to achieve an overall group maneuvering velocity, all the robots are required to maneuver with the same velocity, i.e. $\dot{p}_i = \mu_d, i \in \mathcal{V}$. In the formation, only a set of robots are supposed to have access to μ_d. Moreover, $\dot{\mu}_d = [\dot{\mu}_{d,1}, \dot{\mu}_{d,2}]^T$ is assumed to be bounded, i.e., $|\dot{\mu}_{d,1}| \leq \beta_1$ and $|\dot{\mu}_{d,2}| \leq \beta_2$ where $\beta_1 \geq 0$ and $\beta_2 \geq 0$ are unknown constants.

Therefore, the control problem in this chapter is formulated to design the linear and angular velocities, v_i and ω_i, for each robot such that,

$$e_{ij} \to 0, \ \forall (i,j) \in \mathcal{E}, \tag{5.3}$$

$$\dot{p}_i \to \mu_d \quad \forall i \in \mathcal{V}. \tag{5.4}$$

5.2 Controller Design

The controller design can be divided into two steps. In the first step, an adaptive estimator is designed to estimate the desired maneuvering velocity for each robot. In the second step, utilizing the estimated velocity, a modified control law is proposed to design the linear and angular velocities in such a way that e_{ij} will converge to zero and $\dot{p}_i$ will converge to the desired maneuvering velocity.

5.2.1 Adaptive estimator design

Motivated by [113], the following estimator is designed to estimate μ_d for each agent,

$$\dot{\hat{\mu}}_i = -\alpha\vartheta_i - D_i sgn\left(\vartheta_i\right) \tag{5.5}$$

where $\vartheta_i = \sum_{j\in\mathcal{N}_i}\left(\hat{\mu}_i - \hat{\mu}_j\right) + a_i\left(\hat{\mu}_i - \mu_d\right)$, $D_i = \text{diag}\left(\hat{\beta}_i\right)$ with $\hat{\beta}_i$ being the estimation of $\beta = [\beta_1, \beta_2]^T$ of agent i. α is a positive design parameter, and $a_i = 1$ if robot i has access to μ_d and otherwise $a_i = 0$. Define the estimation errors as $\tilde{\mu}_i = \hat{\mu}_i - \mu_d$ and $\tilde{\beta}_i = \hat{\beta}_i - \beta$ and let $\tilde{\mu} = [\tilde{\mu}_1^T, \tilde{\mu}_2^T, \cdots, \tilde{\mu}_n^T]^T$, $\hat{\beta} = [\hat{\beta}_1^T, \hat{\beta}_2^T, \cdots, \hat{\beta}_n^T]^T$, $\tilde{\beta} = [\tilde{\beta}_1^T, \tilde{\beta}_2^T, \cdots, \tilde{\beta}_n^T]^T$ and $D = diag(\hat{\beta})$. Then we can have the following estimation error dynamics,

$$\begin{aligned}\dot{\tilde{\mu}} &= -\alpha\left[\left(\mathcal{L}\otimes I_2\right)\tilde{\mu} + \left(B\otimes I_2\right)\tilde{\mu}\right] - Dsgn\left[\left(\mathcal{L}\otimes I_2\right)\tilde{\mu} + \left(B\otimes I_2\right)\tilde{\mu}\right] - 1_n\otimes\dot{\mu}_d \\ &= -\alpha\left(H\otimes I_2\right)\tilde{\mu} - Dsgn\left[\left(H\otimes I_2\right)\tilde{\mu}\right] - 1_n\otimes\dot{\mu}_d\end{aligned} \tag{5.6}$$

where $\mathcal{L}$ is the Laplacian matrix associated with graph $\mathcal{G}$, $B = diag(b_1, b_2, \cdots, b_n)$ with at least one nonzero b_i, and $H \triangleq \mathcal{L} + B$. Since $\mathcal{G}$ is rigid, it is connected and H is positive definite [127].

Consider the Lyapunov function

$$V_0 = \frac{1}{2}\tilde{\mu}^T\left(H\otimes I_2\right)\tilde{\mu} + \frac{1}{2\gamma}\tilde{\beta}^T\tilde{\beta}. \tag{5.7}$$

The time derivative of V_0 can be computed as

$$\begin{aligned}\dot{V}_0 &= \tilde{\mu}^T\left(H\otimes I_2\right)\dot{\tilde{\mu}} + \frac{1}{\gamma}\tilde{\beta}^T\dot{\tilde{\beta}} \\ &= -\alpha\tilde{\mu}^T\left(H\otimes I_2\right)^2\tilde{\mu} - \tilde{\mu}^T\left(H\otimes I_2\right)Dsgn\left[\left(H\otimes I_2\right)\tilde{\mu}\right] \\ &- \tilde{\mu}^T\left(H\otimes I_2\right)\left(1_n\otimes\dot{\mu}_d\right) + \frac{1}{\gamma}\tilde{\beta}^T\dot{\hat{\beta}} \\ &\leq -\alpha\tilde{\mu}^T\left(H\otimes I_2\right)^2\tilde{\mu} - \hat{\beta}^T\left|\left(H\otimes I_2\right)\tilde{\mu}\right| + \left|\tilde{\mu}^T\left(H\otimes I_2\right)\right|\left(1_n\otimes\beta\right) + \frac{1}{\gamma}\tilde{\beta}^T\dot{\hat{\beta}} \\ &\leq -\alpha\tilde{\mu}^T\left(H\otimes I_2\right)^2\tilde{\mu} - \tilde{\beta}^T\left|\left(H\otimes I_2\right)\tilde{\mu}\right| + \frac{1}{\gamma}\tilde{\beta}^T\dot{\hat{\beta}}\end{aligned} \tag{5.8}$$

The update law for $\hat{\beta}_i$ is designed as follows,

$$\dot{\hat{\beta}}_i = \gamma \left| \vartheta_i \right| \tag{5.9}$$

which yields,

$$\dot{\hat{\beta}} = \gamma \left| \left(H \otimes I_2 \right) \tilde{\mu} \right| \tag{5.10}$$

Substituting (5.10) into (5.8) yields,

$$\begin{aligned} \dot{V}_0 &\leq -\alpha \tilde{\mu}^T \left(H \otimes I_2 \right)^2 \tilde{\mu} \\ &\leq -\alpha \lambda_{\min} \tilde{\mu}^T \tilde{\mu} \end{aligned} \tag{5.11}$$

where $\lambda_{\min}$ is the minimum eigenvalue of matrix $(H \otimes I_2)^2$.

Remark 5.1. Note that for the robots with $b_i = 0$, the only information available about the desired maneuvering velocity is $|\dot{\mu}_{d,1}| \leq \beta_1$ and $|\dot{\mu}_{d,2}| \leq \beta_2$ with β_1 and β_2 being unknown constants. Such a condition is much weaker than that in [128] where $\dot{\mu}$ is linearly parameterized and the corresponding basis functions are known by all the robots in the group. Unlike designing two different estimators to respectively estimate time-varying and constant μ_d in [113], in this chapter, the proposed adaptive estimator can perform well for both constant and time-varying μ_d, which will be proved hereinafter. Furthermore, the upper bounds of $\dot{\mu}_d$, β_1 and β_2 which are supposed to be known in [113], are unknown and would be estimated and compensated by adaptive technique in this chapter.

5.2.2 Modified gradient controller design

Utilizing the estimated velocity $\hat{\mu}$, we need to design linear and angular velocities for each robot to realize the formulated objective. Consider the following Lyapunov function

$$V_1 = V_0 + \frac{1}{4} \sum_{(i,j) \in \mathcal{E}} e_{ij}^2. \tag{5.12}$$

Then the time derivative of V_1 is given as

$$\begin{aligned}\dot{V}_1 &= \dot{V}_0 + \sum_{(i,j)\in\mathcal{E}} e_{ij}\left(p_i - p_j\right)^T\left(\dot{p}_i - \dot{p}_j\right) \\ &= \dot{V}_0 + \sum_{i\in\mathcal{V}} \phi_i^T \dot{p}_i\end{aligned} \tag{5.13}$$

where $\phi_i = \sum_{j\in\mathcal{N}_i} e_{ij}\left(p_i - p_j\right)$.

Note that the kinematics of nonholonomic mobile robots in (5.1) is a nonlinear model. To realize exact linearization for controller design, we firstly introduce a virtual gradient control law $\dot{p}_i^c$ that involves the estimated maneuvering velocity $\hat{\mu}_i$ as follows,

$$\dot{p}_i^c = \begin{bmatrix} \dot{p}_{i,1}^c \\ \dot{p}_{i,2}^c \end{bmatrix} = -k\phi_i + \hat{\mu}_i \tag{5.14}$$

where k is a positive design parameter. To make ϕ_i converge to zero and $\dot{p}_i$ converge to $\hat{\mu}_i$, it requires to design v_i and ω_i such that,

$$\dot{p}_i = v_i h_i = \dot{p}_i^c \tag{5.15}$$

where $h_i = [\cos\theta_i, \sin\theta_i]^T$. Define the deviation between $\dot{p}_i$ and $\dot{p}_i^c$ as $\varepsilon_i = v_i h_i - \dot{p}_i^c$. Thus, the control objective can be expressed as to make ε_i converge to zero. Then we introduce the following relationship,

$$\begin{bmatrix} h_i^T \\ \left(h_i^\perp\right)^T \end{bmatrix} \varepsilon_i = \begin{bmatrix} v_i - h_i^T \dot{p}_i^c \\ -\left(h_i^\perp\right)^T \dot{p}_i^c \end{bmatrix} \tag{5.16}$$

where $h_i^\perp = [-\sin\theta_i, \cos\theta_i]^T$. Note that h_i is perpendicular to $h_i^\perp$. Since the matrix on the left side of above equation is nonsingular, $v_i - h_i^T \dot{p}_i^c$ and $\left(h_i^\perp\right)^T \dot{p}_i^c$ converging to zero is equivalent to ε_i converging to zero.

Thus, to make sure ε_i converge to zero, the linear velocity can be designed as,

$$v_i = h_i^T \dot{p}_i^c. \tag{5.17}$$

Furthermore, from (5.16), it is required that

$$\left(h_i^{\perp}\right)^T \dot{p}_i^c = \|\dot{p}_i^c\| \sin\tilde{\theta}_i = 0 \tag{5.18}$$

where $\tilde{\theta}_i = \theta_i^c - \theta_i$ and $\theta_i^c = atan2\left(\dot{p}_{i,2}^c, \dot{p}_{i,1}^c\right)$, which indicates we should have $\sin\tilde{\theta}_i = 0$.

With the control command v_i, the nonholonomic model in (5.1) can be expressed as

$$\begin{aligned} \dot{p}_{i,1} &= v_i \cos\theta_i \\ &= \dot{p}_{i,1}^c \cos^2\theta_i + \dot{p}_{i,2}^c \cos\theta_i \sin\theta_i \\ &= \dot{p}_{i,1}^c - \left(\dot{p}_{i,1}^c \sin\theta_i - \dot{p}_{i,2}^c \cos\theta_i\right) \sin\theta_i \\ &= \dot{p}_{i,1}^c + \|\dot{p}_i^c\| \sin\tilde{\theta}_i \sin\theta_i \end{aligned} \tag{5.19}$$

and

$$\begin{aligned} \dot{p}_{i,2} &= v_i \sin\theta_i \\ &= \dot{p}_{i,1}^c \cos\theta_i \sin\theta_i + \dot{p}_{i,2}^c \sin^2\theta_i \\ &= \dot{p}_{i,2}^c + \left(\dot{p}_{i,1}^c \sin\theta_i - \dot{p}_{i,2}^c \cos\theta_i\right) \cos\theta_i \\ &= \dot{p}_{i,2}^c - \|\dot{p}_i^c\| \sin\tilde{\theta}_i \cos\theta_i \end{aligned}, \tag{5.20}$$

which can be summarized as

$$\dot{p}_i = \dot{p}_i^c - \|\dot{p}_i^c\| \sin\tilde{\theta}_i h_i^{\perp}. \tag{5.21}$$

Therefore, (5.13) can be rewritten as

$$\begin{aligned} \dot{V}_1 &= \dot{V}_0 + \sum_{i\in\mathcal{V}} \phi_i^T \left(\dot{p}_i^c + \|\dot{p}_i^c\| \sin\tilde{\theta}_i h_i^{\perp}\right) \\ &= \dot{V}_0 + \sum_{i\in\mathcal{V}} \left(-k\phi_i^T\phi_i + \phi_i^T\hat{\mu}_i - \|\dot{p}_i^c\| \phi_i^T h_i^{\perp} \sin\tilde{\theta}_i\right) \end{aligned} \tag{5.22}$$

Next, in terms of ω_i, it will be designed to ensure $\sin\tilde{\theta}_i \to 0$ by considering the following Lyapunov function

$$V_2 = V_1 + \left(1 - \cos\tilde{\theta}_i\right). \tag{5.23}$$

Then the time derivative of V_2 can be given as

$$\dot{V}_2 = \dot{V}_0 + \sum_{i\in\mathcal{V}} \left(-k\phi_i^T\phi_i + \phi_i^T\hat{\mu}_i\right) + \sum_{i\in\mathcal{V}} \left(\dot{\theta}_i^c - \omega_i - \|\dot{p}_i^c\|\phi_i^T h_i^\perp\right)\sin\tilde{\theta}_i. \tag{5.24}$$

Choosing the following angular velocity

$$\omega_i = k_\theta \sin\tilde{\theta}_i - \|\dot{p}_i^c\|\phi_i^T h_i^\perp + \dot{\theta}_i^c \tag{5.25}$$

we can have,

$$\begin{aligned} \dot{V}_2 &= \dot{V}_0 + \sum_{i\in\mathcal{V}} \left(-k\phi_i^T\phi_i - k_\theta \sin^2\tilde{\theta}_i + \phi_i^T\hat{\mu}_i\right) \\ &\leq -\alpha\lambda_{\min}\tilde{v}^T\tilde{v} - k\phi^T\phi - k_\theta\eta^T\eta + \phi^T\hat{\mu} \end{aligned} \tag{5.26}$$

where $\phi = [\phi_1^T, \phi_2^T, \cdots, \phi_n^T]^T$ and $\eta = [\sin\tilde{\theta}_1, \sin\tilde{\theta}_2, \cdots, \sin\tilde{\theta}_n]^T$.

Remark 5.2. Based on the virtual gradient control law in (5.14) and the transformation in (5.16), linearization is realized by designing the linear and angular velocity as in (5.17) and (5.25). Unlike the controller design without linearization in [129, 130] which can only ensure formation shape stabilization, distance-based formation maneuvering can be achieved with the modified gradient based controller design in this chapter.

Let $\xi = \left[q^T, \tilde{\mu}^T, \tilde{\beta}^T\right]^T$, where $q = [q_1^T, q_2^T, \cdots, q_n^T]^T$ with $q_i = [x_i, y_i, \theta_i]^T$, and define a level set $\Omega(r) = \{\xi : V_2(\xi) \leq r\}$ where $r > 0$. The main results are stated in the following theorem.

Theorem 5.1. For a group of nonholonomic mobile robots modeled by (5.1), under the control of designed linear and angular velocities respectively in (5.17) and (5.25) with the estimator (5.12), if $\xi(0) \in \Omega(r_0)$ with $r_0 > 0$ and the design parameters

are according to the conditions that

$$\alpha\lambda_{\min} > \frac{1}{2}, k > \frac{1}{2}, \tag{5.27}$$

asymptotic convergence of the system to the desired formation $(\mathcal{G}, p^*)$ and an overall maneuvering velocity μ_d is ensured.

Proof. Since $\phi = R(p)^T e$ with $e = [\cdots, e_{ij}, \cdots]^T$, and $\tilde{\mu} = \hat{\mu} - (1_n \otimes \mu_d)$, from the property of $R(p)$, it can be obtained that $e^T R(p)(1_n \otimes \mu_d) = 0$. Then it follows that,

$$\begin{aligned} \dot{V}_2 &\leq -\alpha\lambda_{\min}\|\tilde{\mu}\|^2 - k\|e^T R(p)\|^2 - k_\theta\|\eta\|^2 + e^T R(p)\tilde{\mu} \\ &\leq -\left(\alpha\lambda_{\min} - \frac{1}{2}\right)\|\tilde{\mu}\|^2 - \left(k - \frac{1}{2}\right)\|e^T R(p)\|^2 \\ &\quad - k_\theta\|\eta\|^2 \leq 0 \end{aligned} \tag{5.28}$$

Since $\dot{V}_2 \leq 0$, $\Omega(V_2(\xi(0))) \subseteq \Omega(r_0)$ is positively invariant. Let $\mathcal{M} = \{\xi : V_2(\xi) = 0\}$, the system starting from any point in $\Omega(V_2(\xi(0)))$ converges to the largest invariant set in $\mathcal{M} \cap \Omega(V_2(\xi(0)))$ by the invariance principle [131]. Then from (5.28) we can get $\|\tilde{\mu}\| \to 0$, $\|e^T R(p)\| \to 0$ and $\|\eta\| \to 0$. For some sufficiently small r_0 and for all points in the set $\Omega(r)$, the formation $(\mathcal{G}, p)$ is minimally infinitesimally rigid and close to the desired formation, which implies that $R(p)$ is of full row rank [126, 132]. Under this condition, it can be obtained that $R(p)^T e = 0 \Rightarrow e = 0$, i.e., the system asymptotically converges to the desired formation. From (5.14) and (5.15), it can be obtained that $\dot{p}_i \to \hat{\mu}_i$. Since $\tilde{\mu} \to 0$, it follows that $\dot{p}_i \to \mu_d$. In summary, under the proposed control scheme, the system asymptotically converges to the desired formation and maneuvering velocity.

□

5.3 Simulation

To verify the established theoretical results, simulation study has been carried out. In the simulation, a group of four unicycle mobile robots is considered. The desired formation is a square as shown in Figure 1 with the robots located at the four vertices. There are five edges as shown in the figure. It can be verified that the formation is minimally infinitesimally rigid. Besides, the desired distances between robots that represent the desired formation are set as $d_{12} = d_{14} = d_{23} = d_{34} = 2$ and $d_{13} = 2\sqrt{2}$. In the formation, only robot 1 and robot 2 have access to μ_d, i.e. $a_1 = a_3 = 1$ and $a_2 = a_4 = 0$. The units of all variables are the SI units.

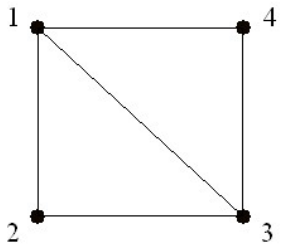

FIGURE 5.1: The desired formation.

The initial positions and orientations of the four robots are set as $q_1(0) = [1.35, 3.05, 0.785]^T$, $q_2(0) = [0.36, 0.52, -0.785]^T$, $q_3(0) = [2.81, 0.125, 0]^T$ and $q_4(0) = [3.32, 2.61, -1.571]^T$. The proposed control scheme consists of an adaptive estimator and a modified gradient controller. The initial estimations, $\hat{\mu}_i(0)$ and $\hat{\beta}_i(0)$, are set as zero. Furthermore, according to (5.27), the control parameters are designed as $\alpha = 12$, $\gamma = 0.8$, $k = 1$ and $k_\theta = 3$.

In the simulation, both time-varying and constant maneuvering velocities are taken into account to demonstrate the effectiveness of the proposed control scheme.

5.3.1 Case 1: time-varying case

In the time-varying case, μ_d is set as

$$\mu_d(t) = \begin{bmatrix} 2 + 0.5\sin(0.15t) \\ 1.5\cos(0.15t) \end{bmatrix}.$$

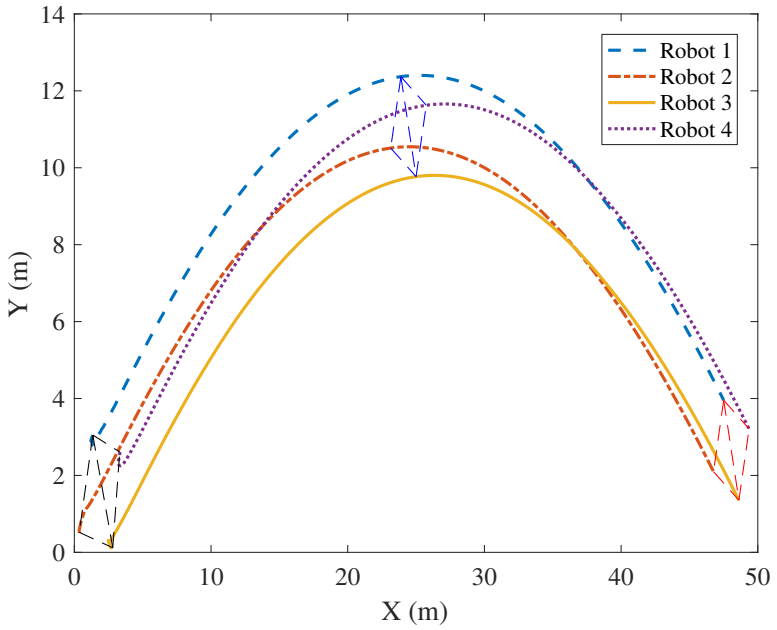

FIGURE 5.2: The trajectories of the four robots. Black, blue and red shapes denote the formation shapes of the system at $0s$, $10s$ and $20s$, respectively.

Overall, the trajectories of the four robots are shown in Figure 5.2, from which, it can be seen that the four robots achieve and maintain the formation during their motions. The estimation errors $\tilde{\mu}_i$ of the proposed estimator are shown in Figure 5.3, from which it can been shown that the proposed estimator can estimate the desired maneuvering velocity for each robot.

Now the performance of the controller is assessed. The formation shape control performance in terms of distance errors e_{ij}, $\forall (i,j) \in \mathcal{E}$ is illustrated in Figure 5.4. As observed from the figure, the distance errors between pairs of robots converge to zero, which means the system converge to the desired formation. Additionally, in terms of the maneuvering velocities of four robots $\dot{p}_i = [\dot{x}_i, \dot{y}_i]^T$, which are shown

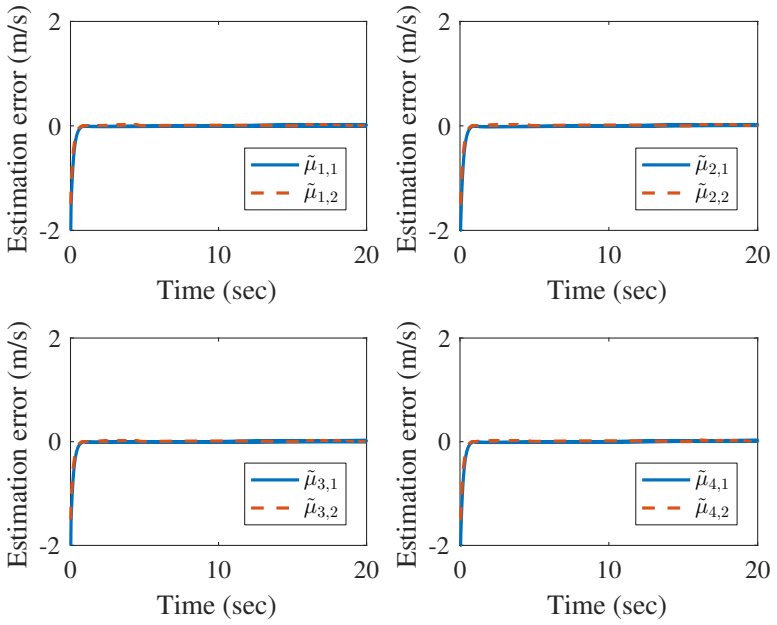

FIGURE 5.3: The estimation error $\tilde{\mu}_{i,j}$, $i = 1, 2, 3, 4$, $j = 1, 2$.

in Figure 5.5, it can be found that all agents approach the desired maneuvering velocity and then maintain this velocity with the proposed controller.

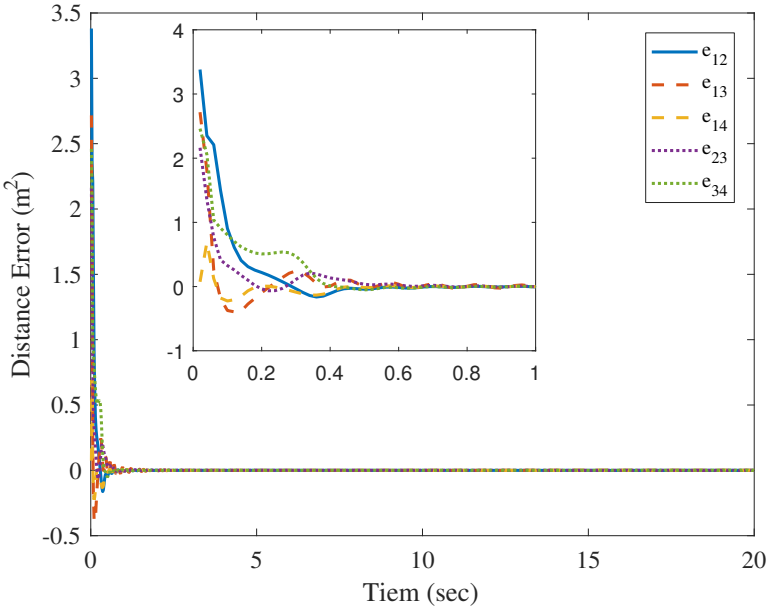

FIGURE 5.4: The distance errors between pairs of robots.

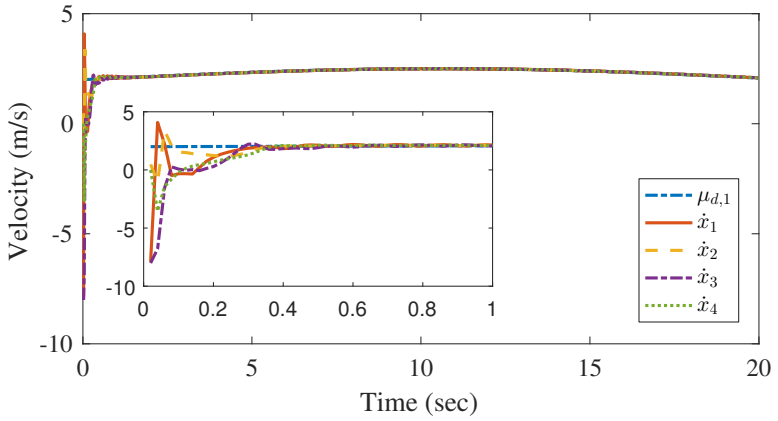

(a)

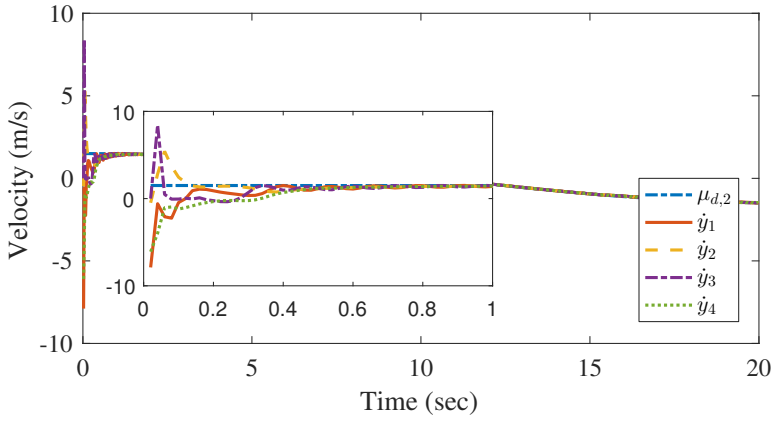

(b)

FIGURE 5.5: The maneuvering velocities $\dot{p}_i = [\dot{x}_i, \dot{y}_i]^T$ of four robots. Figures in (a) and (b) respectively show $\dot{x}_i$ and $\dot{y}_i$, $i = 1, 2, 3, 4$.

5.3.2 Case 2: constant case

In the constant case, μ_d is set as $\mu_d = [1.5, 1.5]^T$.

The trajectories of the four robots are shown in Figure 5.6, from which, it can also be seen that the four robots achieve and maintain the formation during their motions. Meanwhile, the distance errors between pairs of agents converge to zero as observed from Figure 5.7. Additionally, as can be seen in Figure 5.8, all agents approach the desired maneuvering velocity.

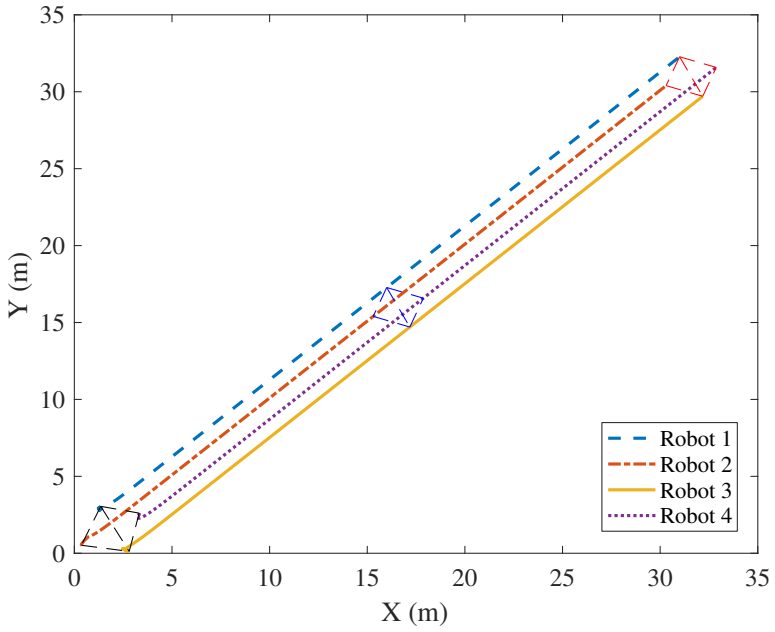

FIGURE 5.6: The trajectories of the four robots.

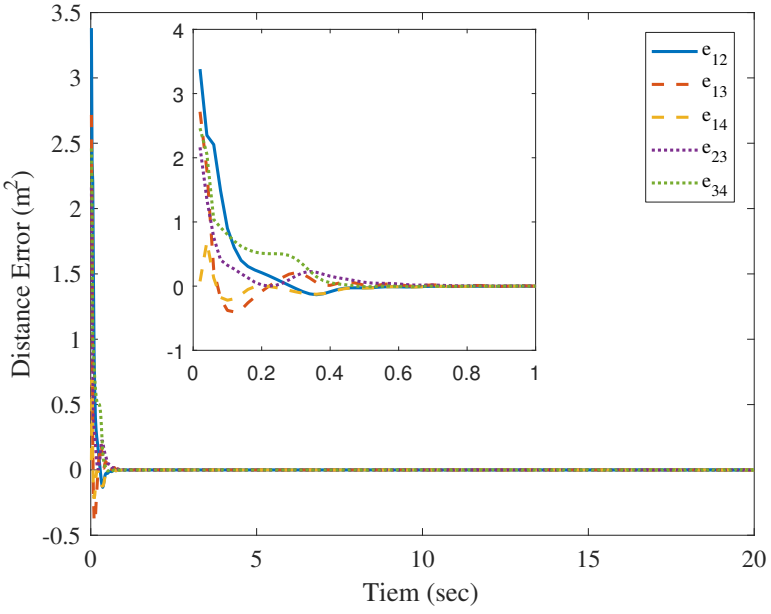

FIGURE 5.7: The distance errors between pairs of robots.

5.4 Conclusion

An adaptive control scheme for formation maneuvering control of mobile robots subject to nonholonomic constraint is proposed in this chapter. The control objective is to achieve the desired distance-based formation shape and a overall maneuvering velocity, which can be either constant or time-varying. The control scheme

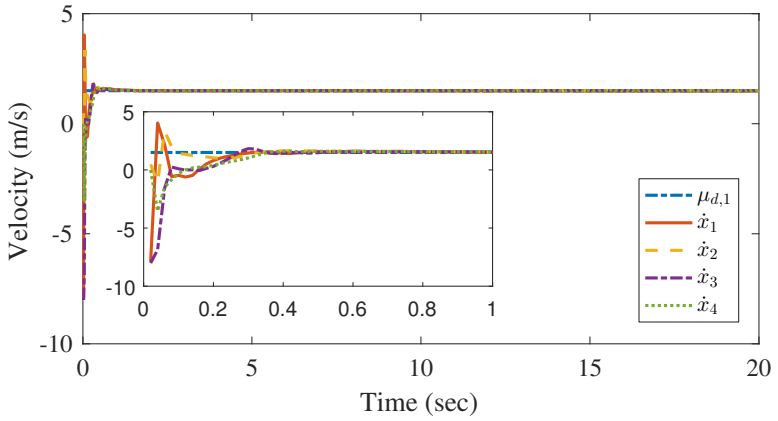

(a)

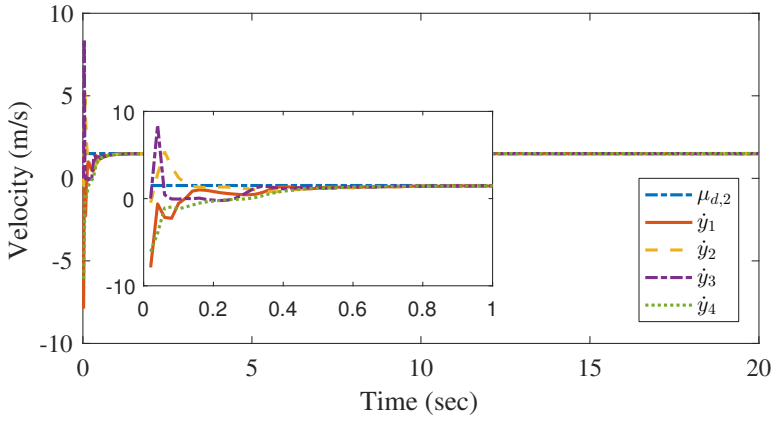

(b)

FIGURE 5.8: The maneuvering velocities $\dot{p}_i$ of four robots. Figures in (a) and (b) respectively show $\dot{x}_i$ and $\dot{y}_i$, $i = 1, 2, 3, 4$

.

consists of two main steps. In the first step, an adaptive estimator is designed to estimate the desired maneuvering velocity for each robot. In the second step, utilizing the estimated velocity, a modified gradient control law is designed based on the nonholonomic kinematics to ensure the system achieve the desired formation shape and maneuver with the desired velocity. Choosing appropriate control parameters, local asymptotic convergence of the system is established. Meanwhile, simulation study is carried out to verify the effectiveness of the proposed control scheme.

Chapter 6

Distributed Adaptive Control for Distance-based Formation and Flocking control of Multi-Agent Systems

In the previous chapter, flocking with distance-based formation control of multiple nonholonomic mobile robots with undirected formation shape graph is addressed. However, the proposed control scheme can only be applied to first-order dynamics without parametric uncertainty under undirected formation shape graph. In this chapter, an adaptive control strategy for distance-based formation and flocking control of multi-agent systems is proposed. Since it is really difficult to consider general directed graphs, similar to most existing works, we focus on minimally persistent graph. We first study a system with LFF type triangular structure, which means the system only consists of three agents, i.e., the leader with time-varying velocity, the first follower and the follower. The three agents are modeled by nonidentical second-order dynamics with parametric uncertainty. To solve our formulated problem, adaptive technique is employed to estimate and compensate for the unknown parameters. Furthermore, by introducing two new variables that

involve distance error and velocity error and utilizing them in the controller design, it is established that all agents in the formation globally converge to the desired formation and to the velocity of the leader. Then, the LFF type system is inductively extended to N-agent system, in which the proposed control strategy can be applied.

Consequently, the contributions and novelty of this paper are summarized as follows:

- Global convergence of all agents in the system to the desired formation and to the time-varying velocity of the leader is achieved simultaneously.
- The agents are modeled as nonidentical second-order dynamics with parametric uncertainty. In controller design, adaptive update laws are designed to estimate and compensate for the unknown parameters.

6.1 Problem Formulation

Consider a group of N agents moving in the 2D Euclidean space, which can be modeled as follows,

$$\begin{aligned} \dot{p}_i &= v_i \\ \dot{v}_i &= u_i + \varphi_i \left(v_i\right)^T \theta_i \end{aligned} \qquad \forall i \in \mathcal{V} \tag{6.1}$$

where $p_i \in \Re^2$, $v_i \in \Re^2$ and $u_i \in \Re^2$ are the position, velocity and input of agent i. $\theta_i \in \Re^{l_i}$ is a vector of unknown constants and $\varphi_i(v_i)$ is a matrix with appropriate dimensions of known smooth nonlinear functions. The system model described in (6.1) allows the agents to have nonidentical dynamics with parametric uncertainty. Clearly this class of systems is more general than those described as single- or double-integrator in most of existing work including [1, 2, 118] and those exactly known second-order dynamics in [133].

Suppose that the interactions and information transmission among the N agents can be modeled by a directed graph $\mathcal{G}$. In distance-based formation control, the

objective is to realize the desired formation which is formulated by the desired distances between agents. For a given graph $\mathcal{G}$, the desired distances are given as $d = (\cdots, d_{ij}, \cdots),\ \forall (i,j) \in \mathcal{E}$ where $d_{ij} > 0$ is the desired distance between agent i and agent j. In this chapter, $z_{ij} \in \Re^2$ and e_{ij} are respectively defined as the relative position and the distance error as follows,

$$z_{ij} = p_i - p_j \quad \forall (i,j) \in \mathcal{E} \tag{6.2}$$

$$e_{ij} = \|z_{ij}\|^2 - d_{ij}^2 \quad \forall (i,j) \in \mathcal{E} \tag{6.3}$$

From (6.3), the distance between agent i and agent j converging to d_{ij} is equivalent to the distance error e_{ij} converging to zero, i.e., $\|z_{ij}\| = d_{ij} \Leftrightarrow e_{ij} = 0$. Therefore, to achieve the desired formation shape, it is required to make all of e_{ij} converge to zero. Furthermore, assign Agent 1 as the leader, to achieve the flocking behavior, the other agents are required to approach the velocity of the leader. Thus, the control objective of this paper can be expressed as designing controller for each agent such that

$$\tilde{v}_{1i} \to 0 \quad \forall i \in \mathcal{V},\ i \neq 1 \tag{6.4}$$

$$\|z_{ij}\| \to d_{ij} \quad \forall (i,j) \in \mathcal{E} \tag{6.5}$$

where $\tilde{v}_{1i} = v_1 - v_i$ is the velocity error between agent 1 and agent i.

Firstly, we focus on the multi-agent system with LFF type triangular structure, as shown in Figure 6.1 where Agent 1 is assigned as the leader, Agent 2 is called the first follower and Agent 3 is the follower. The leader is supposed to perform the following dynamics by human operator or self-navigation,

$$\begin{aligned} \dot{x}_1(t) &= v_1(t) \\ \dot{v}_1(t) &= a_1(t). \end{aligned} \tag{6.6}$$

In this case, the velocity of the leader is time-varying.

Remark 6.1. Note that global convergence for distance-based formation control of an LFF system is achieved in [1], but it assumes each agent to be a single

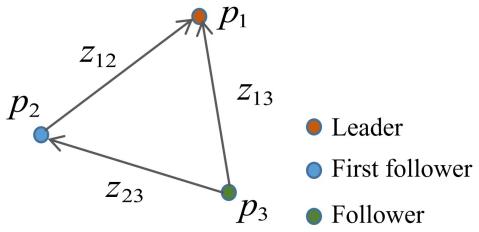

FIGURE 6.1: The system setup of LFF in Cartesian coordinates (Taken from [1]).

integrator and the velocity of the leader is a constant vector. Furthermore, it is pointed out that extending such simple dynamics to high-order dynamic systems is very complicated. As addressed in [2, 120], for distance-based formation control of agents modeled as double-integrators, there is no complete solution that can ensure a global convergence for a group of agents in the constant or time-varying leading velocity case. Thus, it is actually an important yet difficult problem to achieve global stability for agents with unknown second-order dynamics in the case that the leading velocity is time-varying.

To solve the mentioned distance-based formation and flocking control problem of a LFF system, we need the following assumptions:

Assumption 6.1. The information, $v_1(0)$ and $a_1(t)$ expressed in (6.6), of the leader can be obtained by all the agents in the formation. Moreover, $v_1(t)$ and $a_1(t)$ are assumed to be bounded.

Assumption 6.1 is equivalent to that $v_1(t)$ is known, as it can be derived from $v_1(0)$ and $a_1(t)$. Actually, for the case of double-integrator agents in [112] and [2], the velocity of the leader is also assumed to be known, but it is a constant which implies a_1 is 0.

Assumption 6.2. The desired formation for the system given in Figure 1 is realizable. The necessary and sufficient condition for the existence of a realization is given as follows,

$$d_{12} < d_{13} + d_{23}$$
$$d_{23} < d_{12} + d_{13}$$
$$d_{13} < d_{12} + d_{23}$$

Assumption 6.3. [1, 114] The desired formation is minimally persistent obtained as the result of a Henneberg sequence.

6.2 Controller Design

In this section, the control laws for the first follower and follower in the LFF system will be designed separately, and then the extension of LFF system to N-agent system will be derived.

6.2.1 Controller Design for the First Follower

Introduce a new variable $\bar{v}_{12} = \tilde{v}_{12} + k_{p2}h_2$ where

$$h_2 = e_{12}z_{12}, \tag{6.7}$$

k_{p2} is a positive design parameter.

Remark 6.2. The introduction of variable $\bar{v}_{12}$ is a key technique to achieve global stability in the proposed control strategy. Note that, $\bar{v}_{12}$ involves distance error e_{12} and velocity error $\tilde{v}_{12}$. If $\bar{v}_{12} \to 0$ and $h_2 \to 0$, then $\tilde{v}_{12} \to 0$. Utilizing $\bar{v}_{12}$, the proposed controller makes h_2 and the velocity error $\tilde{v}_{12}$ converge to zero, which will be established subsequently. Afterwards, based on the stability analysis, it can be proved that the first follower will converge to the desired formation by choosing appropriate control parameters.

Firstly we derive an adaptive law to estimate the unknown parameter in the dynamic model of the first follower. Define $\hat{\theta}_2$ as the estimate of θ_2.

Choose a Lyapunov function candidate as

$$V_2 = \frac{1}{4}e_{12}^2 + \frac{1}{2}\bar{v}_{12}^T\bar{v}_{12} + \frac{1}{2}\tilde{\theta}_2^T\Gamma_2\tilde{\theta}_2 \tag{6.8}$$

where $\tilde{\theta}_2 = \theta_2 - \hat{\theta}_2$ and Γ_2 is a user defined positive definite matrix with appropriate dimension. Then, the time derivative of V_2 can be computed as

$$\begin{aligned}\dot{V}_2 &= \frac{1}{2}e_{12}\dot{e}_{12} + \bar{v}_{12}^T\dot{\bar{v}}_{12} + \tilde{\theta}_2^T\Gamma_2\dot{\tilde{\theta}}_2 \\ &= e_{12}z_{12}^T\left(\bar{v}_{12} - k_{p2}h_2\right) + \bar{v}_{12}^T(a_1 - u_2 - \varphi_2^T\theta_2 + k_{p2}\dot{h}_2) - \tilde{\theta}_2^T\Gamma_2\dot{\hat{\theta}}_2.\end{aligned} \tag{6.9}$$

Based on (6.9), the control law and the parameter update law are designed as

$$u_2 = k_{v2}\bar{v}_{12} + a_1 - \varphi_2^T\hat{\theta}_2 + k_{p2}\dot{h}_2 + h_2 \tag{6.10}$$

$$\dot{\hat{\theta}}_2 = -\Gamma_2^{-1}\varphi_2\bar{v}_{12} \tag{6.11}$$

where k_{v2} is a positive design parameter and from (6.7)

$$\dot{h}_2 = 2z_{12}z_{12}^T\tilde{v}_{12} + e_{12}\tilde{v}_{12}. \tag{6.12}$$

Substituting (6.10) and (6.11) into (6.9) yields

$$\dot{V}_2 = -k_{p2}\|h_2\|^2 - k_{v2}\|\bar{v}_{12}\|^2 \leq 0 \tag{6.13}$$

Lemma 6.1. With the application of control law (6.10) and parameter update law (6.11) to the first follower, all the signals in the resulted closed-loop system are bounded. In addition, h_2 and the velocity error $\tilde{v}_{12}$ asymptotically converge to zero, i.e., $h_2 \to 0$ and $\tilde{v}_{12} \to 0$ as $t \to \infty$.

Proof. From (6.8) and (6.13), it can be obtained that $V_2 \geq 0$ and $\dot{V}_2 \leq 0$, therefore, e_{12}, z_{12}, $\bar{v}_{12}$, $\tilde{v}_{12}$ and $\hat{\theta}_2$ are bounded. Then, based on (6.9) and (6.13), it can be established that $\ddot{V}_2$ is bounded. By applying Barbalat's lemma [131], we can obtain $\dot{V}_2 \to 0$, i.e.,

$$\lim_{t\to\infty}\left(\|h_2\| + \|\bar{v}_{12}\|\right) = 0 \tag{6.14}$$

Hence, the asymptotic convergence of the velocity error (i.e., $\tilde{v}_{12} \to 0$ as $t \to \infty$) can be derived from (6.7). □

Remark 6.3. It should be noted that with the existing distance-based gradient control, the results in Lemma 6.1 cannot be obtained. Technically, if applying such an approach here, the following Lyapunov function would be considered

$$W = \frac{1}{4}e_{12}^2 + \frac{1}{2}\tilde{v}_{12}^T\tilde{v}_{12} + \frac{1}{2}\tilde{\theta}_2^T\Gamma_2\tilde{\theta}_2$$

which could yield the control law and parameter update law as $u_2 = k_{v2}\bar{v}_{12} + e_{12}z_{12} + a_1 - \varphi_2^T\hat{\theta}_2$ and $\dot{\hat{\theta}}_2 = -\Gamma_2^{-1}\varphi_2\tilde{v}_{12}$, respectively. Then the resulting time derivative of W would be

$$\dot{W} = -k_{v2}\tilde{v}_{12}^T\tilde{v}_{12} \leq 0,$$

from which only the global convergence of $\tilde{v}_{12}$ to zero could be obtained. In this chapter, based on the introduction of the new variable $\bar{v}_{12}$, the proposed control law (6.10) with parameter update law (6.11) ensures the asymptotic convergence of both h_2 and $\tilde{v}_{12}$, which is crucial in establishing the global convergence of the follower to the desired formation and to the velocity of the leader, as seen in the following analysis.

Lemma 6.2. The states of the first follower converge to one of the following two equilibrium points,

$$1)\ \ e_{12} = 0,\ \tilde{v}_{12} = 0; \tag{6.15}$$

$$2)\ \ z_{12} = 0,\ \tilde{v}_{12} = 0. \tag{6.16}$$

Proof. Based on Lemma 6.1, $e_{12}z_{12}$ and $\tilde{v}_{12}$ converge to zero. From the definition of e_{12} in (6.3), it can be found that e_{12} and z_{12} cannot be zero at the same time. Therefore, the states of the first follower can only converge to one of the two equilibrium points: $e_{12} = 0$ and $\tilde{v}_{12} = 0$ or $z_{12} = 0$ and $\tilde{v}_{12} = 0$. □

From Lemma 6.2, there are two global equilibrium points in the solution space and the one in (6.15) is the desired equilibrium point. If the equilibrium point (6.16) is unstable, then from Lemma 6.2 the other one (6.15) is globally stable which will ensure the first follower converges to the desired formation. By analyzing the

stability of the system and choosing the design parameters appropriately, this can be achieved, as summarized in following theorem.

Theorem 6.1. The convergence of the first follower to the desired formation, i.e., $e_{12} \to 0$ and $\tilde{v}_{12} \to 0$ as $t \to \infty$, is ensured by the control law (6.10) and parameter update law (6.11) with the design parameters k_{p2} and k_{v2} chosen according to the following guideline,

$$k_{p2} d_{12}^2 - k_{v2} > 0.$$

Proof of Theorem 6.1. Define $\phi = [\phi_1^T \ \phi_2^T]^T = [z_{12}^T \ \tilde{v}_{12}^T]^T$ and consider the following dynamics:

$$\begin{aligned}
\dot{\phi}_1 &= \tilde{v}_{12} = f_1 \\
\dot{\phi}_2 &= -\varphi_2^T \tilde{\theta}_2 - k_{v2} \bar{v}_{12} - k_{p2} \dot{h}_2 - h_2 = f_2.
\end{aligned}$$

Let $f = [f_1^T \ f_2^T]^T$. To analyze the stability of the equilibrium point (6.16), the above dynamics is linearized as follows,

$$\begin{aligned}
\left.\frac{\partial f}{\partial \phi}\right|_{\phi=0} &= \left.\begin{bmatrix} \frac{\partial f_1}{\partial \phi_1} & \frac{\partial f_1}{\partial \phi_2} \\ \frac{\partial f_2}{\partial \phi_1} & \frac{\partial f_2}{\partial \phi_2} \end{bmatrix}\right|_{\phi=0} \\
&= \begin{bmatrix} O_{2\times 2} & I_2 \\ \gamma_{21} I_2 & \gamma_{22} I_2 \end{bmatrix} = A.
\end{aligned}$$

where $\gamma_{21} = (k_{p2} k_{v2} + 1)\, d_{12}^2$ and $\gamma_{22} = k_{p2} d_{12}^2 - k_{v2}$. Calculating $\det(\lambda I_4 - A) = 0$, the characteristic equation of matrix A is given as

$$\lambda^4 - 2\gamma_{22}\lambda^3 + \left(\gamma_{22}^2 - 2\gamma_{21}\right)\lambda^2 + 2\gamma_{21}\gamma_{22}\lambda + \gamma_{21}^2 = 0 \tag{6.17}$$

Utilizing the Routh-Hurwitz stability criterion, it can be obtained that, there is at least one solution which has positive real part if $\gamma_{22} > 0$. Therefore, if k_{p2} and k_{v2} are chosen such that $k_{p2} d_{12}^2 - k_{v2} > 0$, the equilibrium point (6.16) is unstable. In this case, since the system is asymptotically stable from Lemma 6.1, the other equilibrium point (6.15) is globally stable. It means that the first follower will

converge to the desired formation stated in (6.4) and (6.5) if k_{p2} and k_{v2} satisfy $k_{p2}d_{12}^2 - k_{v2} > 0$. □

Remark 6.4. The above proof process is a common way to analyze the stability of such systems which has been used in [116] and [1]. However, in contrast to the approach there, we need to consider how to choose appropriate control parameters based on the stability analysis to make sure that only the equilibrium point (6.15) is stable in this chapter.

6.2.2 Controller Design for the Follower

Using a similar controller design process as done for the first follower, a new variable $\bar{v}_{13} = \tilde{v}_{13} + k_{p3}h_3$ is firstly introduced for the follower by defining

$$h_3 = e_{13}z_{13} + e_{23}z_{23} \tag{6.18}$$

where k_{p3} is a positive design parameter. It can also be noted that, if $\bar{v}_{13} \to 0$ and $h_3 \to 0$, then $\tilde{v}_{13} \to 0$.

The control law and parameter update laws for the follower are designed as

$$u_3 = k_{v3}\bar{v}_{13} + a_1 - \varphi_3^T\hat{\theta}_3 + k_{p3}\dot{h}_3 + h_3 \tag{6.19}$$

$$\dot{\hat{\theta}}_3 = -\Gamma_3^{-1}\varphi_3\bar{v}_{13} \tag{6.20}$$

where k_{v3} is another positive design parameter, Γ_3 is also a user defined positive definite matrix with appropriate dimension, $\hat{\theta}_3$ is the estimate of θ_3, and based on (6.18)

$$\dot{h}_3 = 2z_{13}z_{13}^T\tilde{v}_{13} + e_{13}\tilde{v}_{13} + 2z_{23}z_{23}^T(v_2 - v_3) + e_{23}(v_2 - v_3), \tag{6.21}$$

in which v_2 is the velocity of the first follower.

To analyze the stability of the proposed controller for the follower, consider the following Lyapunov function,

$$V_3 = \frac{1}{4}e_{13}^2 + \frac{1}{4}e_{23}^2 + \frac{1}{2}\bar{v}_{13}^T\bar{v}_{13} + \frac{1}{2}\tilde{\theta}_3^T\Gamma_3\tilde{\theta}_3 \tag{6.22}$$

where $\tilde{\theta}_3 = \theta_3 - \hat{\theta}_3$.

Then, the time derivative of V_3 is given as

$$\begin{aligned}
\dot{V}_3 &= \frac{1}{2}e_{13}\dot{e}_{13} + \frac{1}{2}e_{23}\dot{e}_{23} + \bar{v}_{13}^T\dot{\bar{v}}_{13} + \tilde{\theta}_3^T\Gamma_3\dot{\tilde{\theta}}_3 \\
&= e_{13}z_{13}^T\tilde{v}_{13} + e_{23}z_{23}^T\left(\tilde{v}_{13} - \tilde{v}_{12}\right) - \tilde{\theta}_3^T\Gamma_3\dot{\hat{\theta}}_3 \\
&+ \bar{v}_{13}^T\left(a_1 - u_3 - \varphi_3^T\theta_3 + k_{p3}\dot{h}_3\right) \\
&= -k_{p3}\left(e_{13}z_{13}^T + e_{23}z_{23}^T\right)h_3 - e_{23}z_{23}^T\tilde{v}_{12} \\
&- \bar{v}_{13}^T\varphi_3^T\tilde{\theta}_3 - k_{v3}\bar{v}_{13}^T\bar{v}_{13} - \tilde{\theta}_3^T\Gamma_3\dot{\hat{\theta}}_3 \\
&= -k_{p3}\|h_3\|^2 - k_{v3}\|\bar{v}_{13}\|^2 - e_{23}z_{23}^T\tilde{v}_{12} \\
&\leq -k_{p3}\|h_3\|^2 - k_{v3}\|\bar{v}_{13}\|^2 + \|e_{23}z_{23}\|\|\tilde{v}_{12}\|.
\end{aligned} \tag{6.23}$$

Lemma 6.3. [1] Applying the proposed control (6.19) and parameter update law (6.20) to the follower, all the signals in the resulted closed-loop system are bounded.

Lemma 6.4. $\|h_3\|$ and $\|\bar{v}_{13}\|$ shown in (6.23) converge to zero, i.e., $\|h_3\| \to 0$ and $\|\bar{v}_{13}\| \to 0$, as $t \to \infty$.

Proof. From Lemma 6.3, V_3 is bounded, thus, there exists $\eta > 0$ such that $\|e_{23}z_{23}\| < \eta$. Furthermore from Lemma 6.1, $\tilde{v}_{12} \to 0$ as $t \to \infty$. Therefore, for any $\epsilon > 0$, there exists $T > 0$ such that $\|\tilde{v}_{12}\| < \epsilon$ when $t > T$. Then, it can be obtained that for $t > T$

$$-\mu(t) - \zeta < \dot{V}_3 < -\mu(t) + \zeta$$

where $\mu(t) = k_{p3}\|h_3\|^2 + k_{v3}\|\bar{v}_{13}\|^2$ and $\zeta = \epsilon\eta$. If $\lim_{t\to\infty}\mu(t) = 0$, then the proof is completed. Otherwise, $\dot{V}_3 \leq 0$ for all sufficiently large t. Therefore, V_3 is a decreasing function and

$$\lim_{t\to\infty} V_3 = M \geq 0$$

Hence, applying Barbalat's lemma, it can be obtained that $\dot{V}_3 \to 0$, then $\lim_{t\to\infty}\|h_3\| = 0$ and $\lim_{t\to\infty}\|\tilde{v}_{13}\| = 0$. □

As it is proved that $\|h_3\|$ and $\|\bar{v}_{13}\|$ converge to zero in Lemma 6.4, and moreover, it is obvious that e_{13} (e_{23}) and z_{13} (z_{23}) cannot be zero at the same time, the states of the follower will converge to one the following three equilibrium points:

$$1)\ \ e_{13} \neq 0,\ z_{13} = -\frac{e_{23}}{e_{13}} z_{23},\ \tilde{v}_{13} = 0; \tag{6.24}$$

$$2)\ \ e_{23} \neq 0,\ z_{23} = -\frac{e_{13}}{e_{23}} z_{13},\ \tilde{v}_{13} = 0; \tag{6.25}$$

$$3)\ \ e_{13} = 0,\ e_{23} = 0,\ \tilde{v}_{13} = 0. \tag{6.26}$$

Note that, the equilibrium point (6.26) represents the desired formation of the follower. Therefore, the convergence of the follower to the desired formation is equivalent to that the equilibrium points (6.24) and (6.25) are unstable. Applying a similar proof process as done for the first follower, we will show that the equilibrium points (6.24) and (6.25) are unstable. Before proceeding with stability analysis, the following two lemmas are presented.

Lemma 6.5. [1] When the states of the follower converge to the equilibrium point (6.24) or (6.25), it can be obtained that $z_{13,1}z_{23,2} - z_{13,2}z_{23,1}$, where $z_{13} = [z_{13,1}\ z_{13,2}]^T$ and $z_{23} = [z_{23,1}\ z_{23,2}]^T$.

Lemma 6.6. [134] When the states of the follower converge to the equilibrium point (6.24) or (6.25) and further $e_{12} = 0$, it can be obtained that $e_{13} + e_{23} < 0$.

Then we can establish the results presented in following theorem.

Theorem 6.2. Under the control law (6.19) with parameter update law (6.20), the follower converges to the desired formation, i.e., $e_{13} \to 0$, $e_{23} \to 0$ and $\tilde{v}_{13} \to 0$ as $t \to \infty$.

Proof of Theorem 6.2. Define $\psi = [\psi_1^T \ \psi_2^T]^T = [z_{13}^T \ z_{23}^T]^T$, hence, the dynamics of ψ can be given as follows:

$$\ddot{\psi}_1 = -\varphi_3^T\tilde{\theta}_3 - k_{v3}\bar{v}_{13} - k_{p3}\dot{h}_3 - h_3 = g_1$$
$$\ddot{\psi}_2 = u_2 + \varphi_2^T\theta_2 - a_1 - \varphi_3^T\tilde{\theta}_3 - k_{v3}\bar{v}_{13} - k_{p3}\dot{h}_3 - h_3 = g_2.$$

Let $g = [g_1^T \ g_2^T]^T$, the following Jacobian matrix can be obtained

$$\frac{\partial g}{\partial \psi} = \begin{bmatrix} \frac{\partial g_1}{\partial \psi_1} & \frac{\partial g_1}{\partial \psi_2} \\ \frac{\partial g_2}{\partial \psi_1} & \frac{\partial g_2}{\partial \psi_2} \end{bmatrix} = B.$$

From Lemma 6.1 and Lemma 6.4, $\tilde{v}_{12} \to 0$ and $\tilde{v}_{13} \to 0$, hence, $v_2 - v_3 (= \tilde{v}_{13} - \tilde{v}_{12}) \to 0$. To analyze the stability of the equilibrium points (6.24) and (6.25), substituting $\tilde{v}_{13} = 0$ and $v_2 - v_3 = 0$ into the above Jacobian matrix, we have,

$$B = -k \begin{bmatrix} \gamma_{31} & \gamma_{32} \\ \gamma_{31} & \gamma_{32} \end{bmatrix}$$

where $k = k_{p3}k_{v3} + 1$, $\gamma_{31} = e_{13}I_2 + 2z_{13}z_{13}^T$ and $\gamma_{32} = e_{23}I_2 + 2z_{23}z_{23}^T$. Therefore, the characteristic equation of matrix B can be calculated as

$$\lambda^4 + ks_1\lambda^3 + k^2\left(s_2 + s_3\right)\lambda^2 = 0 \tag{6.27}$$

where

$s_1 = 2\left(e_{13} + e_{23} + \|z_{13}\|^2 + \|z_{23}\|^2\right)$,

$s_2 = \left(e_{13} + e_{23}\right)\left(e_{13} + e_{23} + 2\|z_{13}\|^2 + 2\|z_{23}\|^2\right)$,

$s_3 = 4\left(z_{13,1}z_{23,2} - z_{13,1}z_{23,2}\right)^2$.

According to Lemma 6.5, $z_{13,1}z_{23,2} - z_{13,1}z_{23,2} = 0$, i.e., $s_3 = 0$. Therefore, the above characteristic equation can be rewritten as follows,

$$\lambda^4 + k\left(\alpha + \beta\right)\lambda^3 + k^2\alpha\beta\lambda^2 = 0 \tag{6.28}$$

where $\alpha = e_{13} + e_{23}$ and $\beta = e_{13} + e_{23} + 2\|z_{13}\|^2 + 2\|z_{23}\|^2$.

In Theorem 6.1, the convergence of e_{12} is proved. From Lemma 6.6, if the states of the system reach the equilibrium point (6.24) or (6.25) and further $e_{12} = 0$, then $\alpha < 0$. The system is unstable if at least one of the solutions of the above characteristic equation has positive real part. According to the Routh-Hurwitz stability criterion, the stability of the system with characteristic equation (6.28) is related to the sign of $k(\alpha + \beta)$ and $k^2\alpha\beta$. Since $\alpha < 0$ and $k > 0$, we consider the following three cases to analyze the stability of the system:

- 1) $\beta > 0$

  Thus $k^2\alpha\beta < 0$, there is at least one solution that has positive real part.

- 2) $\beta < 0$

  Thus $k(\alpha + \beta) < 0$, there is at least one solution that has positive real part.

- 3) $\beta = 0$

  Thus $k(\alpha + \beta) < 0$ and $k^2\alpha\beta = 0$, there is one solution that has positive real part.

In conclusion, when the states of the system converge to the equilibrium point (6.24) or (6.25), at least one solution of (6.28) has positive real part, hence, the equilibrium points (6.24) and (6.25) are unstable. Therefore, the states of the follower will converge to the equilibrium point (6.26). □

Combining Theorem 6.1 and Theorem 6.2, it can be concluded that, the proposed control strategy makes the LFF system converge to the desired formation and to the velocity of the leader as described in (6.4) and (6.5).

6.2.3 Extension to N-agent Case

In the previous parts, global convergence of an LFF system to the desired formation and to the velocity of the leader is proved. Now the convergence of an

N-agent system to the desired formation can be inferred inductively. Without loss of generality, similar to the inductive procedure done in [1], taking the LFF system as a base case, a cycle-free persistent graph $\mathcal{G}$ is obtained as the result of a Henneberg sequence containing only vertex additions. Technically, agent 4 is obtained by adding an agent into graph of LFF using Henneberg sequence, and the resulted graph is still cycle-free persistent graph, subsequent agents are added one by one similarly.

An example of $\mathcal{G}$ for an extended 5-agent system is shown in Figure 6.2. The control law (6.19) with parameter update law (6.20) designed for the follower can be applied to the added agent i as,

$$\begin{aligned} u_i &= k_{vi}\bar{v}_{1i} + u_1 + \varphi_1^T\hat{\theta}_{1i} - \varphi_i^T\hat{\theta}_i + k_{pi}\dot{h}_i + h_i \\ \dot{\hat{\theta}}_i &= -\Gamma_i^{-1}\varphi_i\bar{v}_{1i} \end{aligned} \tag{6.29}$$

where $\bar{v}_{1i} = \tilde{v}_{1i} + k_{pi}h_i$, with $k_{pi} > 0$ and

$$h_i = \sum_{j\in\mathcal{N}_i} e_{ij}z_{ij}.$$

Assume the obtained n-agent graph locally converges to desired formation, then the $n+1$-agent graph is obtained by adding an agent to the n-agent graph using Henneberg sequence. Applying the control law and parameter update law in (6.29) to the added agent, then from the above lemmas and theorems, it can be proved that the $n+1$ agents locally converge to the desired formation. Based on the results established for the LFF system (i.e. the base case), by mathematical induction, the cycle-free persistent graph locally converges to the desired formation by applying the designed control law.

Even though it has been established that the LFF system globally converges to the desired formation, with the same analysis as in [1], the N-agent system locally converges to the desired formation because there are two positions that satisfies $e_{ij} = 0$ for each agent. For example, consider the system in Figure 6.3, agent 4 has another position $\bar{p}_4$ satisfies $e_{14} = e_{24} = 0$. If agent 4 converges to $\bar{p}_4$, in this case

, it may have $\|\bar{p}_{34}\| > d_{35} + d_{45}$, which makes it impossible for agent 5 to achieve $e_{35} = e_{45} = 0$, i.e., the system cannot converge to the desired formation.

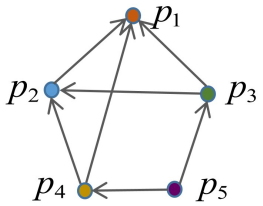

FIGURE 6.2: The system setup of 5-agent system in Cartesian coordinates.

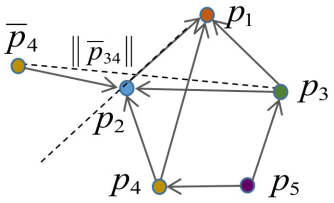

FIGURE 6.3: An example of two positions of agent 4 that satisfies $e_{14} = e_{24} = 0$.

6.3 Simulation

To verify the established theoretical results, simulation study has been carried out. In the simulation, a group of five agents, whose interaction structure is shown in Figure 6.2, is considered. Besides, the desired distances between agents that represent the desired formation are set as $d_{12} = d_{13} = d_{23} = d_{14} = d_{24} = 4$ and $d_{35} = d_{45} = 5$. The function matrices and constant vectors in the dynamics of each

agent (6.1) are given as follows,

$$\varphi_2 = \begin{bmatrix} 0 & \sin(v_{2,2}) \\ \cos(v_{2,1}) & 0 \end{bmatrix},\ \theta_2 = \begin{bmatrix} 1 \\ 0.5 \end{bmatrix};$$
$$\varphi_3 = \begin{bmatrix} v_{3,1}\sin(t) & 0 \\ 0 & v_{3,2}\cos(t) \end{bmatrix},\ \theta_3 = \begin{bmatrix} 0.7 \\ 0.3 \end{bmatrix};$$
$$\varphi_4 = \begin{bmatrix} v_{4,2} & \sin(v_{4,2}) \\ \cos(v_{4,1}) & v_{4,1} \end{bmatrix},\ \theta_4 = \begin{bmatrix} 0.6 \\ 0.9 \end{bmatrix};$$
$$\varphi_5 = \begin{bmatrix} \sin^2(v_{5,1}) & 0 \\ 0 & \cos^2(v_{5,2}) \end{bmatrix},\ \theta_5 = \begin{bmatrix} 0.8 \\ 0.45 \end{bmatrix}.$$

where $v_i = [v_{i,1} v_{i,2}]^T$, $i = 2, 3, 4, 5$.

The initial positions of the five agents are set as,

$$p_1(0) = \begin{bmatrix} 4 & 0.2 \end{bmatrix}^T,\ p_2(0) = \begin{bmatrix} 0.23 & -2.1 \end{bmatrix}^T,$$
$$p_3(0) = \begin{bmatrix} -0.19 & 2.2 \end{bmatrix}^T,\ p_4(0) = \begin{bmatrix} 4.3 & -4.2 \end{bmatrix}^T,$$
$$p_5(0) = \begin{bmatrix} -1.2 & -3.2 \end{bmatrix}^T.$$

The initial velocity and acceleration of the leader are respectively set as $v_1(0) = [2, 1]^T$ and $a_1(t) = [0.5\cos(0.5t), 0.5\cos(0.5t)]^T$. The initial values of the estimates are set as 50% of their true values. Furthermore, the design parameters of the proposed control scheme are set as $k_{pi} = 1$, $k_{vi} = 4$ and $\Gamma_i^{-1} = 0.5 I_2$.

Note that no theoretical result is established for this example system by using existing methods and thus so far no method is applicable it. However, in the simulation, a comparison with the control scheme proposed in [2] is conducted, even though its control scheme is designed for the constant leading velocity case and based on double-integrator model. Also since there is no adaptive law to address the dynamic uncertainty, thus the initial value $\hat{\theta}_i(0)$ is used in the control law. Let L be the Laplacian matrix of the graph in Figure 6.2 with the following

form,

$$L = \begin{bmatrix} 0_{1\times 1} & 0_{1\times 4} \\ L_{21} & L_{22} \end{bmatrix} \tag{6.30}$$

There exists a diagonal positive definite matrix P such that $Q := PL_{22} + L_{22}^T P > 0$ [135]. Then the control law in [2] can be given as follows,

$$u = -(\bar{L} \otimes I_2)v + (P^{-1} \otimes I_2)h - \Phi^T \hat{\Theta}(0) + 1_{n-1} \otimes a_1 \tag{6.31}$$

where $u = [u_2^T, \cdots, u_5^T]^T$, $h = [h_2^T, \cdots, h_5^T]^T$, $\bar{L} = [L_{21}\ L_{22}]$, $\Phi = diag([\varphi_2, \cdots, \varphi_5])$ and $\hat{\Theta} = [\hat{\theta}_2^T, \cdots, \hat{\theta}_5^T]^T$. In the simulation, $P = diag([2, 2, 2, 2])$.

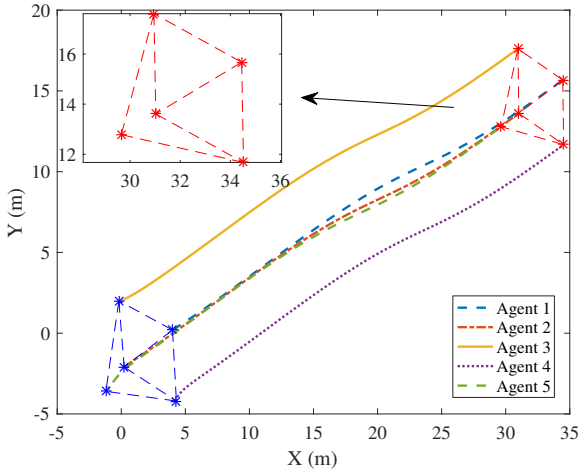

FIGURE 6.4: The trajectories of the five agents generated by the proposed control scheme.

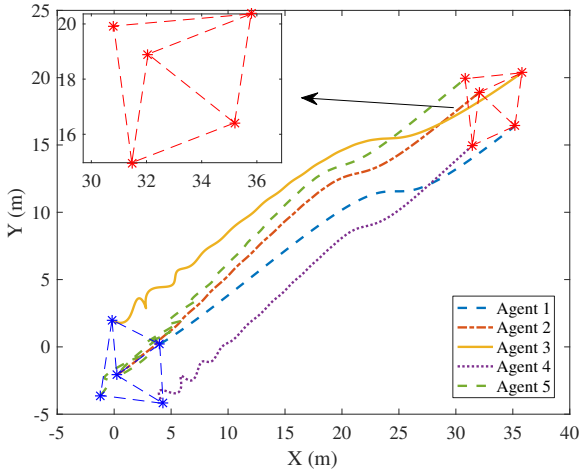

FIGURE 6.5: The trajectories of the five agents generated by [2].

Overall, the trajectories of the five agents generated by the two control schemes are respectively shown in the Figure 6.4 and Figure 6.5, from which, it can be seen that the five agents achieve and maintain the formation during their motions with both control schemes. Now the control performance is assessed by the formation shape control performance and velocity consensus performance. The formation shape control performance of two control schemes in terms of distance errors $e_{ij},\ \forall (i,j) \in \mathcal{E}$ are illustrated in Figure 6.6 and Figure 6.7, respectively. As observed, the distances between pairs of agents converge to zero under the proposed control scheme, however, such control objective is not achieved with the control scheme in [2]. Additionally, from the velocities of agents as shown in Figure 6.8 and Figure 6.9, it can be seen that all agents approach the velocity of the leader and then maintain the same velocity with the proposed control scheme, whereas , there exists deviations between the velocities of leader and other agents with the control scheme in [2]. These simulations illustrate the effectiveness of the proposed scheme and also verify the theoretical results established.

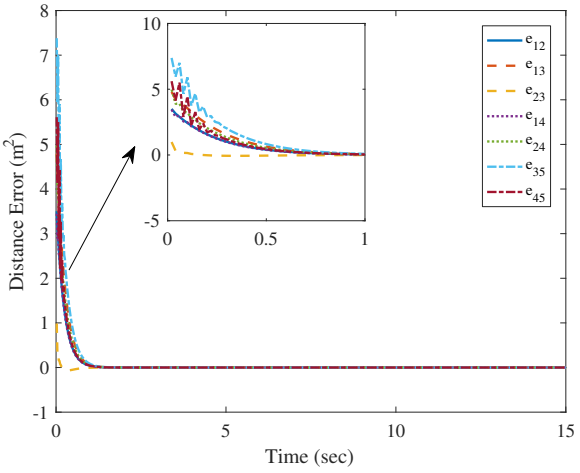

FIGURE 6.6: The distance errors between agents of the proposed control scheme.

6.4 Conclusion

A distributed adaptive strategy is proposed for distance-based formation and flocking control of LFF systems in this chapter. Different from existing research works

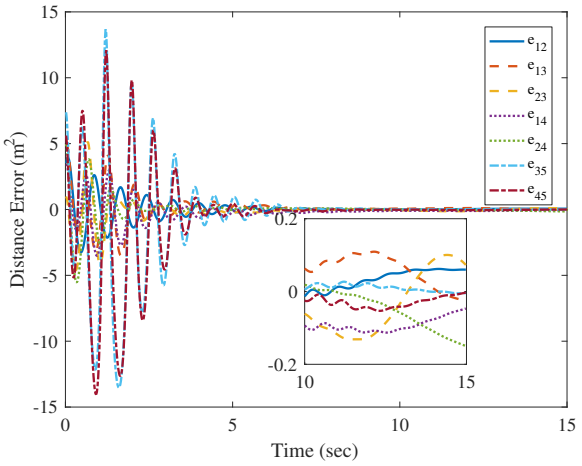

FIGURE 6.7: The distance errors between agents of the control scheme in [2].

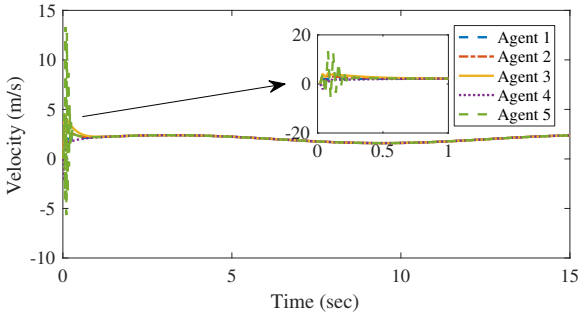

(a)

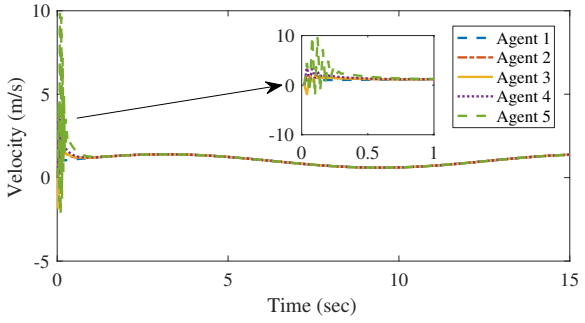

(b)

FIGURE 6.8: The velocities of the five agents of the proposed control scheme. (a) and (b) respectively show the two components, $v_{i,1}$ and $v_{i,2}$, of v_i, $i = 1, 2, 3, 4, 5$.

in this area, the global stability is established in the case that the leading velocity is time-varying, and all agents are supposed to have nonidentical second-order dynamics with parametric uncertainty. By employing adaptive technique, the unknown parameters are estimated and compensated. The introduction of two new variables that involve distance error and velocity error makes sure that the system globally converges to the desired formation and all agents share a common velocity.

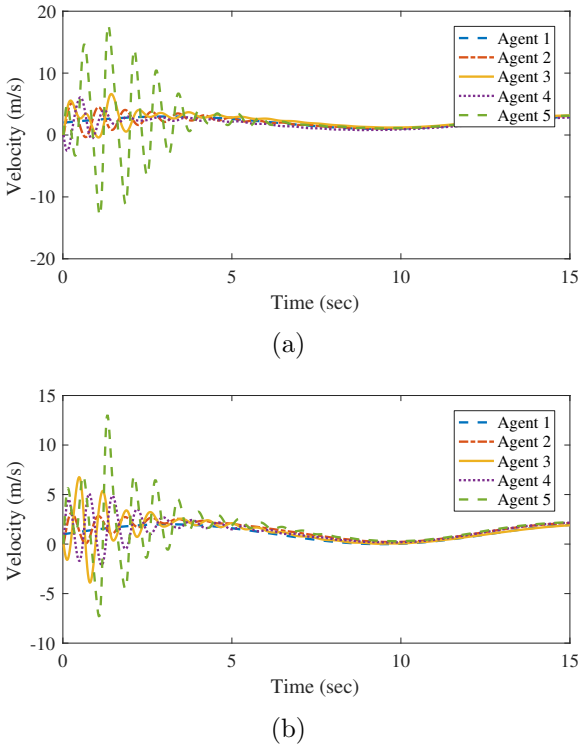

FIGURE 6.9: The velocities of the five agents of the control scheme in [2].

The stability and effectiveness of the proposed control strategy is analyzed in theory and verified through simulation results, respectively. Additionally, the result is extended from LFF system to N-agent case.

Chapter 7

Conclusion and Future Work

In this chapter, the main results of this thesis are summarized and suggestions for future research are provided.

7.1 Conclusion

This thesis investigates two categories consensus problems, the first one is distributed output feedback consensus tracking control of multiple nonholonomic mobile robots with directed graphs in two situations (i) sensor faults occur (ii) only position information of the leader is available to a subset of follower robots. The other consensus problem is the flocking with distance-based formation shape control with undirected graph and LFF system.

The obtained results are summarized as follows.

1 In Chapter 3, distributed output feedback consensus tracking control of multiple nonholonomic mobile robots with directed communication graph in the presence of sensor faults is studied. The proposed control scheme involves a fully distributed estimator and an observer-based output feedback controller.

The estimator, which is independent of global information of communication network topology, is constructed to estimate the reference trajectory for each robot. Due to the presence of sensor faults, an observer-based output feedback control law is designed to compress the effects of sensor faults and realize trajectory tracking based on backstepping technique and the estimated information. With the proposed control scheme, the boundedness of all the signals in the resulting closed-loop system is guaranteed and the convergence of consensus tracking error to an adjustable neighborhood of zero is established.

2 In Chapter 4, distributed output feedback consensus tracking control for multiple nonholonomic mobile robots under directed graph is addressed by using only position information of leader. Since only the position of the leader is available to a set of robots, a fully distributed estimator is firstly constructed to estimate the position of the leader for each robot without using any global information of the graph. To handle unknown parameters and realize trajectory tracking for each robot, an observer-based output feedback control law is designed based on the estimated position information. The proposed control scheme can guarantee the boundedness of all the signals in the resulting closed-loop system and the convergence of consensus error to an adjustable neighborhood of zero.

3 In Chapter 5, formation maneuvering control problem is investigated for mobile robots subject to nonholonomic constraint. To achieve a common velocity for the whole group, an adaptive estimator is firstly designed to estimate the desired maneuvering velocity for each robot. Utilizing the estimated velocity, a modified gradient control law is designed based on the nonholonomic kinematics to achieve the desired formation shape and maneuvering velocity. With the proposed control scheme and appropriate control parameters, local asymptotic convergence of the system is established.

4 In Chapter 6, a distributed adaptive strategy is proposed for distance-based formation and flocking control of LFF systems. Two new variables that involve distance error and velocity error are introduced in the controller design to makes sure that the system globally converges to the desired formation and all agents share a common velocity. To handle the unknown parameters, adaptive laws are designed to estimate unknown parameters and the estimates are employed in the controller design. With the proposed control strategy, the global stability is established in the case that the leading velocity is time-varying and the agent dynamics contain parametric uncertainty. Additionally, the result of LFF system is extended to N-agent case.

7.2 Future Work

Although the consensus of multi-robot systems has been investigated in depth in the literature and this thesis, there are still several interesting research problems that are worthy for further research, which are outlined as follows.

1 Distributed output feedback consensus tracking control of multiple nonholonomic mobile robots in the presence of sensor faults is significant in many practical applications and has been investigated in Chapter 3. With application of the developed smooth control law, we can only ensure that the consensus error converges to an adjustable neighborhood of zero. Asymptotic convergence may be achieved by using sign function to design a non-smooth control law to achieve distributed tracking and compress the effects of sensor faults. It can be an interesting issue for future research. It can be noted that only position is controlled and position sensor faults are considered. Therefore, how to realize consensus on both position and orientation in presence of position and orientation sensor faults is worthy for further investigation. Furthermore, dynamic uncertainty is also an important issue in practical applications. However, it is not simple to realize distributed output feedback

consensus tracking control of multiple nonholonomic mobile robots in the presence of both sensor faults and dynamic uncertainty. Thus, solving this problem is also an interesting future work.

2 Distributed output feedback consensus tracking control of multiple nonholonomic mobile robots is addressed in Chapter 4 using only position information of the leader. Note that, the proposed control scheme focuses on controlling the position without considering the orientation as done in some existing works on multiple nonholonomic mobile robots. Thus, a controller design that can achieve consensus of both position and orientation is worthy for future research. Furthermore, the communication networks considered in Chapter 4 is fixed. However, in some applications, a switching communication network is required. Thus, this is another interesting research problem.

3 An adaptive estimator-based control scheme is designed for formation maneuvering control of nonholonomic mobile robots in Chapter 5. In the proposed control scheme, unmodelled dynamics and exogenous disturbances are not considered in the system model. It is noted that [136] addressed the issue of disturbance attenuation in distance-based formation control for a group of single-integrators in 2D space under an undirected complete graph. Inspired by this, studying the robustness of the proposed scheme with respect to these uncertainties is an interesting problem in distance-based formation control under general undirected graph network topology. However, the problem is rather challenging and requires new techniques, perhaps by following some ideas in [137]. Thus, how to deal with such problems is worthy for further research.

4 Distributed distance-based formation and flocking control of multi-agent systems is solved in Chapter 6. However, the controller is designed based on the assumption that the information of the leader needs to be known by each agent. Therefore, how to relax this condition is worthy for further investigation. Furthermore, collision avoidance is also an important issue in the formation control. However, it is not simple and requires much effort to

achieve collision avoidance and global stability simultaneously because of nonlinear dynamics. Finally, motion constraint such as nonholonomic dynamics is not considered in Chapter 6, thus an extension to control such multiple nonholonomic mobile robots would also be an interesting future research.

Author's Publications

Journal Papers

1. Y. Zou, C. Wen, and M. Guan. "Distributed adaptive control for distance-based formation and flocking control of multi-agent systems," *IET Control Theory & Applications*, vol. 13, no. 6, 878-885, 2019.

2. Y. Zou, C. Wen, and M. Guan. "Adaptive Estimator-based Formation Maneuvering Control of Nonholonomic Mobile Robots," *International Journal of Adaptive Control and Signal Processing*, https://doi.org/10.1002/acs.3078.

3. Y. Zou, C. Wen, M. Shan and M. Guan. "An Adaptive Control Strategy for Indoor Leader-following of Wheeled Mobile Robot," *Journal of the Franklin Institute*, DOI: 10.1016/j.jfranklin.2019.11.054.

Conference Papers

1. Y. Zou, C. Wen, M. Shan and M. Guan. "Image-based visual tracking adaptive control for mobile robots." in *proceedings of the 2016 14th International Conference on Control, Automation, Robotics and Vision (ICARCV)*, 2016, pp.1-6.

2. Y. Zou, M. Shan, M. Guan, C. Wen, and K. Lim. "A trajectory reconstruction approach for leader-following of multi-robot system." in *proceedings of the 2017 12th IEEE Conference on Industrial Electronics and Applications (ICIEA)*, 2017, pp. 1534-1539.

3. M. Shan, Y. Zou, M. Guan, C. Wen, K. Lim, C. Ng, and P. Tan. "Probabilistic trajectory estimation based leader following for multi-robot systems." in *proceedings of the 2016 14th International Conference on Control, Automation, Robotics and Vision (ICARCV)*, 2016, pp. 1-6.

Papers under Review

1. Y. Zou, C. Wen, and M. Guan. "Distributed output feedback consensus tracking control of multiple nonholonomic mobile robots with directed communication graph and sensor faults," submitted to International Journal of Control.

2. Y. Zou, C. Wen, and C. Deng. "Distributed output feedback consensus tracking control of multiple nonholonomic mobile robots with only position information of leader," submitted to IEEE Transactions on Systems, Man and Cybernetics: Systems.

Bibliography

[1] S.-M. Kang and H.-S. Ahn, "Design and realization of distributed adaptive formation control law for multi-agent systems with moving leader," *IEEE Transactions on Industrial Electronics*, vol. 63, no. 2, pp. 1268–1279, 2016.

[2] M. Deghat, B. D. Anderson, and Z. Lin, "Combined flocking and distance-based shape control of multi-agent formations," *IEEE Transactions on Automatic Control*, vol. 61, no. 7, pp. 1824–1837, 2016.

[3] R. M. Murray, "Recent research in cooperative control of multivehicle systems," *Journal of Dynamic Systems, Measurement, and Control*, vol. 129, no. 5, pp. 571–583, 2007.

[4] K.-K. Oh, M.-C. Park, and H.-S. Ahn, "A survey of multi-agent formation control," *Automatica*, vol. 53, pp. 424–440, 2015.

[5] Y. Cao, W. Yu, W. Ren, and G. Chen, "An overview of recent progress in the study of distributed multi-agent coordination," *IEEE Transactions on Industrial informatics*, vol. 9, no. 1, pp. 427–438, 2012.

[6] R. Olfati-Saber, J. A. Fax, and R. M. Murray, "Consensus and cooperation in networked multi-agent systems," *Proceedings of the IEEE*, vol. 95, no. 1, pp. 215–233, 2007.

[7] S. Knorn, Z. Chen, and R. H. Middleton, "Overview: Collective control of multiagent systems," *IEEE Transactions on Control of Network Systems*, vol. 3, no. 4, pp. 334–347, 2015.

[8] R. Olfati-Saber and R. M. Murray, "Consensus problems in networks of agents with switching topology and time-delays," *IEEE Transactions on automatic control*, vol. 49, no. 9, pp. 1520–1533, 2004.

[9] G. Hu, "Robust consensus tracking for an integrator-type multi-agent system with disturbances and unmodelled dynamics," *International journal of control*, vol. 84, no. 1, pp. 1–8, 2011.

[10] S. Djaidja and Q. Wu, "Leader-following consensus for single-integrator multi-agent systems with multiplicative noises in directed topologies," *International Journal of Systems Science*, vol. 46, no. 15, pp. 2788–2798, 2015.

[11] S. Djaidja and Q. Wu, "Leader-following consensus of single-integrator multi-agent systems under noisy and delayed communication," *International Journal of Control, Automation and Systems*, vol. 14, no. 2, pp. 357–366, 2016.

[12] W. Ren and E. Atkins, "Distributed multi-vehicle coordinated control via local information exchange," *International Journal of Robust and Nonlinear Control: IFAC-Affiliated Journal*, vol. 17, no. 10-11, pp. 1002–1033, 2007.

[13] S. Li, H. Du, and X. Lin, "Finite-time consensus algorithm for multi-agent systems with double-integrator dynamics," *Automatica*, vol. 47, no. 8, pp. 1706–1712, 2011.

[14] S. Yu and X. Long, "Finite-time consensus for second-order multi-agent systems with disturbances by integral sliding mode," *Automatica*, vol. 54, pp. 158–165, 2015.

[15] Z.-H. Guan, F.-L. Sun, Y.-W. Wang, and T. Li, "Finite-time consensus for leader-following second-order multi-agent networks," *IEEE Transactions on Circuits and Systems I: Regular Papers*, vol. 59, no. 11, pp. 2646–2654, 2012.

[16] Y. Zhang and Y. Yang, "Finite-time consensus of second-order leader-following multi-agent systems without velocity measurements," *Physics letters A*, vol. 377, no. 3-4, pp. 243–249, 2013.

[17] H.-Y. Yang, X.-L. Zhu, and S.-Y. Zhang, "Consensus of second-order delayed multi-agent systems with leader-following," *European Journal of Control*, vol. 16, no. 2, pp. 188–199, 2010.

[18] H. Li, X. Liao, T. Huang, and W. Zhu, "Event-triggering sampling based leader-following consensus in second-order multi-agent systems," *IEEE Transactions on Automatic Control*, vol. 60, no. 7, pp. 1998–2003, 2014.

[19] J. Fu and J. Wang, "Finite-time coordinated tracking for high-order uncertain nonlinear multi-agent systems with directed communication graphs," in *Proceedings of the 33rd Chinese Control Conference*. IEEE, 2014, pp. 1081–1086.

[20] H. Du, S. Li, Y. He, and Y. Cheng, "Distributed high-order finite-time consensus algorithm for multi-agent systems," in *Proceedings of the 32nd Chinese Control Conference*. IEEE, 2013, pp. 603–608.

[21] Z. Li, Z. Duan, G. Chen, and L. Huang, "Consensus of multiagent systems and synchronization of complex networks: A unified viewpoint," *IEEE Transactions on Circuits and Systems I: Regular Papers*, vol. 57, no. 1, pp. 213–224, 2009.

[22] Y. Hong, G. Chen, and L. Bushnell, "Distributed observers design for leader-following control of multi-agent networks," *Automatica*, vol. 44, no. 3, pp. 846–850, 2008.

[23] W. Ni and D. Cheng, "Leader-following consensus of multi-agent systems under fixed and switching topologies," *Systems & Control Letters*, vol. 59, no. 3-4, pp. 209–217, 2010.

[24] H. Zhang, F. L. Lewis, and A. Das, "Optimal design for synchronization of cooperative systems: state feedback, observer and output feedback," *IEEE Transactions on Automatic Control*, vol. 56, no. 8, pp. 1948–1952, 2011.

[25] Z. Li, Z. Duan, and L. Huang, "Leader-follower consensus of multi-agent systems," in *2009 American control conference*. IEEE, 2009, pp. 3256–3261.

[26] W. Zhu and Z.-P. Jiang, "Event-based leader-following consensus of multi-agent systems with input time delay," *IEEE Transactions on Automatic Control*, vol. 60, no. 5, pp. 1362–1367, 2014.

[27] G. Wen, Z. Li, Z. Duan, and G. Chen, "Distributed consensus control for linear multi-agent systems with discontinuous observations," *International Journal of Control*, vol. 86, no. 1, pp. 95–106, 2013.

[28] W. Ni, C. Xiong, and J. Yang, "Leader-following consensus of high-order multi-agent linear systems with bounded transmission channels," *International Journal of Systems Science*, vol. 44, no. 9, pp. 1711–1725, 2013.

[29] X.-J. Li and G.-H. Yang, "Adaptive fault-tolerant synchronization control of a class of complex dynamical networks with general input distribution matrices and actuator faults," *IEEE Transactions on Neural Networks and Learning Systems*, vol. 28, no. 3, pp. 559–569, 2015.

[30] Z. Li, X. Liu, W. Ren, and L. Xie, "Distributed tracking control for linear multiagent systems with a leader of bounded unknown input," *IEEE Transactions on Automatic Control*, vol. 58, no. 2, pp. 518–523, 2012.

[31] X. Wang and G.-H. Yang, "Distributed h_∞ consensus tracking control for multi-agent networks with switching directed topologies," *Neurocomputing*, vol. 207, pp. 693–699, 2016.

[32] Z. Li, W. Ren, X. Liu, and L. Xie, "Distributed consensus of linear multi-agent systems with adaptive dynamic protocols," *Automatica*, vol. 49, no. 7, pp. 1986–1995, 2013.

[33] Z. Li, W. Ren, X. Liu, and M. Fu, "Consensus of multi-agent systems with general linear and lipschitz nonlinear dynamics using distributed adaptive protocols," *IEEE Transactions on Automatic Control*, vol. 58, no. 7, pp. 1786–1791, 2012.

[34] C. Wang and H. Ji, "Leader-following consensus of multi-agent systems under directed communication topology via distributed adaptive nonlinear protocol," *Systems & Control Letters*, vol. 70, pp. 23–29, 2014.

[35] Z. Li, G. Wen, Z. Duan, and W. Ren, "Designing fully distributed consensus protocols for linear multi-agent systems with directed graphs," *IEEE Transactions on Automatic Control*, vol. 60, no. 4, pp. 1152–1157, 2014.

[36] Z. Li and Z. Ding, "Distributed adaptive consensus and output tracking of unknown linear systems on directed graphs," *Automatica*, vol. 55, pp. 12–18, 2015.

[37] Y. Zhao, Z. Li, and Z. Duan, "Distributed consensus tracking of multi-agent systems with nonlinear dynamics under a reference leader," *International Journal of Control*, vol. 86, no. 10, pp. 1859–1869, 2013.

[38] Z. Li, Z. Duan, and F. L. Lewis, "Distributed robust consensus control of multi-agent systems with heterogeneous matching uncertainties," *Automatica*, vol. 50, no. 3, pp. 883–889, 2014.

[39] J. Sun and Z. Geng, "Adaptive consensus tracking for linear multi-agent systems with heterogeneous unknown nonlinear dynamics," *International Journal of Robust and Nonlinear Control*, vol. 26, no. 1, pp. 154–173, 2016.

[40] Y. Lv, Z. Li, Z. Duan, and J. Chen, "Distributed adaptive output feedback consensus protocols for linear systems on directed graphs with a leader of bounded input," *Automatica*, vol. 74, pp. 308–314, 2016.

[41] X. Wang, D. Xu, and Y. Hong, "Consensus control of nonlinear leader–follower multi-agent systems with actuating disturbances," *Systems & Control Letters*, vol. 73, pp. 58–66, 2014.

[42] Y. Cao and W. Ren, "Finite-time consensus for multi-agent networks with unknown inherent nonlinear dynamics," *Automatica*, vol. 50, no. 10, pp. 2648–2656, 2014.

[43] G. Wen, C. P. Chen, Y.-J. Liu, and Z. Liu, "Neural network-based adaptive leader-following consensus control for a class of nonlinear multiagent state-delay systems," *IEEE transactions on cybernetics*, vol. 47, no. 8, pp. 2151–2160, 2016.

[44] H. Yu and X. Xia, "Adaptive consensus of multi-agents in networks with jointly connected topologies," *Automatica*, vol. 48, no. 8, pp. 1783–1790, 2012.

[45] T. H. Lee, J. H. Park, D. Ji, and H. Y. Jung, "Leader-following consensus problem of heterogeneous multi-agent systems with nonlinear dynamics using fuzzy disturbance observer," *Complexity*, vol. 19, no. 4, pp. 20–31, 2014.

[46] C. Hua, X. You, and X. Guan, "Adaptive leader-following consensus for second-order time-varying nonlinear multiagent systems," *IEEE transactions on cybernetics*, vol. 47, no. 6, pp. 1532–1539, 2016.

[47] H. Du, Y. Cheng, Y. He, and R. Jia, "Second-order consensus for nonlinear leader-following multi-agent systems via dynamic output feedback control," *International Journal of Robust and Nonlinear Control*, vol. 26, no. 2, pp. 329–344, 2016.

[48] X. Jin, S. Wang, J. Qin, W. X. Zheng, and Y. Kang, "Adaptive fault-tolerant consensus for a class of uncertain nonlinear second-order multi-agent systems with circuit implementation," *IEEE Transactions on Circuits and Systems I: Regular Papers*, vol. 65, no. 7, pp. 2243–2255, 2017.

[49] G.-X. Wen, C. P. Chen, Y.-J. Liu, and Z. Liu, "Neural-network-based adaptive leader-following consensus control for second-order non-linear multi-agent systems," *IET Control Theory & Applications*, vol. 9, no. 13, pp. 1927–1934, 2015.

[50] C. Wang, X. Wang, and H. Ji, "Leader-following consensus for a class of second-order nonlinear multi-agent systems," *Systems & Control Letters*, vol. 89, pp. 61–65, 2016.

[51] G. Wen, Z. Peng, A. Rahmani, and Y. Yu, "Distributed leader-following consensus for second-order multi-agent systems with nonlinear inherent dynamics," *International Journal of Systems Science*, vol. 45, no. 9, pp. 1892–1901, 2014.

[52] J. Huang, C. Wen, W. Wang, and Y.-D. Song, "Adaptive finite-time consensus control of a group of uncertain nonlinear mechanical systems," *Automatica*, vol. 51, pp. 292–301, 2015.

[53] Q. Shen and P. Shi, "Output consensus control of multiagent systems with unknown nonlinear dead zone," *IEEE Transactions on Systems, Man, and Cybernetics: Systems*, vol. 46, no. 10, pp. 1329–1337, 2015.

[54] C. P. Chen, C.-E. Ren, and T. Du, "Fuzzy observed-based adaptive consensus tracking control for second-order multiagent systems with heterogeneous nonlinear dynamics," *IEEE Transactions on Fuzzy Systems*, vol. 24, no. 4, pp. 906–915, 2015.

[55] H. Su, G. Chen, X. Wang, and Z. Lin, "Adaptive second-order consensus of networked mobile agents with nonlinear dynamics," *Automatica*, vol. 47, no. 2, pp. 368–375, 2011.

[56] W. Yu, W. Ren, W. X. Zheng, G. Chen, and J. Lü, "Distributed control gains design for consensus in multi-agent systems with second-order nonlinear dynamics," *Automatica*, vol. 49, no. 7, pp. 2107–2115, 2013.

[57] H. Yu, Y. Shen, and X. Xia, "Adaptive finite-time consensus in multi-agent networks," *Systems & Control Letters*, vol. 62, no. 10, pp. 880–889, 2013.

[58] X. Jin, "Adaptive iterative learning control for high-order nonlinear multi-agent systems consensus tracking," *Systems & Control Letters*, vol. 89, pp. 16–23, 2016.

[59] P. Shi and Q. Shen, "Observer-based leader-following consensus of uncertain nonlinear multi-agent systems," *International Journal of Robust and Nonlinear Control*, vol. 27, no. 17, pp. 3794–3811, 2017.

[60] W. Liu and J. Huang, "Adaptive leader-following consensus for a class of higher-order nonlinear multi-agent systems with directed switching networks," *Automatica*, vol. 79, pp. 84–92, 2017.

[61] C. Chen, C. Wen, Z. Liu, K. Xie, Y. Zhang, and C. P. Chen, "Adaptive consensus of nonlinear multi-agent systems with non-identical partially unknown control directions and bounded modelling errors," *IEEE Transactions on Automatic Control*, vol. 62, no. 9, pp. 4654–4659, 2016.

[62] T. Liu and Z. Jiang, "Distributed output-feedback control of nonlinear multi-agent systems," *IEEE Transactions on Automatic Control*, vol. 58, no. 11, pp. 2912–2917, 2013.

[63] X. Zhang, L. Liu, and G. Feng, "Leader–follower consensus of time-varying nonlinear multi-agent systems," *Automatica*, vol. 52, pp. 8–14, 2015.

[64] C.-C. Hua, X. You, and X.-P. Guan, "Leader-following consensus for a class of high-order nonlinear multi-agent systems," *Automatica*, vol. 73, pp. 138–144, 2016.

[65] W. Wang, C. Wen, and J. Huang, "Distributed adaptive asymptotically consensus tracking control of nonlinear multi-agent systems with unknown parameters and uncertain disturbances," *Automatica*, vol. 77, pp. 133–142, 2017.

[66] Y. Zhang, H. Liang, H. Ma, Q. Zhou, and Z. Yu, "Distributed adaptive consensus tracking control for nonlinear multi-agent systems with state constraints," *Applied Mathematics and Computation*, vol. 326, pp. 16–32, 2018.

[67] W. Wang, D. Wang, Z. Peng, and T. Li, "Prescribed performance consensus of uncertain nonlinear strict-feedback systems with unknown control directions," *IEEE Transactions on Systems, Man, and Cybernetics: Systems*, vol. 46, no. 9, pp. 1279–1286, 2015.

[68] S. J. Yoo, "Distributed consensus tracking for multiple uncertain nonlinear strict-feedback systems under a directed graph," *IEEE Transactions on Neural Networks and Learning Systems*, vol. 24, no. 4, pp. 666–672, 2013.

[69] W. Wang, J. Huang, C. Wen, and H. Fan, "Distributed adaptive control for consensus tracking with application to formation control of nonholonomic mobile robots," *Automatica*, vol. 50, no. 4, pp. 1254–1263, 2014.

[70] Z. Ding and Z. Li, "Distributed adaptive consensus control of nonlinear output-feedback systems on directed graphs," *Automatica*, vol. 72, pp. 46–52, 2016.

[71] Y. Kozlovsky, I. Cohen, I. Golding, and E. Ben-Jacob, "Lubricating bacteria model for branching growth of bacterial colonies," *Physical Review E*, vol. 59, no. 6, p. 7025, 1999.

[72] I. Cohen, I. Golding, I. Ron, and E. Ben-Jacob, "Biofluiddynamics of lubricating bacteria," *Mathematical methods in the applied sciences*, vol. 24, no. 17-18, pp. 1429–1468, 2001.

[73] Y. Cao, Y. Li, W. Ren, and Y. Chen, "Distributed coordination algorithms for multiple fractional-order systems," in *2008 47th IEEE Conference on Decision and Control*. IEEE, 2008, pp. 2920–2925.

[74] F. Wang and Y. Yang, "Leader-following consensus of nonlinear fractional-order multi-agent systems via event-triggered control," *International Journal of Systems Science*, vol. 48, no. 3, pp. 571–577, 2017.

[75] Z. Yu, H. Jiang, and C. Hu, "Leader-following consensus of fractional-order multi-agent systems under fixed topology," *Neurocomputing*, vol. 149, pp. 613–620, 2015.

[76] G. Ren, Y. Yu, and S. Zhang, "Leader-following consensus of fractional nonlinear multiagent systems," *Mathematical Problems in Engineering*, vol. 2015, 2015.

[77] B. Ning and Q.-L. Han, "Prescribed finite-time consensus tracking for multi-agent systems with nonholonomic chained-form dynamics," *IEEE Transactions on Automatic Control*, vol. 64, no. 4, pp. 1686–1693, 2018.

[78] S. Shi, S. Xu, and H. Feng, "Robust fixed-time consensus tracking control of high-order multiple nonholonomic systems," *IEEE Transactions on Systems, Man, and Cybernetics: Systems*, 2019.

[79] J. Wang, T. Gao, and G. Zhang, "Finite-time leader-following consensus for multiple non-holonomic agents," in *Proceedings of the 33rd Chinese Control Conference*. IEEE, 2014, pp. 1580–1585.

[80] W. Dong, "Distributed observer-based cooperative control of multiple nonholonomic mobile agents," *International Journal of Systems Science*, vol. 43, no. 5, pp. 797–808, 2012.

[81] Q. Yang, H. Fang, M. Cao, and J. Chen, "Distributed trajectory tracking control for multiple nonholonomic mobile robots," *IFAC-PapersOnLine*, vol. 49, no. 4, pp. 31–36, 2016.

[82] W. Dong and V. Djapic, "Leader-following control of multiple nonholonomic systems over directed communication graphs," *International Journal of Systems Science*, vol. 47, no. 8, pp. 1877–1890, 2016.

[83] S. Khoo, L. Xie, and Z. Man, "Leader-follower consensus control of a class of nonholonomic systems," in *2010 11th International Conference on Control Automation Robotics & Vision*. IEEE, 2010, pp. 1381–1386.

[84] X. Zhang, Z. Peng, S. Yang, G. Wen, and A. Rahmani, "Distributed fixed-time consensus-based formation tracking for multiple nonholonomic wheeled mobile robots under directed topology," *International Journal of Control*, pp. 1–10, 2019.

[85] T. Liu and Z. Jiang, "Distributed formation control of nonholonomic mobile robots without global position measurements," *Automatica*, vol. 49, pp. 592–600, 2013.

[86] M. Ou, S. Gu, B. Wang, and Q. Lan, "Finite-time tracking control for multiple nonholonomic mobile robots with external disturbances and uncertainties," in *2016 35th Chinese Control Conference (CCC)*. IEEE, 2016, pp. 7913–7919.

[87] M. Ou, H. Sun, S. Gu, and Y. Zhang, "Distributed finite-time trajectory tracking control for multiple nonholonomic mobile robots with uncertainties and external disturbances," *International Journal of Systems Science*, vol. 48, no. 15, pp. 3233–3245, 2017.

[88] M. Ou, H. Du, and S. Li, "Finite-time formation control of multiple nonholonomic mobile robots," *International Journal of Robust and Nonlinear Control*, vol. 24, no. 1, pp. 140–165, 2014.

[89] Z. Peng, S. Yang, G. Wen, and A. Rahmani, "Distributed consensus-based robust adaptive formation control for nonholonomic mobile robots with partial known dynamics," *Mathematical Problems in Engineering*, vol. 2014, 2014.

[90] L. Liu, J. Yu, J. Ji, Z. Miao, and J. Zhou, "Cooperative adaptive consensus tracking for multiple nonholonomic mobile robots," *International Journal of Systems Science*, pp. 1–12, 2019.

[91] L. Liu, X. Wang, L. Xiang, Z. Miao, and J. Zhou, "Consensus tracking control for switched multiple nonholonomic mobile robots," in *Chinese Intelligent Systems Conference*. Springer, 2019, pp. 699–707.

[92] L. He, X. Sun, and L. Yan, "Distributed output-feedback formation tracking control for unmanned aerial vehicles," *International Journal of Systems Science*, vol. 47, no. 16, pp. 3919–3928, 2016.

[93] Y. Cheng, R. Jia, H. Du, G. Wen, and W. Zhu, "Robust finite-time consensus formation control for multiple nonholonomic wheeled mobile robots via output feedback," *International Journal of Robust and Nonlinear Control*, vol. 28, no. 6, pp. 2082–2096, 2018.

[94] W. Ren and E. Atkins, "Distributed multi-vehicle coordinated control via local information exchange," *International Journal of Robust and Nonlinear Control*, vol. 17, no. 10-11, p. 1002–1033, 2007.

[95] J. Fax and R. Murray, "Information flow and cooperative control of vehicle formations," *IEEE Transactions on Automatic Control*, vol. 49, no. 9, pp. 75–88, 2004.

[96] M. Caruso, "Applications of magnetic sensors for low cost compass systems," in *2000 IEEE position location and navigation symposium*, 2005, p. 177–184.

[97] W. Ren, R. Beard, and E. Atkins, "A survey of consensus problems in multiagent coordination," in *2005 American control conference*, 2007, p. 1859–1864.

[98] Z. Lin, B. Francis, and M. Maggiore, "State agreement for continuous-time coupled nonlinear systems," *SIAM Journal on Control and Optimization*, vol. 46, no. 1, p. 288–307, 2007.

[99] K.-K. Oh and H.-S. Ahn, "Distance-based undirected formations of single-integrator and double-integrator modeled agents in n-dimensional space," *International Journal of Robust and Nonlinear Control*, vol. 24, no. 12, pp. 1809–1820, 2014.

[100] M.-C. Park, K. Jeong, and H.-S. Ahn, "Formation stabilization and resizing based on the control of inter-agent distances," *International Journal of Robust and Nonlinear Control*, vol. 25, no. 14, pp. 2532–2546, 2015.

[101] K.-K. Oh and H.-S. Ahn, "Formation control of mobile agents based on inter-agent distance dynamics," *Automatica*, vol. 47, no. 10, pp. 2306–2312, 2011.

[102] F. He, Y. Wang, Y. Yao, L. Wang, and W. Chen, "Distributed formation control of mobile autonomous agents using relative position measurements," *IET Control Theory & Applications*, vol. 7, no. 11, pp. 1540–1552, 2013.

[103] J. Shao, G. Xie, and L. Wang, "Leader-following formation control of multiple mobile vehicles," *IET Control Theory & Applications*, vol. 1, no. 2, pp. 545–552, 2007.

[104] D. V. Dimarogonas and K. H. Johansson, "Bounded control of network connectivity in multi-agent systems," *IET control theory & applications*, vol. 4, no. 8, pp. 1330–1338, 2010.

[105] Z. Peng, J. Wang, and D. Wang, "Distributed maneuvering of autonomous surface vehicles based on neurodynamic optimization and fuzzy approximation," *IEEE Transactions on Control Systems Technology*, vol. 26, no. 3, pp. 1083–1090, 2017.

[106] Z. Peng, J. Wang, and D. Wang, "Distributed containment maneuvering of multiple marine vessels via neurodynamics-based output feedback," *IEEE Transactions on Industrial Electronics*, vol. 64, no. 5, pp. 3831–3839, 2017.

[107] S. A. Barogh and H. Werner, "Cooperative source seeking with distance-based formation control and single-integrator agents," *IFAC-PapersOnLine*, vol. 50, no. 1, pp. 7911–7916, 2017.

[108] L. Asimow and B. Roth, "The rigidity of graphs, ii," *Journal of Mathematical Analysis and Applications*, vol. 68, no. 1, pp. 171–190, 1979.

[109] L. Wang and Q. Guo, "Distance-based formation stabilization and flocking control for distributed multi-agent systems," in *2018 IEEE International Conference on Mechatronics and Automation (ICMA)*. IEEE, 2018, pp. 1580–1585.

[110] Z. Sun, S. Mou, M. Deghat, and B. D. Anderson, "Finite time distributed distance-constrained shape stabilization and flocking control for d-dimensional undirected rigid formations," *International Journal of Robust and Nonlinear Control*, vol. 26, no. 13, pp. 2824–2844, 2016.

[111] Z. Sun, S. Mou, M. Deghat, B. Anderson, and A. S. Morse, "Finite time distance-based rigid formation stabilization and flocking," *IFAC Proceedings Volumes*, vol. 47, no. 3, pp. 9183–9189, 2014.

[112] B. D. Anderson, Z. Lin, M. Deghat *et al.*, "Combining distance-based formation shape control with formation translation," *Developments in Control Theory Towards Glocal Control*, vol. 1, pp. 121–130, 2012.

[113] L. Bai, F. Chen, and W. Lan, "Distributed tracking of a rigid formation for multi-agent systems," ser. 33rd Chinese Control Conference, Nanjing, 2014.

[114] J. M. Hendrickx, B. D. Anderson, J.-C. Delvenne, and V. D. Blondel, "Directed graphs for the analysis of rigidity and persistence in autonomous agent systems," *International Journal of Robust and Nonlinear Control: IFAC-Affiliated Journal*, vol. 17, no. 10-11, pp. 960–981, 2007.

[115] T. H. Summers, C. Yu, S. Dasgupta, and B. D. Anderson, "Control of minimally persistent leader-remote-follower and coleader formations in the plane," *IEEE Transactions on Automatic Control*, vol. 56, no. 12, pp. 2778–2792, 2011.

[116] J. Guo, Z. Lin, M. Cao, and G. Yan, "Adaptive leader-follower formation control for autonomous mobile robots," in *American Control Conference (ACC), 2010*. IEEE, 2010, pp. 6822–6827.

[117] J. Guo, Z. Lin, M. Cao, and G. Yan, "Adaptive control schemes for mobile robot formations with triangularised structures," *IET control theory & applications*, vol. 4, no. 9, pp. 1817–1827, 2010.

[118] S.-M. Kang, M.-C. Park, B.-H. Lee, and H.-S. Ahn, "Distance-based adaptive formation control for three agents moving with reference velocity," *Submitted for a publication*, 2014.

[119] S.-M. Kang, M.-C. Park, B.-H. Lee, and H.-S. Ahn, "Distance-based formation control with a single moving leader," in *American Control Conference (ACC), 2014*. IEEE, 2014, pp. 305–310.

[120] Y.-Y. Chen and Y.-P. Tian, "A backstepping design for directed formation control of three-coleader agents in the plane," *International Journal of Robust and Nonlinear Control: IFAC-Affiliated Journal*, vol. 19, no. 7, pp. 729–745, 2009.

[121] T. Das and I. N. Kar, "Design and implementation of an adaptive fuzzy logic-based controller for wheeled mobile robots," *IEEE Transactions on Control Systems Technology*, vol. 14, no. 3, pp. 501–510, 2006.

[122] H. Zhang and F. L. Lewis, "Adaptive cooperative tracking control of higher-order nonlinear systems with unknown dynamics," *Automatica*, vol. 48, no. 7, pp. 1432–1439, 2012.

[123] W. Lin and C. Qian, "Adaptive control of nonlinearly parameterized systems: a nonsmooth feedback framework," *IEEE Transactions on Automatic control*, vol. 47, no. 5, pp. 757–774, 2002.

[124] C. Wang and Y. Lin, "Decentralized adaptive tracking control for a class of interconnected nonlinear time-varying systems," *Automatica*, vol. 54, pp. 16–24, 2015.

[125] J. Yu, X. Dong, Q. Li, and Z. Ren, "Practical time-varying formation tracking for multiple non-holonomic mobile robot systems based on the distributed extended state observers," *IET Control Theory & Applications*, vol. 12, no. 12, pp. 1737–1747, 2018.

[126] L. Krick, M. E. Broucke, and B. A. Francis, "Stabilisation of infinitesimally rigid formations of multi-robot networks," *International Journal of control*, vol. 82, no. 3, pp. 423–439, 2009.

[127] J. Mei, W. Ren, and G. Ma, "Distributed coordinated tracking with a dynamic leader for multiple euler-lagrange systems," *IEEE Transactions on Automatic Control*, vol. 56, no. 6, pp. 1415–1421, 2011.

[128] Bai, He and Arcak, Murat and Wen, John T, "Adaptive motion coordination: Using relative velocity feedback to track a reference velocity," *Automatica*, vol. 45, no. 4, pp. 1020–1025, 2009.

[129] S. Zhao, D. V. Dimarogonas, Z. Sun, and D. Bauso, "A general approach to coordination control of mobile agents with motion constraints," *IEEE Transactions on Automatic Control*, vol. 63, no. 5, pp. 1509–1516, 2018.

[130] S. Zhao, "Affine formation maneuver control of multiagent systems," *IEEE Transactions on Automatic Control*, vol. 63, no. 12, pp. 4140–4155, 2018.

[131] H. K. Khalil, "Noninear systems," *Prentice-Hall, New Jersey*, vol. 2, no. 5, pp. 5–1, 1996.

[132] Z. Sun, S. Mou, B. D. Anderson, and M. Cao, "Exponential stability for formation control systems with generalized controllers: A unified approach," *Systems & Control Letters*, vol. 93, pp. 50–57, 2016.

[133] H. Rezaee and F. Abdollahi, "A decentralized cooperative control scheme with obstacle avoidance for a team of mobile robots," *IEEE Transactions on Industrial Electronics*, vol. 61, no. 1, pp. 347–354, 2014.

[134] M. Cao, B. D. Anderson, A. S. Morse, and C. Yu, "Control of acyclic formations of mobile autonomous agents," in *Decision and Control, 2008. CDC 2008. 47th IEEE Conference on*. IEEE, 2008, pp. 1187–1192.

[135] Z. Lin, B. Francis, and M. Maggiore, *Distributed control and analysis of coupled cell systems*. VDM Publishing, 2008.

[136] Bae, Yoo-Bin and Lim, Young-Hun and Kang, Sung-Mo and Ahn, Hyo-Sung, "Disturbance Attenuation in Distance-Based Formation Control: A Linear Matrix Inequality Approach," ser. IEEE Conference on Control Technology and Applications (CCTA), Copenhagen, 2018.

[137] Chakrabortty, Aranya and Arcak, Murat, "Robust stabilization and performance recovery of nonlinear systems with unmodeled dynamics," *IEEE Transactions on Automatic Control*, vol. 54, no. 6, pp. 1351–1356, 2009.